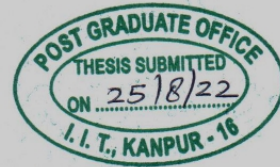# Spectral and energy efficiency optimization of non-concurrent two-way relaying

A Thesis Submitted

in Partial Fulfilment of the Requirements

for the Degree of

Doctor of Philosophy

by

Pandava Sudharshan Babu

Roll No. 16204275

To the

Department of Electrical Engineering

INDIAN INSTITUTE OF TECHNOLOGY KANPUR

August, 2022

CERTIFICATE

It is certified that the work contained in the thesis titled "Spectral and energy efficiency optimization of non-concurrent two-way relaying" by Pandava Sudharshan Babu has been carried out under our supervision and that this work has not been submitted elsewhere for a degree.

Dr. Rohit Budhiraja
Associate Professor,
Department of Electrical Engineering,
Indian Institute of Technology,
IIT Kanpur - 208016.

Dr. A. K. Chaturvedi
Professor,
Department of Electrical Engineering,
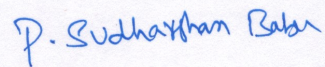Indian Institute of Technology,
IIT Kanpur - 208016.

August 2022

DECLARATION

This is to certify that the thesis titled "**Spectral and energy efficiency optimization of non-concurrent two-way relaying**" has been authored by me. It presents the research conducted by me under the supervision of **Dr. Rohit Budhiraja** and **Dr. A. K. Chaturvedi**.

To the best of my knowledge, it is an original work, both in terms of the research content and narrative, and has not been submitted elsewhere, in part or in full, for a degree. Further, due credit has been attributed to the relevant state-of-the-art and collaborations with appropriate citations and acknowledgements, in line with established norms and practices.

August 2022

P. Sudharshan Babu

Pandava Sudharshan Babu

Ph.D Programme,

Department of Electrical Engineering,

Indian Institute of Technology,

Kanpur-208016.

Abstract

Two-way relaying (TWR) enables two source nodes to exchange data in two-channel uses and is shown to be spectrally-efficient than one-way relaying (OWR), which requires four-channel uses for this data exchange. TWR assumes that a node wants to exchange data with its partner node. If TWR is incorporated in cellular networks, it will assume that a user also wants to exchange data with the base station (BS). In cellular networks, a user, however, does not usually exchange data with the BS. Consider a transmit-only user (TU) who is uploading a large file to a cloud, or a user RU, who is downloading a multimedia data from a server. We see that neither TU nor RU exchanges data with the BS, and consequently, the BS cannot serve them using TWR. The BS, however, can serve them using one-way relaying, but will require four-channel uses, i.e., two each for TU and RU. In the non-concurrent TWR (ncTWR) protocol considered in the literature, the BS can serve both TU and RU in two-channel uses, but the RU now experiences interference from the TU transmit data.

In the first part of the thesis, we consider an orthogonal frequnecy division (OFDM) based ncTWR system, and design an overhearing-based interference cancellation scheme for the RU. It collects side-information by overhearing the TU transmit signal, and uses that to cancel the interference. We then maximize the spectral efficiency (SE) of this system by allocating power across the OFDM subbands jointly at the TU, BS, and the relay nodes. We use successive convex approximation approach to approximate the non-convex sum-rate maximization as a convex geometric program (GP). The algorithm is shown to outperform several other state-of-the-art techniques. In the second part of the thesis, we maximize the global energy efficiency (GEE) of the aforementioned ncTWR system using quadratic transformation (QT)-based optimization. We show that the proposed approach outperforms GP-based sum-rate maximization, one-way relaying, equal and random power allocation. We also show that the GEE reduces with increase in the number of subbands. This happens due to increase in circuit power consumption with the increase in number of subbands.

In the last part of the thesis, we extend the system model to MIMO AF ncTWR with a single subcarrier. We first construct a novel transceiver using GSVD, which reduces the end-to-end MIMO channels into triangular channels. This enables the decoding of transmit symbols using successive interference cancellation. We maximize the system SE by proposing

an iterative GP based optimization framework. We also optimize the system GEE by combining GP with that of the Dinkelbach approach. We also numerically show that the proposed algorithms yield much better performance that the existing state-of-the-art algorithms.

Dedicated to

my family members

Acknowledgments

I express my most profound gratitude to my thesis supervisor, Prof. Rohit Budhiraja, for providing his constant motivation and valuable guidance. His expert directions have taught me beneficial qualities I will treasure throughout my life. Without his meticulous scrutiny, I could not imagine this thesis in its current shape. Apart from his technical suggestions, his patience, jovial nature, and moral support have taught me valuable qualities I will cherish throughout my life. He has never hesitated in lending a helping hand during my journey's most challenging times and tried his best to get me going. I could not imagine having a better advisor and mentor for my research.

I also thank my other thesis supervisor, Prof. A. K. Chaturvedi, for his valuable input during my journey whenever required. It is great working with him and learning many things during the initial days of my Ph.D. Another thing I will treasure throughout my life is his insightful wisdom. His handling of the administrative duties is a treat to watch, and I wish I had learned them more.

I am very thankful to the institution, IIT Kanpur, for providing a pleasurable stay and an entirely promising direction for my future. All of the department's faculty members have my deepest gratitude. I want to express my gratitude to Dr. A. Banerjee for providing me with the opportunity to participate in various departmental events. My travel was made more pleasurable by his constant encouragement and reassuring presence.

I am thankful to all the members of the WiSDOM lab for their constant support. I specifically thank Dheeraj, Anupama, Vishal, Venkatesh, Rajesh, Likith, and Aravind for maintaining the research and lively environment in the lab for me.

I'm grateful to all of my friends, especially Mohan, Bharadwaj, Srujan, Hrushikesh, Sravan, and the rest of my cohort, for their unwavering support and for helping to make my time on campus enjoyable and memorable. I also treasure the moments with Jany, Madhu, Vivek, Krishna, Vijay, Ganesh, Prachi, Krati, Pushpender, and the rest of my M.tech classmates.

Every Sunday during my stay at IITK, we played cricket matches with Jaipal, Raghu, Viswanath, Hari Krishna, Kunwar Pritiraj, Prem, Ayush, Surender, and all our other teammates were memorable and fun. I also thank my badminton group, who encouraged me to improve my game every morning, especially Mohan, Bharadwaj, Vishnu, Siva, Prof. Gopa

Contents

List of Figures

List of Tables

List of Symbols

a	vector a
$\mathbf{A}$	Matrix A
$(.)^*$	Complex conjugate of a scalar
$(\mathbf{A})^*$	Complex conjugate of matrix $\mathbf{A}$
$(\mathbf{A})^T$	Transpose of matrix $\mathbf{A}$
$(\mathbf{A})^H$	Conjugate transpose of matrix $\mathbf{A}$
$\text{Tr}(\mathbf{A})$	Trace of matrix $\mathbf{A}$
$[\mathbf{A}_{i,j}]$	$(i,j)^{th}$ element of a matrix $\mathbf{A}$
$\gg$	much greater than
$\ll$	much less than
$\approx$ approximately equal to	
$\mathbf{a}_n$	n^{th} element of a vector $\mathbf{a}$
$diag(\mathbf{a})$	a diagonal matrix with $\mathbf{a}$ as elements on its main diagonal
$E[.]$	expectation operator
$Var[.]$	variance operator
$diag\,(\mathbf{a})$	a diagonal matrix with elements $\mathbf{a}$ on its diagonal
$|c|$	magnitude of a scalar c
$\mathbf{I}_N$	an N $\times$ Identity matrix
$\mathcal{CN}(0,1)$	complex normal distribution
$\mathbb{R}^{p \times q}$	a real matrix of dimension $p \times q$
$\mathbb{C}^{p \times q}$	a complex matrix of dimension $p \times q$
$n_r[k]$	noise at the relay on k^{th} subband

$\mathbf{p}_j$	power vector at node j
P_r	maximum transmit power at the relay
P_c	system circuit power
K	number of subbands

List of Abbreviations

4G	Fourth-generation wireless
5G	Fifth-generation wireless
AF	Amplify and forward
AWGN	Additive white Gaussian noise
BER	Bit error rate
BI	Back propagating interference
BS	Base station
CCFP	Concave-Convex fractional program
CSI	Channel state information
DN	Destination node
EPA	Equal power allocation
FD	Full duplex
GEE	Global energy efficiency
GP	Geometric programming
GSVD	Generalized singular value decomposition
ncTWR	Non-concurrent two way relaying
HD	Half duplex
i.i.d	Independent and identically distributed
KKT	Karush-Kuhn-Tucker
LP	Linear processing
MIMO	Multiple inpur and Multiple output
OFDM	Orthogonal frequency division multiplexing

OWR	One-way relaying
PC	Pseudo Concave
QoS	Quality of Service
QT	Quadratic transform
RN	Relay node
RPA	Random power allocation
RU	Receive only user
SCA	Successive convex approximation
SE	Spectral efficiency
SIC	Successive interference cancellation
SNR	Signal-to-noise ratio
SR	Sum-rate
TC	Transceiver chain
TU	Transmit only user
TWR	Two-way relaying

Chapter 1

Introduction

A cellular system, whose schematics is shown in Fig. 1.1, consists of three nodes: core network, base station (BS), and the user. The core network is connected to the BS with wired backhaul links, while the users are connected to the BS using wireless access links. Such an architecture works well only when a user has a strong link with the BS. For a coverage-
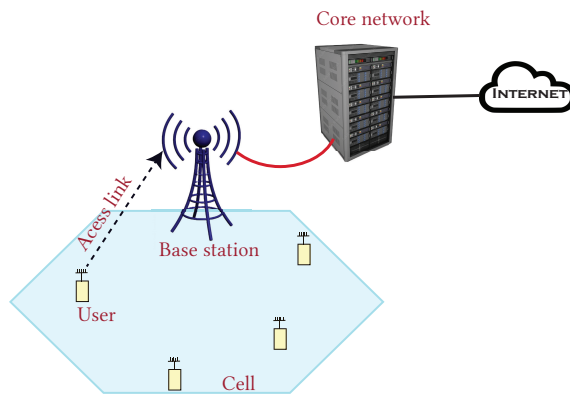
Figure 1.1: Cellular system architecture.

extension situation in Fig. 1.2, which is labelled as 1, a large distance between a user and the BS, considerably reduces the access link signal strength. Similarly in a coverage-hole scenario shown in Fig. 1.2, which labelled as 2, the user-BS link is poor due to high penetration loss. In these scenarios, it is challenging for the BS to deliver a high data rate to such users. Since

users in coverage-limited areas experience poor channel conditions for a significant portion of their communication session, the BS cannot enable high data rate connectivity to these users by just resending lost data packets to them. Any such retransmission will encounter adverse channel yet again, and the user will not be able to decode the signal they receive.
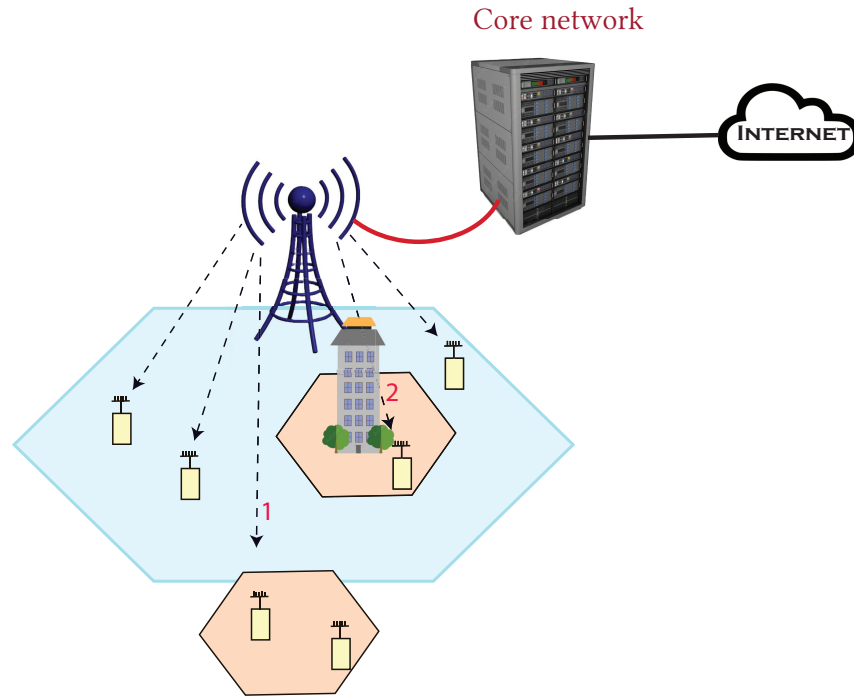
Figure 1.2: Coverage limited scenarios with a weak direct BS $\rightarrow$ user link.

1.1 Solutions

This thesis focuses on providing connectivity to such users who cannot directly communicate directly with the BS, due to a weak direct link. We begin by considering two possible network architecture to serve such users.

1.1.1 Use of low-power BS which are in close proximity to the BS

The users in a coverage-limited scenario will receive a strong signal if, as indicated in Fig. 1.3, a secondary, low-powered BS is installed nearby. Each such BS will have a wired backhaul

link to the core network, which will increase the system installation cost. Further, there might not be many users with such restricted coverage to justify such a cost increase.
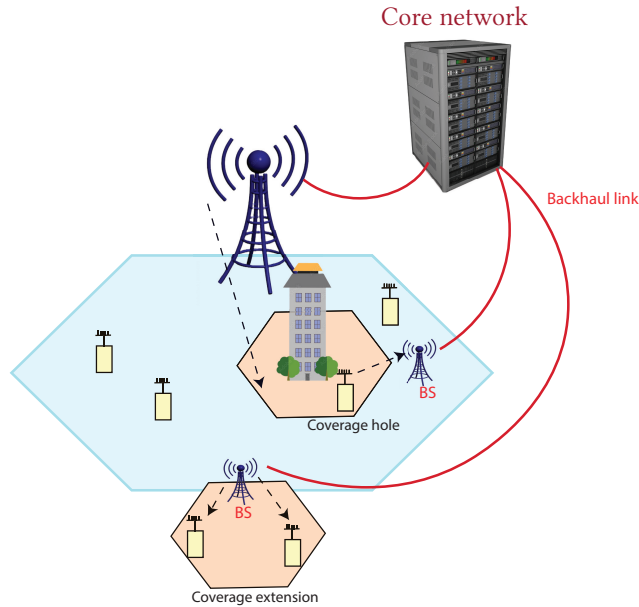
Figure 1.3: Cellular layout with low-power proximate BS.

1.1.2 Installation of Relays

Using a relay, instead of a proximate BS, can reduce the system cost. As shown in Fig. 1.4, a relay is connected to the BS via a wireless link. A relay cannot generate data. It is a transceiver that receives the downlink signal transmitted by the BS, and then retransmits it to the user after suitable processing. Similarly it receives the in the uplink signal transmitted by the user, and after suitable processing, transmits it to the BS. Depending on the relay capabilities, it can for example be implemented as computationally simple amplify-and-forward (AF) [1, 2, 3] device or computationally-complex decode-and-forward (DF) [4, 5, 6] device.

1.2 Motivation

Relays can operate in either half-duplex (HD) or full-duplex (FD) mode. A FD relay uses the same spectral resource to simultaneously transmit and receive signals [4, 7, 8, 9, 10, 11,
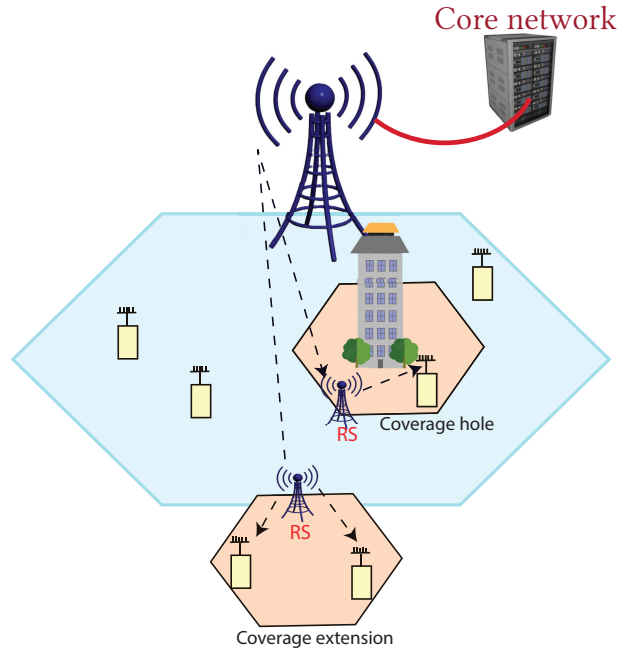
Figure 1.4: Illustration of the cellular layout after relays have been set up to serve users in capacity-restricted areas

12, 13, 14]. As shown in Fig. 1.5, the relay high-power transmit signal causes significant self-interference to its received signal. Various self interference cancellation schemes are studied in [15, 16]. However, a FD relay implementation in practical systems is not anticipated soon. The HD technology is well-established and nearly all commercial cellular systems are HD. We consider HD relays in this thesis which require two uses of channel (frequency/time slots) for transmission and reception.

In the literature, one-way [2, 17, 18, 19, 20, 21] and two-way [1, 22, 23, 24, 25, 26, 27, 28, 22, 29, 30, 31, 32] HD relaying techniques have been extensively investigated. As seen in Fig. 1.6, one-way relaying (OWR) involves a HD relay that receives the signal from Node 1 (BS) in the first use of channel, and processes and retransmits it to Node 2 (user) in the second use of channel. As a result, two uses of the channel are required to send one unit of data in the downlink (BS → user), or equivalently four uses of channel are needed to exchange
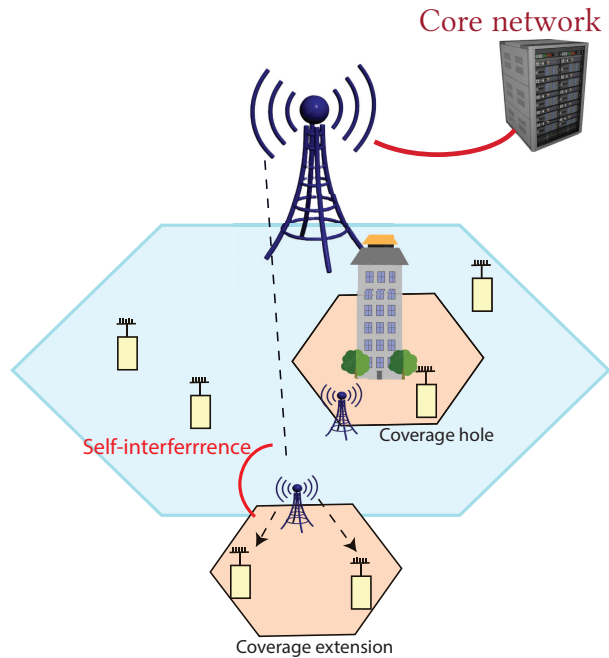
Figure 1.5: Illustration of the self-interference in a full-duplex system
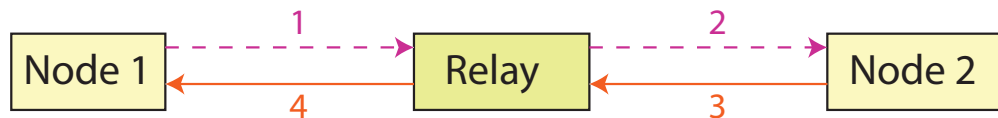
Figure 1.6: Protocol for one-way relaying : Relay receives Node 1 (resp. Node 2) transmit signal in the first (resp. third) use of channel, and relay retransmits to Node 2 (resp. Node 1) in the second (resp. fourth) use of channel.

two units of data on the uplink and downlink. This is twice the number of uses of channel required for two nodes to communicate to one another directly without the aid of a relay. Although OWR strengthens the signal, it reduces the spectral efficiency (SE) of the system.

If two nodes want to exchange data, two-way relaying (TWR) can avoid this spectral loss

[33]. As shown in Fig. 1.7, in the first use of channel in TWR, two source nodes concurrently transmit their signals to the relay, which then receives the combination of these two signals. The relay then transmits a function of this combined signal to the same two nodes in the second use of channel. We see that both these nodes not only receive the desired signal but

(a) First channel use.

(b) Second channel use.
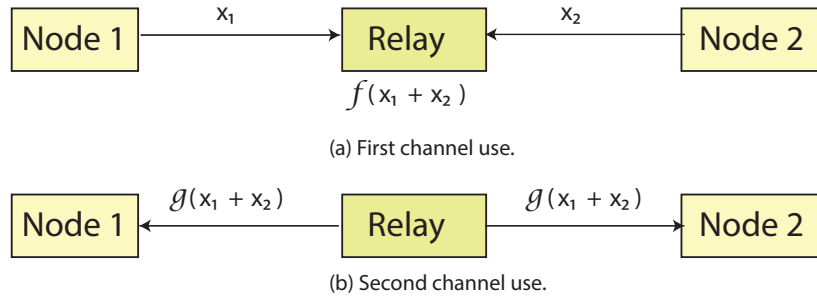
Figure 1.7: In the first use of channel in TWR, two source nodes simultaneously transmit their signals to the relay, which receives a combination of two signals. In the second use of the channel, the relay transmits a function of the combined signal received in the first use of channel.

also their respective transmit signal which they transmitted in the first use of the channel. In TWR, the key idea is that each node is aware of its own transmit signal, it is possible for them to cancel from their receive signal the interference which back propagates due to their own transmit signal [34]. TWR enables the use of two channels to exchange two data units after cancellation of this back-propagating interference (BI). TWR improves the SE of conventional half-duplex relaying by reducing the number of uses of channel [33].

It is assumed in TWR that if Node 1 transmits data to Node 2, Node 1 also has data to receive from Node 2 at the same time. Therefore, the first use of channel is used for transmission by both the nodes. The fundamental idea in TWR is that two different flows of data from two separate nodes are combined to create a two-way flow of data. However, in a cellular system, due to non-concurrent uplink and downlink traffic requirements, combining two data flows between a user and the BS is not always feasible. Consider, for instance, a transmit-only user (TU) in the uplink who wants to send a video to cloud. In this case, as

illustrated in Fig. 1.8a, user TU does not request data from the BS. It only sends data to the BS. Consider, for example, another receive-only user (RU), who is streaming an HD video from a service provider. In this case, as illustrated in Fig. 1.8b, user RU does not have any data to transmit to the BS, and is only requesting data from it. These two traffic directions TU→ RS →BS and BS →RS → RU, both lead to one-way data flow. The BS will not be able to employ TWR with either TU or RU without a two-way data flow between the two.
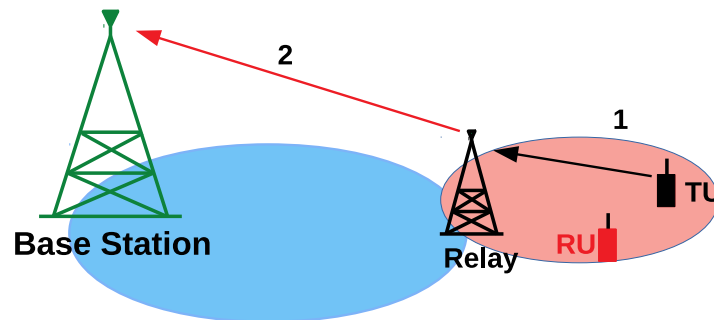
(a) TU only sends data to BS
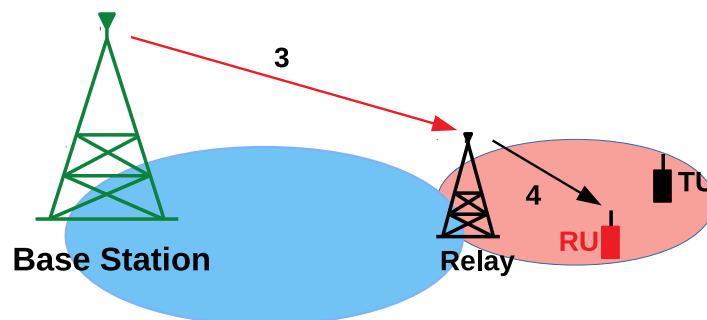
(b) RU only receives data from BS

Figure 1.8: Non-Concurrent traffic scenarios in cellular systems

The BS, as shown in the system model below in Fig. 1.9, can however serve them by employing OWR, but will require four uses of channel – two each for TU and RU. The OWR will establish two separate end-to-end links. With four uses of channel, OWR will have a degraded SE.

The non-concurrent two-way relaying (ncTWR) protocol proposed in [35, 36], enables the BS to assist TU and RU in two uses of channel, and offers a higher SE than OWR protocol.
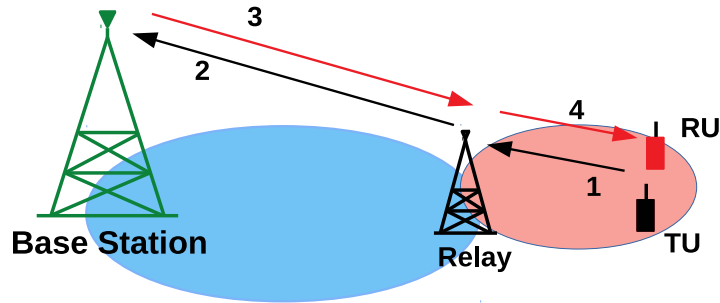
Figure 1.9: An example of a situation where BS uses one-way relaying to serve TU and RU. For the BS to assist both TU and RU, four uses of channel are required.

This protocol extends the fundamental TWR idea of aggregating two flows. It achieves this objective by aggregating the uplink data flow from the TU, and the downlink data flow destined for the RU. In the first use of channel in the ncTWR protocol, both TU and BS send their respective data signals to the relay (see Fig. 1.10). While the TU transmits its data which is destined for the BS, the BS transmits data which is destined for the RU. The relay receives a signal which is a sum of the signals transmitted by the TU and the BS. It then sends a function of the sum signal to both BS and RU in the second use of channel of ncTWR (Fig. 1.10). The first use of channel of ncTWR is usually called the multiple access (MAC) phase, and the second use of channel is usually called the broadcast (BC) phase.

Unlike conventional TWR, the ncTWR protocol does not necessitate that a user concurrently transmits and requests data from the BS. As a result, ncTWR re-establishes data flow in the uplink and the downlink directions across the relay. In two uses of channel, two data units are transferred, leading to an increased SE. Now, the BI experienced by the BS in ncTWR protocol is due to its own transmit data in the MAC phase. The BS can cancel its BI, just like in traditional TWR. However, the BI that the RU in ncTWR experiences is not it's own but rather a transmit signal from TU. Without an access of TU data, the RU cannot cancel BI. Thus, only the TU $\rightarrow$ RS $\rightarrow$ BS link is BI-free using the ncTWR protocol, whereas the BS $\rightarrow$ RS $\rightarrow$ RU link encounters BI. This is unlike the OWR system discussed previously, where both of these links are BI-free. As with OWR, one goal of this protocol is to guarantee that the BS$\rightarrow$RS$\rightarrow$RU link is likewise BI-free and to establish two end-to-end
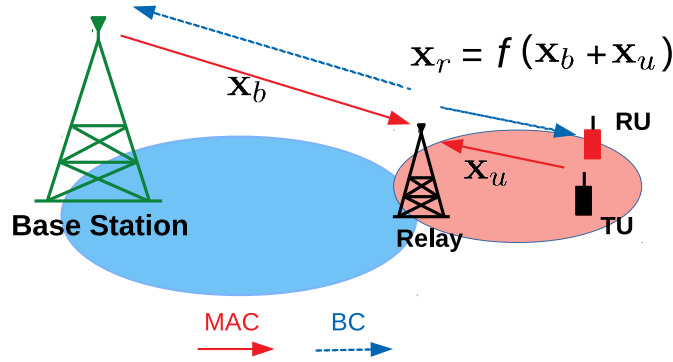
Figure 1.10: Non-Concurrent TWR (ncTWR) protocol: In the MAC phase, TU transmits data which is intended for the BS. Similarly the BS transmits data, which is intended for the user RU. In the BC phase, relay transmits a function of the MAC-phase sum-signal received earlier, to both BS and RU.

BI-free links. References [37, 38] gives brief overview of the similar kind of specific problems we are going to solve.

References [35, 36] designed a relay precoder to mitigate the BI, whereas references [39, 40, 41] assumed that the RU can overhear the MAC-phase TU transmit signal of the TU, and then use it to cancel the BI in the BC phase. *All the aforementioned references [36, 39, 40, 41, 35, 42] have considered single-carrier systems, and have ignored the use of orthogonal frequency division multiplexing (OFDM) in their system design, which is an important technology component of the 4G and 5G systems.*

1.3   Contributions and organization of the thesis

The summary of the thesis contributions and its organization are as follows:

- Chapter 2 extends the ncTWR protocol to handle the non-concurrent traffic in practical OFDM cellular system. An overhearing-based BI-cancellation technique is proposed, wherein the RU cancels the BI by overhearing the TU broadcast signal. The OFDM ncTWR system, with the aid of overhearing technique, provides two non-interfering connections and only requires two uses of channel to serve both these users. In this chapter, we also formulate optimizations to maximize the SE and global energy effi-

ciency (GEE), which is the ratio of network SE and its power consumption, for OFDM ncTWR protocol. We perform the studies in this thesis for an amplify-and-forward (AF) relay as it is easy to implement [23, 36].

- Chapter 3 maximizes the SE of OFDM AF ncTWR by cooperatively allocating power across the OFDM subbands at the TU, BS, and relay nodes. We propose a successive convex approximation (SCA) method to approximate the non-convex SE maximization as a convex geometric problem [43]. We numerically demonstrate that the proposed SE maximization, based on SCA strategy, outperforms various existing SE optimizations. The GEE metric, unlike SE is a fractional function of the optimization variables, and the SCA-based approach cannot be trivially extended to optimize it. We then extend the quadratic transformation (QT) based approach from [44] to optimize it. We again show the efficacy of the proposed GEE optimization approach using numerical simulations.

- Chapter 2 and Chapter 3 consider OFDM ncTWR system with single-antenna nodes. In Chapter 4, we consider a ncTWR system with multiple-input multiple-output (MIMO) nodes. We additionally assume that the weak direct links between the BS, TU and RU can be exploited to increase the SE. The focus in this chapter is on a novel MIMO ncTWR transceiver design with direct link. We do not consider OFDM herein for the sake of brevity. This makes it easier for us to discuss how the precoder design decomposes end-to-end MIMO channels into triangular channels using GSVD. We achieve this with the novel precoder and decoder design to jointly beamform for relay and direct links. The triangular channel structure makes it possible to detect the transmit symbols at the RU and BS.

- Chapter 5 maximizes the SE and GEE for MIMO AF ncTWR, which are non-convex problems. We again use the GP framework to maximize the SE. We then combine GP with Dinkelbach's method to optimize GEE. We numerically demonstrate that the proposed technique outperforms other techniques known in the literature.

- Chapter 6 concludes the thesis with the summary of the work done in this thesis. It discuss briefly about future research directions.

Chapter 2

System model of OFDM-based SISO AF ncTWR

2.1 System Model of OFDM ncTWR

Consider a non-concurrent AF TWR system, as shown in Fig. 2.1 , wherein a HD relay is used by two users, TU and RU, to communicate with the BS. The data is sent from the BS to the RU on the downlink, and from the TU to the BS on the uplink. Because of excessive path attenuation and shadowing, the two users aae unable to establish direct connections with the BS [35, 36]. We also assume that all the nodes are equipped with a single antenna. We consider an OFDM-based system with K subbands.[1] In the first use of channel in ncTWR, both BS and TU transmit their respective downlink and uplink OFDM signals to the relay, which receives a sum of these two signals. The relay received sum signal on the kth subband is

$$y_r[k] = h_b[k]x_b[k] + h_u[k]x_u[k] + n_r[k], \quad \text{for} \quad k = 1, \ldots, K. \tag{2.1}$$

Here $h_b[k]$, $h_u[k]$ are the kth subband channels for the BS→Relay and the TU→Relay links, respectively. We express $x_i[k] = \sqrt{p_i[k]}\tilde{x}_i[k]$ for $i = u, k$, where $\tilde{x}_i[k]$ has zero mean

---

[1]A group of subcarriers is termed as a subband.
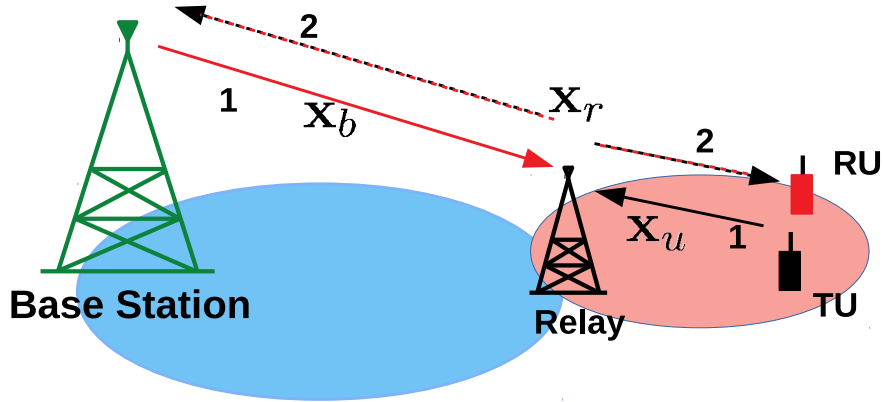
Figure 2.1: Non-current TWR: In the first use of channel (labeled '1'), both BS and TU send their respective data signals to the relay. The relay amplifies its receive sum-signal, and transmits it to both BS and RU in the second channel use (labeled '2').

and unit variance such that

$$\mathbb{E}\left[\sum_{k=1}^{K}|x_i[k]|^2\right] = \sum_{k=1}^{K} p_i[k] \leq P_i \quad \text{for} \quad i = u, b \tag{2.2}$$

The relay noise $n_r[k]$, which is independent and identically distributed (i.i.d) across subbands, has complex normal distribution, denoted as $\mathcal{CN}(0,1)$. We assume that, similar to,[39, 41], the RU overhears the TU transmit signal, and utilizes it to suppress its BI in the second channel use. The signal overheard by the RU in the kth subband is

$$y_u^1[k] = h_o[k]x_u[k] + n_u^1[k]. \tag{2.3}$$

The superscript here and in the sequel denotes the channel use of the RU receive signal. The term $h_o[k]$ is the kth subband channel for the TU→RU overhearing-link. The first-channel-use RU noise $n_u^1[k]$, iid across subbands, is distributed as $\mathcal{CN}(0,1)$. We assume, similar to [35, 36], a quasi-static channel model where channel is constant over multiple channel uses, and can be estimated perfectly, and are accessible to all the nodes. The relay amplifies the signal it receives and sends it to both BS and RU during the second channel use of ncTWR. The relay transmit sigal $x_r[k]$ for the kth subband is

$$x_r^k = \sqrt{p_r[k]}y_r[k] = \sqrt{p_r[k]}(h_b[k]x_b[k] + h_u[k]x_u[k] + n_r[k]),$$

where $p_r[k]$ is the amplification factor for the kth subband. The relay signal satisfies the maximum transmit power constraint, which is specified as

$$\sum_{k=1}^{K} p_r[k]|h_b[k]|^2 p_b[k] + p_r[k]|h_u[k]|^2 p_u[k] + p_r[k] \leq P_r \qquad (2.4)$$

The relay transmit signal $x_r[k]$ is normalized to satisfy its transmit power constraint. The above transmit power constraint, similar to the existing literature [36, 43, 45], also ensures that $x_r[k]$ does not go against the relay power constraint. In the second channel use, the BS and RU's respective kth-subband signals are represented as

$$y_b[k] = \sqrt{p_r[k]} g_b[k] \Big(\underbrace{h_b[k] x_b[k]}_{\text{BI}} + h_u[k] x_u[k] \Big) + \bar{n}_b[k]$$

$$y_u^2[k] = \sqrt{p_r[k]} g_u[k] \Big(h_b[k] x_b[k] + \underbrace{h_u[k] x_u[k]}_{\text{BI}} \Big) + \bar{n}_u^2[k]. \qquad (2.5)$$

Here $g_b[k]$ and $g_u[k]$ are the kth subband channel for the Relay→BS and Relay→RU links, respectively. Also, the effective noise at the BS and the RU in the second channel use are

$$\bar{n}_b[k] = \sqrt{p_r[k]} g_b[k] n_r[k] + n_b[k] \qquad (2.6)$$

$$\bar{n}_u^2[k] = \sqrt{p_r[k]} g_u[k] n_r[k] + n_u^2[k], \qquad (2.7)$$

where $n_b[k] \sim \mathcal{CN}(0,1)$ and $n_u^2[k] \sim \mathcal{CN}(0,1)$.

2.1.1 Challenges in design

The OFDM ncTWR system design has two challenging design aspects:

- a suitable BI cancelling scheme for the RU.

- a novel optimal power allocation scheme to maximize the system SE by jointly allocating power at the BS, TU and the relay nodes, and crucially also across OFDM subbands.

2.1.2 Contributions of this chapter

The main contribution of this chapter which addresses the challenges mentioned above are as follows:

- Motivated by the overhearing-based BI-cancellation approach in [39, 41], the RU herein also cancels the BI by overhearing the TU transmit signal. This approach is crucial for the OFDM ncTWR system as it yields signal-to-noise ratio (SNR) expressions which allows us to maximize the system SE using geometric programming.

- For the proposed OFDM-based ncTWR system, we formulate the SE and GEE optimizations.

2.1.3 Overhearing based BI cancellation

The BS uses its self-data to cancel the BI in $y_b[k]$ in (2.5) as follows.

$$\tilde{y}_b[k] = \sqrt{p_r[k]} g_b[k] h_u[k] x_u[k] + \bar{n}_b[k]. \tag{2.8}$$

If RU can overhear a noise-free TU signal, it can directly cancel the BI in (2.5), which is, however, impractical. We, therefore, consider a practical scenario where RU overhears a noisy version of the TU transmit signal, which is given in (2.3). The RU then cancels the interference as shown in (2.9).

The RU, by using the signal overheard in the first channel use in (2.3), cancels its BI as follows.

$$\begin{aligned}
\tilde{y}_u[k] &= y_u^2[k] - \frac{\sqrt{p_r[k]} g_u[k] h_u[k]}{h_0[k]} y_u^1[k] \\
&= \sqrt{p_r[k]} g_u[k] h_b[k] x_b[k] + \bar{n}_u^2[k] - \frac{\sqrt{p_r[k]} g_u[k] h_u[k]}{h_0[k]} n_u^1[k].
\end{aligned} \tag{2.9}$$

2.1.4 Rate expressions for end-to-end links

The rate expressions for the kth subband for the end-to-end TU→Relay→BS and BS→Relay→RU links. These expressions, derived using (2.8) and (2.9), are given respectively as

$$R_b[k] = \frac{1}{2} \log_2 \left(1 + \text{SNR}_b[k]\right) \tag{2.10}$$

$$R_u[k] = \frac{1}{2} \log_2 \left(1 + \text{SNR}_u[k]\right), \text{ where} \tag{2.11}$$

$$\text{SNR}_b[k] = \frac{|h_u[k] g_b[k]|^2 p_r[k] p_u[k]}{1 + |g_b[k]|^2 p_r[k]}$$

$$\text{SNR}_u[k] = \frac{|g_u[k] h_b[k]|^2 p_r[k] p_b[k]}{1 + |g_u[k]|^2 p_r[k] + |\frac{g_u[k] h_u[k]}{h_o[k]}|^2 p_r[k]}. \tag{2.12}$$

The factor of $1/2$ is because the HD relay cannot transmit and receive simulataneously on the same spectral resource. The system SE for the K subbands is as

$$R_{\text{sum}} = \sum_{k=1}^{K} R_b[k] + R_u[k]. \tag{2.13}$$

2.2 SE problem formulation

At the relay, BS, and TU, we will now jointly allocate the power over K subbands to maximize R_{sum} by imposing power constraints at each transmit node. Before doing that, we define power vectors $\mathbf{p}_j = (p_j[1], \ldots, p_j[K])^T$ for $j = r, b, u$ which we will later optimize. We now write R_{sum} as $R_{\text{sum}}(\mathbf{p}_u, \mathbf{p}_b, \mathbf{p}_r)$ to make it explicit that R_{sum} is a function of the optimization variables $\mathbf{p}_u, \mathbf{p}_b$, and $\mathbf{p}_r$. The SE maximization problem can now be stated as following.

$$\textbf{P1} : \underset{\mathbf{p}_r, \mathbf{p}_b, \mathbf{p}_u}{\text{Max}} \; R_{\text{sum}}(\mathbf{p}_r, \mathbf{p}_b, \mathbf{p}_u) \tag{2.14a}$$

$$\text{s.t.} \quad \sum_{k=1}^{K} p_r[k]|h_b[k]|^2 p_b[k] + p_r[k]|h_u[k]|^2 p_u[k] + p_r[k] \le P_r \tag{2.14b}$$

$$\sum_{k=1}^{K} p_b[k] \le P_b \tag{2.14c}$$

$$\sum_{k=1}^{K} p_u[k] \le P_u. \tag{2.14d}$$

The three constraints are respectively on the maximum transmit power of the relay, TU, and BS. We will show that this problem can be solved using SCA, wherein each approximated problem is cast as a geometric program (GP) in the next chapter. A logarithmic modification in the variables allows GPs, a family of non-linear, presumably non-convex optimizations, to be reformulated as convex problems and solved by software packages [46]. Geometric programming has been used to allocate power in communication systems in [35, 47, 48]. The objective function in GP is posynomial, and the inequality constraints are upper-bounded posynomials and equality constraints are monomials [45, 49]. We refer the reader to Appendix B.1 for a brief discussion on GP.

2.3 GEE problem formulation

The design of energy-efficient wireless systems in search of a green and sustainable future has recently attracted attention. The GEE metric has received attention as a performance benchmark as it achieves a pareto-efficiency between the SE and power consumption [50]. We observe from ncTWR references in Table 3.1 that the GEE for OFDM ncTWR has not yet been optimized. The GEE is defined as the ratio of the network SE and its total power consumption [44] i.e.,

$$\text{GEE} = \frac{R_{\text{sum}}}{\sum_{k=1}^{K} \frac{1}{\xi}(p_r[k] + p_b[k] + p_u[k]) + P_c}. \tag{2.15}$$

Here P_c is the system circuit power. The GEE optimization problem can now be expressed in the following manner:

$$\textbf{P2}: \underset{\mathbf{p}_r, \mathbf{p}_b, \mathbf{p}_u}{\text{Max}} \frac{R_{\text{sum}}}{\sum_{k=1}^{K} \frac{1}{\xi}(p_r[k] + p_b[k] + p_u[k]) + P_c} \tag{2.16a}$$

$$\sum_{k=1}^{K} p_r[k]|h_b[k]|^2 p_b[k] + p_r[k]|h_u[k]|^2 p_u[k] + p_r[k] \leq P_r \tag{2.16b}$$

$$\sum_{k=1}^{K} p_b[k] \leq P_b \tag{2.16c}$$

$$\sum_{k=1}^{K} p_u[k] \leq P_u. \tag{2.16d}$$

The three constraints are, respectively, on the relay's maximum transmit power, TU, and BS. The GEE optimizes the system energy to achieve a given SE [51]. Further, the individual transmit constraint make sure that they are not violated while optimizing the system power. The GEE is a function of the non-concave SE, and the consumed power. We will show that it can be optimized using QT in the next chapter.

2.3.1 Power consumption model

The consumed system power $P_{total} = P_c + P_{tx}$, where P_c is the circuit power and P_{tx} is the transmission power. The circuit power P_c consists of the i) per-band signal processing power of users TU, RU, and the BS denoted as $P_s^t[k]$, $P_s^r[k]$, $P_s^b[k]$ respectively, which linearly scales with number of subbands; and ii) fixed power P_f^b and P_f^u, required to operate the

electronic devices of the BS and the user, respectively. The circuit power P_c is therefore [51] $P_c = \sum_{k=1}^{K}(P_s^b[k] + P_s^t[k] + P_s^r[k]) + P_f^b + P_f^u$. The transmission power P_{tx} is given as [51] $P_{tx} = \sum_{k=1}^{K} \frac{1}{\xi}(p_r[k] + p_u[k] + p_b[k])$. Here, the power amplifier efficiency is denoted as $\xi \in (0,1)$.

2.3.2 Implementation issues

Before we summarize this chapter, we will briefly discuss the implementation issues of the proposed model. The relay requires the channels $h_b[k]$ and $h_u[k]$, which it estimates using pilots transmitted by the BS and TU, respectively. The BS requires the composite channels $g_b[k]h_b[k]$ and $g_b[k]h_u[k]$ to cancel the BI, and to decode data. The relay can help BS estimate them by sending pilots precoded with $h_b[k]$ and $h_u[k]$, respectively. The RU requires the composite channels $g_u[k]h_b[k]$ and $\frac{g_u[k]h_u[k]}{h_o[k]}$ to decode data and to cancel the BI. The relay can help RU estimate $g_u[k]h_b[k]$ and $g_u[k]h_u[k]$ by sending pilots precoded with $h_b[k]$ and $h_u[k]$, respectively. The TU can help RU estimate $h_o[k]$ by sending un-precoded pilot. The relay also requires the channels $g_b[k]$ and $g_u[k]$ to solve the optimization, which it can estimate using the techniques from [52]. As it is easy for the relay to estimate channel of all the links, it executes the optimization and distributes the power variables.

2.4   Summary

This chapter starts with an OFDM-based ncTWR where a receive-only user RU experiences BI. The RU cancels the BI by overhearing the transmit-only user signal. We formulated non-convex SE and GEE optimization problem for the proposed system model. We finally explained the implementation issues and practical power consumption model.

Chapter 3

Optimization for OFDM non-concurrent two-way relaying

In this chapter, we will optimize the spectral efficiency (SE) and Global energy efficiecny (GEE) metrics for OFDM-based AF ncTWR. The non-convex SE maximization is approximated as a convex GP with the help of successive convex approximation (SCA) approach. We then employ quadratic transformation (QT) to maiximize the GEE, which have the relationship between non-concave SE and the consumed power. We first give a quick overview of the relevant ncTWR literature.

3.1 Literature overview on SE and GEE optimization of ncTWR

A high diversity precoder for ncTWR that suppresses the BI and enables the decoding of received data with a high diversity order is developed in [53]. In [36], the SE of a single-carrier ncTWR is optimized utilizing GP. To optimize the SE with single-carrier ncTWR and QoS restrictions, GP is utilized in [45]. Using semidefinite relaxation, Chunguo Li [39] proposed an overhearing precoder for single carrier ncTWR in order to maximize the SE. All of these studies [53, 36, 45, 39] have considered single-carrier systems, and avoided the use of OFDM in their system designs, despite the fact that OFDM is a major technology component of the current 4G and emerging 5G systems. Reference [43] used successive convex approximation method for approximating the non-convex SE maximization as a convex GP. In [54], a QT

Table 3.1: An overview of the literature on SE and GEE optimization of ncTWR.

ncTWR	Main contribution	Metric optimized	Approach
[53]	Quantized precoder, single carrier	None	Diversity enhancing precoder
[36]	Power allocation, single carrier	Sum-rate	Geometric programming with approximated objective
[45]	Power allocation, single carrier	Sum-rate+QoS	Geometric programming
[39]	Overhearing precoder, single carrier	Sum-rate	Semidefinte relaxation
[43] Current work	Power allocation, OFDM	Sum-rate	Geometric programming
[54] Current work	Power allocation, OFDM	GEE	Iterative quadratic transformation

method for maximizing the GEE is devised for a joint power allocation algorithm.

3.1.1   Contributions of this chapter

The following are the chapter's contributions:

- The SE is maximized by allocating power across the OFDM subbands jointly at the TU, BS and the relay nodes. We use SCA approach to approximate the non-convex SE maximization as a convex GP. The approximation is then successively improved by proposing an algorithm, which is numerically shown to converge within few iterations.

- We will show that the proposed algorithm has better SE than the other state-of-the-art optimizations.

- We propose a QT-based approach to optimize GEE which in its numerator and denominator contains the SE and the total power consumed by the network, respectively.

3.2   SE maximization using SCA

In this section, we will show that SE maximization can be solved using SCA, wherein each approximated problem is cast as a GP. The SE maximizationis re-stated as follows.

$$\mathbf{P1} : \underset{\mathbf{p}_r, \mathbf{p}_b, \mathbf{p}_u}{\text{Max}} \ R_{\text{sum}}(\mathbf{p}_r, \mathbf{p}_b, \mathbf{p}_u) \tag{3.1a}$$

$$\text{s.t.} \quad \sum_{k=1}^{K} p_r[k]|h_b[k]|^2 p_b[k] + p_r[k]|h_u[k]|^2 p_u[k] + p_r[k] \leq P_r \tag{3.1b}$$

$$\sum_{k=1}^{K} p_b[k] \leq P_b \tag{3.1c}$$

$$\sum_{k=1}^{K} p_u[k] \leq P_u. \tag{3.1d}$$

We know from [55] that a GP has a posynomial objective, and upper-bounded posynomials inequality constraints. We notice that the first inequality constraint in (3.1b) that $\sum_{k=1}^{K} p_r[k]|h_b[k]|^2 p_b[k] + p_r[k]|h_u[k]|^2 p_u[k] + p_r[k] \leq P_r$ is a posynomial in the variables $\mathbf{p}_r, \mathbf{p}_b$ and $\mathbf{p}_u$. This is because the coefficients of the variables $p_r[k], p_b[k]$ and $p_u[k]$ are non-negative. Also the posynomial is upper-bounded by $P_r \ \forall \ k = 1, \cdots, K$. Similarly, the constraints $\sum_{k=1}^{K} p_b[k] \leq P_b$ and $\sum_{k=1}^{K} p_u^k \leq P_u$ are posynomials in $\mathbf{p}_b$ and $\mathbf{p}_u$, and are upper-bounded by P_b and P_u, respectively. To optimize $\mathbf{P1}$ in (3.1), we now cast it in the epigraph form [55].

$$\mathbf{P2} : \underset{\mathbf{p}_r, \mathbf{p}_b, \mathbf{p}_u, \gamma_b, \gamma_u}{\text{Max}} \ \sum_{k=1}^{K} \frac{1}{2} \log_2\left(1 + \gamma_b[k]\right) + \frac{1}{2} \log_2\left(1 + \gamma_u[k]\right) \tag{3.2a}$$

$$\text{s.t.} \quad \gamma_b[k] \leq \frac{|h_u[k]g_b[k]|^2 p_r[k] p_u[k]}{1 + |g_b[k]|^2 p_r[k]} \tag{3.2b}$$

$$\gamma_u[k] \leq \frac{|g_u[k]h_b[k]|^2 p_r[k] p_b[k]}{1 + |g_u[k]|^2 p_r[k] + |\frac{g_u[k]h_u[k]}{h_o[k]}|^2 p_r[k]} \tag{3.2c}$$

$$\sum_{k=1}^{K} p_r[k]|h_b[k]|^2 p_b[k] + p_r[k]|h_u[k]|^2 p_u[k] + p_r[k] \leq P_r$$

$$\sum_{k=1}^{K} p_b[k] \leq P_b \quad \sum_{k=1}^{K} p_u[k] \leq P_u.$$

The problem **P2** can equivalently be expressed as

$$\mathbf{P3}: \min_{\mathbf{p}_r,\mathbf{p}_b,\mathbf{p}_u,\boldsymbol{\gamma}_b,\boldsymbol{\gamma}_u} \prod_{k=1}^{K} \Big[\left(1 + \gamma_b[k]\right)\left(1 + \gamma_u[k]\right) \Big]^{-1} \tag{3.3a}$$

$$\text{s.t.} \qquad \gamma_b[k] \leq \frac{|h_u[k]g_b[k]|^2 p_r[k]p_u[k]}{1 + |g_b[k]|^2 p_r[k]}$$

$$\gamma_u[k] \leq \frac{|g_u[k]h_b[k]|^2 p_r[k]p_b[k]}{1 + |g_u[k]|^2 p_r[k] + |\frac{g_u[k]h_u[k]}{h_o[k]}|^2 p_r[k]}$$

$$\sum_{k=1}^{K} p_r[k]|h_b[k]|^2 p_b[k] + p_r[k]|h_u[k]|^2 p_u[k] + p_r[k] \leq P_r$$

$$\sum_{k=1}^{K} p_b[k] \leq P_b \quad \sum_{k=1}^{K} p_u[k] \leq P_u.$$

We have dropped the constant $1/2$ and the monotonically increasing log term from the objective. We now re-cast the constraints (3.2b) and (3.2c) in problem **P3** as follows.

$$\mathbf{P4}: \min_{\mathbf{p}_r,\mathbf{p}_b,\mathbf{p}_u,\boldsymbol{\gamma}_b,\boldsymbol{\gamma}_u} \prod_{k=1}^{K} \Big[\left(1 + \gamma_b[k]\right)\left(1 + \gamma_u[k]\right) \Big]^{-1} \tag{3.4a}$$

$$\text{s.t.} \qquad \gamma_b[k]\Big(p_r[k]^{-1}p_u[k]^{-1} + |g_b[k]|^2 p_u[k]^{-1} \Big) \leq |h_u[k]g_b[k]|^2 \tag{3.4b}$$

$$\gamma_u[k]\Big(p_r[k]^{-1}p_b[k]^{-1} + |g_u[k]|^2 p_b[k]^{-1} + |\frac{g_u[k]h_u[k]}{h_o[k]}|^2 p_b[k]^{-1} \Big) \leq |g_u[k]h_b[k]|^2$$

$$\tag{3.4c}$$

$$\sum_{k=1}^{K} p_r[k]|h_b[k]|^2 p_b[k] + p_r[k]|h_u[k]|^2 p_u[k] + p_r[k] \leq P_r$$

$$\sum_{k=1}^{K} p_b[k] \leq P_b \quad \sum_{k=1}^{K} p_u[k] \leq P_u.$$

$$\tag{3.4d}$$

We observe that the upper-bounded constraints (3.4b), (3.4c) are posynomials in $\boldsymbol{\gamma}_b, \boldsymbol{\gamma}_u, \mathbf{p}_r, \mathbf{p}_b$ and $\mathbf{p}_u$ as the coefficients of $\gamma_b[k], \gamma_u[k], p_r[k], p_b[k]$ and $p_u[k]$ are non-negative. The objective function in **P4** is non-convex as is the inverse of product of two posynomials, and consequently not a posynomial [55]. We handle this non-convexity by approximating these two posynomials as monomials – product of two monomials is a monomial, and its inverse is a monomial [55]. This will enable us to use GP framework to solve the approximated problem. We utilize the following lemma from [56] to accomplish this goal.

Lemma 1 *The monomial approximation of* $1 + \gamma_b[k]$ *is* $c_1[k]\gamma_b[k]^{a_1[k]}$ *where* $a_1[k] = \left(\frac{\widehat{\gamma}_b[k]}{1+\widehat{\gamma}_b[k]}\right)$ *and* $c_1[k] = \widehat{\gamma}_b[k]^{-a_1[k]}(1 + \widehat{\gamma}_b[k])$. *Similarly the posynomial* $1 + \gamma_u[k]$ *is approximated as* $c_2[k]\gamma_u[k]^{a_2[k]}$ *where* $a_2[k] = \left(\frac{\widehat{\gamma}_u[k]}{1+\widehat{\gamma}_u[k]}\right)$ *and* $c_2[k] = \widehat{\gamma}_u[k]^{-a_2[k]}(1 + \widehat{\gamma}_u[k])$. *Here* $\widehat{\gamma}_b[k] > 0$ *and* $\widehat{\gamma}_u[k] > 0$ *are arbitrary points near* $(1 + \widehat{\gamma}_b[k])$ *and* $(1 + \widehat{\gamma}_u[k])$, *respectively.*

By using Lemma 1, the objective can be re-formulated as

$$\underset{\mathbf{p}_r,\mathbf{p}_b,\mathbf{p}_u,\boldsymbol{\gamma}_b,\boldsymbol{\gamma}_u}{\text{Min}} \qquad C \prod_{k=1}^{K} \left[\gamma_b[k]^{\left(\frac{\widehat{\gamma}_b[k]}{1+\widehat{\gamma}_b[k]}\right)} \gamma_u[k]^{\left(\frac{\widehat{\gamma}_u[k]}{1+\widehat{\gamma}_u[k]}\right)} \right]^{-1}, \qquad (3.5)$$

where $C = \prod_{k=1}^{K} \widehat{\gamma}_b[k]^{-a_1[k]}\widehat{\gamma}_u[k]^{-a_2[k]}$ is the net multiplicative constant. We see that the objective, after this approximation, is a monomial. We next iteratively improve the above approximation by proposing Algorithm 1 (on the next page).

Algorithm 1: Joint power allocation using GP

    Input: A maximum number of iterations L, and the tolerance $\epsilon > 0$.

    Output: Optimization variables $\mathbf{p}_r, \mathbf{p}_b$ and $\mathbf{p}_u$.

2 *Initialization*: Calculate initial values of $\widehat{\gamma}_b^1$ and $\widehat{\gamma}_u^1$ by allocating equal power across all K subbands.

4 for $m \leftarrow 1$ **to** L **do**

6   Given a feasible $\mathbf{p}_i, \forall i = r, b, u$ compute $\frac{\gamma_b^{\hat{m}}[k]}{1+\gamma_b^{\hat{m}}[k]}, \frac{\gamma_u^{\hat{m}}[k]}{1+\gamma_u^{\hat{m}}[k]} \forall k = 1, \cdots, K$.

8   Solve the GP to calculate $\mathbf{p}_r, \mathbf{p}_b, \mathbf{p}_u, \boldsymbol{\gamma}_b, \boldsymbol{\gamma}_u$

$$\underset{\mathbf{p}_r,\mathbf{p}_b,\mathbf{p}_u,\boldsymbol{\gamma}_b,\boldsymbol{\gamma}_u}{\text{Min}} \qquad C \prod_{k=1}^{K} \left[\gamma_b[k]^{\left(\frac{\widehat{\gamma}_b[k]}{1+\widehat{\gamma}_b[k]}\right)} \gamma_u[k]^{\left(\frac{\widehat{\gamma}_u[k]}{1+\widehat{\gamma}_u[k]}\right)} \right]^{-1}$$

$$\text{s.t.} \qquad \alpha_l^{-1}\hat{\boldsymbol{\gamma}}_l \leq \boldsymbol{\gamma}_l \leq \alpha_l\hat{\boldsymbol{\gamma}}_l, \text{ for } l \in \{b, u\}$$

$$(3.1\text{b}), (3.1\text{c}), (3.1\text{d}), (3.4\text{b}), (3.4\text{c}). \qquad (3.6)$$

10   Do until convergence

        if $\max |\boldsymbol{\gamma}_b - \widehat{\boldsymbol{\gamma}}_b^m| \leq \epsilon$ *and* $\max |\boldsymbol{\gamma}_u - \widehat{\boldsymbol{\gamma}}_u^m| \leq \epsilon$ **then**

11   break

12   **else** $\widehat{\boldsymbol{\gamma}}_b^{m+1} = \boldsymbol{\gamma}_b$ *and* $\widehat{\boldsymbol{\gamma}}_u^{m+1} = \boldsymbol{\gamma}_u$

14 return $\mathbf{p}_r, \mathbf{p}_b$ *and* $\mathbf{p}_u$.

The initial values of $\widehat{\boldsymbol{\gamma}}_b$ and $\widehat{\boldsymbol{\gamma}}_u$ in step-3 of the algorithm are derived using equal power allocation, and the values of $\left(\frac{\widehat{\gamma}_b}{1+\widehat{\gamma}_b}\right)$, $\left(\frac{\widehat{\gamma}_u}{1+\widehat{\gamma}_u}\right)$ are calculated accordingly. The fourth step solves an approximated GP around the current guesses $\widehat{\boldsymbol{\gamma}}_b$, and $\widehat{\boldsymbol{\gamma}}_u$. The inequality constraints in (3.6), known as trust region constraints, are added to confine the domain of variables γ_b and γ_u around the current guess $\widehat{\gamma}_b^m$ and $\widehat{\gamma}_u^m$, respectively. The parameters α_b and α_u control the desired approximation accuracy and the convergence speed.

This algorithm approximates the posynomial with a monomial and, is therefore, not optimal. But this heuristic approach, as shown in [57, 58], yields a globally optimal solution 96% of the time, and only marginally degrades the SE by 2%.

3.3 GEE maximization using quadratic transform

The GEE optimization problem can be formulated as follows.

$$\textbf{P5}: \underset{\mathbf{p}_r,\mathbf{p}_b,\mathbf{p}_u}{\text{Max}} \frac{R_{\text{sum}}}{\sum_{k=1}^{K} \frac{1}{\xi}(p_r[k] + p_b[k] + p_u[k]) + P_c} \tag{3.7a}$$

$$\text{s.t.} \quad \sum_{k=1}^{K} p_r[k]|h_b[k]|^2 p_b[k] + p_r[k]|h_u[k]|^2 p_u[k] + p_r[k] \leq P_r, \tag{3.7b}$$

$$\sum_{k=1}^{K} p_b[k] \leq P_b \quad \sum_{k=1}^{K} p_u[k] \leq P_u. \tag{3.7c}$$

The three constraints are, respectively, on the relay's maximum transmit power, TU, and BS. The GEE optimization is a fractional function of the non-concave SE and the power consumption, and the SCA technique, developed for SE cannot be directly applied to optimize it. We will apply recently developed QT method to optimize it [44]. To accomplish this objective, we use the following proposition from [44] which will decouple its numerator and denominator in the GEE objective.

3.3.1 GEE optimization using quadratic transformation

Proposition 1 *Consider a function of ratio problem*

$$\underset{x}{Max} f\left(\frac{u(x)}{v(x)}\right) \quad subject \ to \ x \in \chi, \tag{3.8}$$

where $f_k(\cdot)$ is a non-negative function, and χ is a convex set. The numerator and denominator functions are defined as: $u(x) : \mathbb{R}^n \to \mathbb{R}^+$ and $v(x) : \mathbb{R}^n \to \mathbb{R}^{++}$. The aforementioned problem in (3.8) can be equivalently expressed using QT as

$$\underset{x,y}{Max} f\left(2\sqrt{u(x)}y - y^2 v(x)\right) subject\ to\ x \in \chi, y \in \mathbb{R}. \tag{3.9}$$

The functions $u(x)$ and $v(x)$ must be non-negative and positive, respectively, according to Proposition 1. Next, we assert a different result from [44], that is predicated on a particular structure for the functions $u(x)$ and $v(x)$. This proposition, as shown next, will allow us to calculate a stationary (x, y) of (3.9) by iteratively solving a concave problem and a closed-form equation.

Proposition 2 *For the function of ratio problem in* (3.8), *considering that the function f is concave and non-decreasing, if each $u(x)$ is concave and $v(x)$ is convex in concave-convex ratio form of $\frac{u(x)}{v(x)}$, the problem* (3.9) *is a concave problem in x for a given y, and the optimal value of y can be obtained in a closed form as $y^* = \frac{\sqrt{u(x)}}{v(x)}$ for a given x. By iteratively optimizing x and y, the problem* (3.9) *converges to a stationary point of* (3.8) *with a non decreasing objective value after every iteration.*

We now use the QT in Proposition 1 to solve **P5**. Even after using QT, the GEE optimization is challenging due to the non-concave terms. To account for that, we will apply the first-order Taylor series result to linearly approximate these non-concave terms. Using Proposition 1, we now rewrite **P5** using QT as

$$\mathbf{P6}: \underset{\mathbf{p}_r,\mathbf{p}_b,\mathbf{p}_u,\mathbf{y}}{Max} 2y\sqrt{R_{sum}} - y^2\sum_{k=1}^{K}\frac{1}{\xi}(p_r[k]+p_b[k]+p_u[k])+P_c$$

$$\text{s.t.} \quad \sum_{k=1}^{K} p_r[k]|h_b[k]|^2 p_b[k] + p_r[k]|h_u[k]|^2 p_u[k] + p_r[k] \le P_r,$$

$$\sum_{k=1}^{K} p_b[k] \le P_b \quad \sum_{k=1}^{K} p_u[k] \le P_u.$$

Here, y is an auxiliary variable which decouples the numerator and denominator of GEE. We observe from objective in **P6**, the term R_{sum} contains two fractional terms in the form of

$\text{SNR}_b[k]$ and $\text{SNR}_u[k]$. Hence using the proposition 1 twice, we rewrite the **P6** as

$$
\begin{aligned}
\textbf{P7}: \underset{\mathbf{p}_r,\mathbf{p}_b,\mathbf{p}_u,y,\mathbf{w},\mathbf{z}}{\text{Max}} 2y\Big(& \sum_{k=1}^{K}\frac{1}{2}\log_2(1+2w_k\sqrt{C_k}-w_k^2 D_k) \\
& + \sum_{k=1}^{K}\frac{1}{2}\log_2(1+2z_k\sqrt{E_k}-z_k^2 F_k)\Big)^{\frac{1}{2}} \\
& - y^2\sum_{k=1}^{K}\frac{1}{\xi}(p_r[k]+p_b[k]+p_u[k])+P_c
\end{aligned}
\tag{3.11a}
$$

$$
\text{s.t.} \quad \sum_{k=1}^{K}p_r[k]|h_b[k]|^2 p_b[k] + p_r[k]|h_u[k]|^2 p_u[k] + p_r[k] \le P_r,
$$

$$
\sum_{k=1}^{K}p_b[k] \le P_b \quad \sum_{k=1}^{K}p_u[k] \le P_u, y \in \mathbb{R}, \mathbf{w} \in \mathbb{R}^K \quad \text{and} \quad \mathbf{z} \in \mathbb{R}^K.
$$

Here $\mathbf{w}=[w_1,\cdots,w_K]$ and $\mathbf{z}=[z_1,\cdots,z_K]$, where each w_k and z_k decouples the numerator and denominator of each $R_b[k]$ and $R_u[k]$ respectively. For notational convenience, we use C_k, D_k and E_k, F_k for $k=1,\cdots,K$ to denote the numerator and denominator of $\text{SNR}_b[k]$ and $\text{SNR}_u[k]$ in (2.12), respectively. In summary, we use QT twice in Proposition 1 to change **P5** to **P6**. From Proposition 2, **P7** is a concave maximization problem if C_k, E_k and D_k, F_k are concave and convex functions respectively.

We see that the terms C_k and E_k are non-concave in optimization variables $p_r[k]$, $p_u[k]$ and $p_b[k]$. Further the constraint (3.7c) is convex but the LHS of (3.7b) is non-convex. We use first-order Taylor series approximation to linearize $p_r[k]p_b[k]$ and $p_r[k]p_u[k]$ as affine function in $p_r[k],p_b[k],p_u[k]$, which will help us convexify the objective and the constraint, utilizing the following lemma, the proof of which is relegated to Appendix A.

Lemma 2 *The non-convex terms $p_r[k]p_b[k]$ and $p_r[k]p_u[k]$ can be linearly approximated as $p_r[k]p_b[k]=\tilde{p}_r[k]\tilde{p}_b[k]+\tilde{p}_b[k](p_r[k]-\tilde{p}_r[k])+\tilde{p}_r[k](p_b[k]-\tilde{p}_b[k])$ and $p_r[k]p_u[k]=\tilde{p}_r[k]\tilde{p}_u[k]+\tilde{p}_u[k](p_r[k]-\tilde{p}_r[k])+\tilde{p}_r[k](p_u[k]-\tilde{p}_u[k])$ where $\tilde{p}_r[k]$, $\tilde{p}_b[k]$ and $\tilde{p}_u[k]$ are initial values of $p_r[k]$, $p_b[k]$ and $p_u[k]$, respectively.*

Proof. Refer to Appendix B.2.

To convexify the objective, we now use Lemma 2 for affine approximation of C_k and E_k in (3.11a).

$$
\widehat{C}_k = |h_u[k]g_b[k]|^2\Big(\tilde{p}_r[k]\tilde{p}_u[k]+\tilde{p}_u[k](p_r[k]-\tilde{p}_r[k])+\tilde{p}_r[k](p_u[k]-\tilde{p}_u[k])\Big)
\tag{3.12}
$$

$$\widehat{E}_k = |g_u[k]h_b[k]|^2 \Big(\tilde{p}_r[k]\tilde{p}_b[k] + \tilde{p}_b[k](p_r[k] - \tilde{p}_r[k]) + \tilde{p}_r[k](p_b[k] - \tilde{p}_b[k]) \Big). \tag{3.13}$$

Hence both $\widehat{C}_k$ and $\widehat{E}_k$ are concave (affine) and D_k and F_k are convex which makes the objective in **P3** to concave. The constraint (3.7b) is now modified using the Lemma 1 as

$$\sum_{k=1}^{K} |h_b[k]|^2 \Big(\tilde{p}_r[k]\tilde{p}_b[k] + \tilde{p}_b[k](p_r[k] - \tilde{p}_r[k]) + \tilde{p}_r[k](p_b[k] - \tilde{p}_b[k]) \Big)$$
$$+ |h_u[k]|^2 \Big(\tilde{p}_r[k]\tilde{p}_u[k] + \tilde{p}_u[k](p_r[k] - \tilde{p}_r[k])$$
$$+ \tilde{p}_r[k](p_u[k] - \tilde{p}_u[k]) \Big) + p_r[k] \leq P_r. \tag{3.14}$$

The left side of the above constraint in (3.14) is now affine. Using (3.12), (3.13) and (3.14), we rewrite **P7** as **P8**.

$$\textbf{P8}: \underset{\mathbf{p}_r,\mathbf{p}_b,\mathbf{p}_u,y,\mathbf{w},\mathbf{z}}{\text{Max}} 2y\Big(\sum_{k=1}^{K} \frac{1}{2}\log_2(1 + 2w_k\sqrt{\widehat{C}_k} - w_k^2 D_k)$$
$$+ \sum_{k=1}^{K} \frac{1}{2}\log_2(1 + 2z_k\sqrt{\widehat{E}_k} - z_k^2 F_k)\Big)^{\frac{1}{2}}$$
$$- y^2 \sum_{k=1}^{K} \frac{1}{\xi}(p_r[k] + p_b[k] + p_u[k]) + P_c \tag{3.15a}$$

$$\text{s.t.} \qquad (3.14),(3.7c), y \in \mathbb{R}, \mathbf{w} \in \mathbb{R}^K \quad \text{and} \quad \mathbf{z} \in \mathbb{R}^K.$$

The problem **P4** is now concave in $\mathbf{p}_r, \mathbf{p}_b, \mathbf{p}_u$ for a given y, $\mathbf{w}$ and $\mathbf{z}$. After calculating $\mathbf{p}_r, \mathbf{p}_b, \mathbf{p}_u$, using Proposition 2, we determine the optimal values for auxiliary variables y, $\mathbf{w}$ and $\mathbf{z}$ as

$$y = \frac{\sqrt{R_{sum}}}{\sum_{k=1}^{K} \frac{1}{\xi}(p_r[k] + p_b[k] + p_u[k]) + P_c} \tag{3.16a}$$

$$w_k = \frac{\sqrt{|h_u[k]g_b[k]|^2 p_r[k]p_u[k]}}{1 + |g_b[k]|^2 p_r[k]} \tag{3.16b}$$

$$z_k = \frac{\sqrt{|g_u[k]h_b[k]|^2 p_r[k]p_b[k]}}{1 + |g_u[k]|^2 p_r[k] + |\frac{g_u[k]h_u[k]}{h_o[k]}|^2 p_r[k]}. \tag{3.16c}$$

Here $\mathbf{w} = [w_1, \cdots, w_K]$ and $\mathbf{z} = [z_1, \cdots, z_K]$. We iteratively calculate $\mathbf{p}_r, \mathbf{p}_b, \mathbf{p}_u$ by first solving **P3** for a given y, $\mathbf{w}$ and $\mathbf{z}$ and then calculate y, $\mathbf{w}$ and $\mathbf{z}$ from (3.16a), (3.16b), (3.16c), respectively. The process is summarized in Algorithm 2 below on the next page.

Algorithm 2: GEE optimization using quadratic programming

Input: Tolerance $\epsilon > 0$, and the maximum iterations L.

Output: Optimal power allocation variables $\mathbf{p}_r, \mathbf{p}_b$ and $\mathbf{p}_u$.

2 *Initialization*: Allocate equal power across all K subbands to calculate initial feasible values of $\mathbf{p}_r, \mathbf{p}_b$ and $\mathbf{p}_u$, denoted as, $\mathbf{p}_r^1, \mathbf{p}_b^1$ and $\mathbf{p}_u^1$, respectively.

4 for $m \leftarrow 1$ **to** L **do**

6 $\quad$ Given a feasible $\mathbf{p}_i^m, \forall i = r, b, u$ compute y, $\mathbf{w}$ and $\mathbf{z}$ $\forall k = 1, \cdots, K$ from (3.16a), (3.16b) and (3.16c).

8 $\quad$ Solve the following problem to calculate $\mathbf{p}_r, \mathbf{p}_b, \mathbf{p}_u$

$$
\begin{aligned}
\underset{\mathbf{p}_r, \mathbf{p}_b, \mathbf{p}_u}{\text{Max}} \; 2y \Big(&\sum_{k=1}^{K} \frac{1}{2} \log_2(1 + 2w_k\sqrt{\widehat{C}_k} - w_k^2 D_k) \\
&+ \sum_{k=1}^{K} \frac{1}{2} \log_2(1 + 2z_k\sqrt{\widehat{E}_k} - z_k^2 F_k) \Big)^{\frac{1}{2}} \\
&- y^2 \sum_{k=1}^{K} \frac{1}{\xi}(p_r[k] + p_b[k] + p_u[k]) + P_c \qquad\qquad (3.17a)
\end{aligned}
$$

$$
\text{s.t.} \quad (3.14), (3.7c), y \in \mathbb{R}, \mathbf{w} \in \mathbb{R}^K \quad \text{and} \quad \mathbf{z} \in \mathbb{R}^K.
$$

10 $\quad$ Do until convergence

$\qquad$ **if** $\max |\mathbf{p}_r - \mathbf{p}_r^m| \le \epsilon$ *and* $\max |\mathbf{p}_b - \mathbf{p}_b^m| \le \epsilon$ *and* $\max |\mathbf{p}_u - \mathbf{p}_u^m| \le \epsilon$ **then**

11 $\quad$ break

12 $\quad$ **else** $\mathbf{p}_r^{m+1} = \mathbf{p}_r$, $\mathbf{p}_b^{m+1} = \mathbf{p}_b$ and $\mathbf{p}_u^{m+1} = \mathbf{p}_u$

14 return $\mathbf{p}_r, \mathbf{p}_b$ *and* $\mathbf{p}_u$.

3.3.2 Convergence analysis

The auxiliary variables y, $\mathbf{w}$, $\mathbf{z}$ are determined by (3.16a), (3.16b) and (3.16c) respectively, using $\mathbf{p}_r^m$, $\mathbf{p}_b^m$ and $\mathbf{p}_u^m$. The objective in **P1**, **P3** and **P4** are written as $f_o(\mathbf{p}_r^m, \mathbf{p}_b^m, \mathbf{p}_u^m)$, $f_q(\mathbf{p}_r^m, \mathbf{p}_b^m, \mathbf{p}_u^m, y, \mathbf{w}, \mathbf{z})$ and $\tilde{f}_q(\mathbf{p}_r^m, \mathbf{p}_b^m, \mathbf{p}_u^m, y, \mathbf{w}, \mathbf{z})$ respectively at the m-th iteration. First, we state a useful lemma, which can be easily verified.

Lemma 3 $f_o(\mathbf{p}_r, \mathbf{p}_b, \mathbf{p}_u) \geq f_q(\mathbf{p}_r, \mathbf{p}_b, \mathbf{p}_u, y, \boldsymbol{w}, \boldsymbol{z})$, *with equality iff* $y, \boldsymbol{w}, \boldsymbol{z}$ *satisfy* (3.16a), (3.16b) *and* (3.16c) *respectively.*

$$
\begin{aligned}
f_o(\mathbf{p}_r^{m+1}, \mathbf{p}_b^{m+1}, \mathbf{p}_u^{m+1}) \; &\overset{(a)}{=} \; f_q(\mathbf{p}_r^{m+1}, \mathbf{p}_b^{m+1}, \mathbf{p}_u^{m+1}, y^{m+1}, \mathbf{w}^{m+1}, \mathbf{z}^{m+1} | \mathbf{p}_r^m, \mathbf{p}_b^m, \mathbf{p}_u^m) \\
&\overset{(b)}{\geq} \; \tilde{f}_q(\mathbf{p}_r^{m+1}, \mathbf{p}_b^{m+1}, \mathbf{p}_u^{m+1}, y^{m+1}, \mathbf{w}^{m+1}, \mathbf{z}^{m+1} | \mathbf{p}_r^m, \mathbf{p}_b^m, \mathbf{p}_u^m) \\
&\overset{(c)}{\geq} \; \tilde{f}_q(\mathbf{p}_r^{m+1}, \mathbf{p}_b^{m+1}, \mathbf{p}_u^{m+1}, y^m, \mathbf{w}^m, \mathbf{z}^m | \mathbf{p}_r^m, \mathbf{p}_b^m, \mathbf{p}_u^m) \\
&\overset{(d)}{\geq} \; \tilde{f}_q(\mathbf{p}_r^m, \mathbf{p}_b^m, \mathbf{p}_u^m, y^m, \mathbf{w}^m, \mathbf{z}^m | \mathbf{p}_r^m, \mathbf{p}_b^m, \mathbf{p}_u^m) \\
&\overset{(e)}{=} \; f_q(\mathbf{p}_r^m, \mathbf{p}_b^m, \mathbf{p}_u^m, y^m, \mathbf{w}^m, \mathbf{z}^m | \mathbf{p}_r^m, \mathbf{p}_b^m, \mathbf{p}_u^m) \\
&\overset{(f)}{=} \; f_o(\mathbf{p}_r^m, \mathbf{p}_b^m, \mathbf{p}_u^m).
\end{aligned}
$$

In the above equations, the notation $f(\ldots | \mathbf{p}_r^m, \mathbf{p}_b^m, \mathbf{p}_u^m)$ imply "for a given value of $\mathbf{p}_r^m, \mathbf{p}_b^m, \mathbf{p}_u^m$". Equality in (a) is due to Lemma 2. Inequality (b) is due to fact that Taylor series approximation of the first order allows a convex function to be lower bounded [59]. Inequality (c) is because the updates of auxiliary variables y, $\mathbf{w}$, $\mathbf{z}$ in (3.16a), (3.16b) and (3.16c) respectively, maximize $\tilde{f}_q$, with other variables being fixed. Ineqaulity (d) is because the updates of $\mathbf{p}_r$, $\mathbf{p}_b$, $\mathbf{p}_u$ maximize $\tilde{f}_q$, with other variables being fixed. Equality in (e) is because Taylor-series-approximated $\tilde{f}_q$ and f_q are equal at $\mathbf{p}_r^m, \mathbf{p}_b^m, \mathbf{p}_u^m$ [59]. Equality in (f) is because of Lemma 2. The objective f_o is monotonically nondecreasing after each iteration. As the value of f_o is bounded from above, the algorithm must converge to a local optimum.

3.4 Simulation results

We will now compare numerical performance of the proposed joint power allocation algorithm using GP (denoted as JPAGP) for an OFDM asymmetric AF TWRN with K subbands. We

contrast the efficacy of the proposed algorithm with i) conventional equal-power allocation (EPA)[60]; ii) random power allocation (RPA)[60]; and iii) 4-channel-use (denoted as 4CU or OWR) one-way relaying protocol [41] where the BS serves TU and RU in two channel uses each. We also perform a numerical analysis of the GEE obtained using the proposed QT-base algorithm (denoted as QTPA) for an OFDM AF ncTWR with K subbands. We compare the performance of the QTPA algorithm with above mentioned methods along with the scheme where overhearing link is ignored (labelled as QTWOL); and geometric programming-based SE maximization algorithm in [43] (labelled as GPSRM). The GPSRM scheme maximizes the SE using geometric programming and uses the optimal power so obtained for calculating GEE. The QTWOL scheme uses the proposed algorithm to maximize GEE but ignores the overhearing link. The conventional OWR also uses the proposed algorithm to maximize the GEE but the BS now requires four time slots to serve TU and RU - two to receive data from TU and two to send data to RU. The RPA scheme randomly allocates power across the subbands at the TU, relay and BS nodes to satisfy their individual power constraints. We assume that, similar to [35, 36], the channels between the different links are distributed as $\mathcal{CN}(0, \eta_i)$ where $i = b$ for BS↔Relay link, $i = u$ for Relay ↔ RU link and $i = o$ for TU → RU overhearing link. The channel variance η_i for $\{i \in u, b, o\}$ denote the channel gains of the respective links. For notational convenience in simulations, we set $P_r = P_b = P_u = \eta$.

3.4.1   Comaprison of SE with the existing state-of-the-art designs

We plot in Fig. 3.1 the SE by varying η_u. For this study, we fix the noise power as unity, and fix $\eta_b = 10$ dB and $\eta_o = 5$ dB with respect to the noise power. We also assume $P_u = 5$ dB, $P_r = 10$ dB, and $P_b = 10$ dB with respect to the noise power. We choose, similar to [56], $\alpha_b = \alpha_u = 3$. We also fix $\epsilon = 10^{-2}$ and $K = 16$ subbands. We see from the Fig. 3.1 that the proposed algorithm outperforms both sub-optimal EPA and RPA schemes. Further the 4-channel-use one-way relaying, due to four channel uses, has inferior SE than both other schemes.
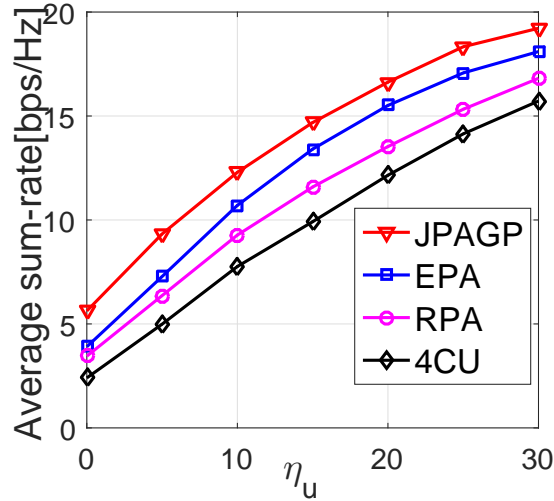
Figure 3.1: Average SE vs η_u for $\eta_b = 10$ dB, $\eta_o = 5$ dB and $K = 16$;

3.4.2 Convergence of JPAGP

We explore in Fig. 3.2 the proposed algorithm convergence behavior by plotting the SE achieved by the algorithm in each iteration. For this study, we consider the same parameters as in Fig. 3.1. Within 8 GP iterations, we see that the algorithm converges for various η_u values.

3.4.3 Comparison of SE by varying number of subbands

We compare in Fig. 3.3 and Fig. 3.4 the proposed algorithm by varying the number of subbands K. In Fig. 3.3, we fix $\eta_u = \eta_b = 10$ dB and $\eta_o = 5$ dB for all K values, whereas in Fig. 3.4 we fix $\eta_u = \eta_b = \eta_o \triangleq \eta = 2$ dB for $K = 5$ subbands, and then we double η with every $K = 5$ subband increment. We observe that the proposed algorithm outperforms both EPA and RPA algorithms for different values of subbands. In Fig. 3.3, for $K = 40$ subbands, it yields 6 bps/Hz and 3.5 bps/Hz higher average SE than the RPA and the EPA, respectively. For larger K values, the proposed algorithm has higher flexibility to optimize the power budget, which increases the SE difference when compared with smaller K values. In Fig. 3.4, for $K = 25$ subbands, the proposed algorithm yields 8.5 bps/Hz and 13.1 bps/Hz higher average SE than the EPA and the RPA, respectively. For $K = 40$, the gap between
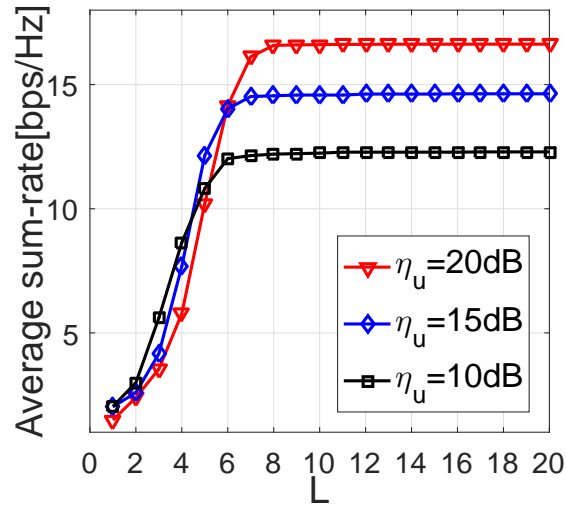
Figure 3.2: Sum-rate vs L for $\eta_b = 10$ dB and $\eta_o = 5$ dB
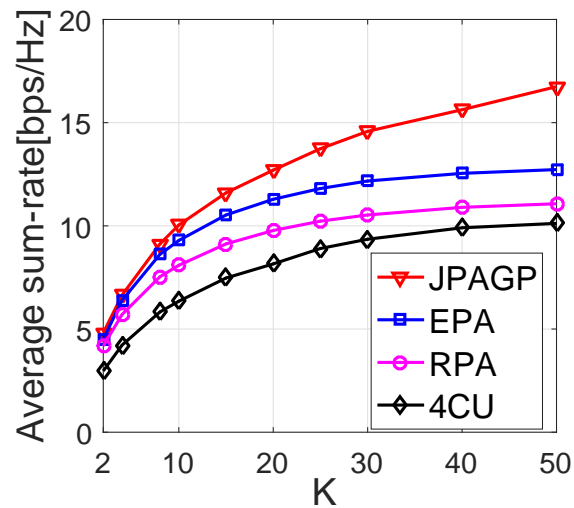
Figure 3.3: Average SE versus K for fixed η_b, η_u and η_o;
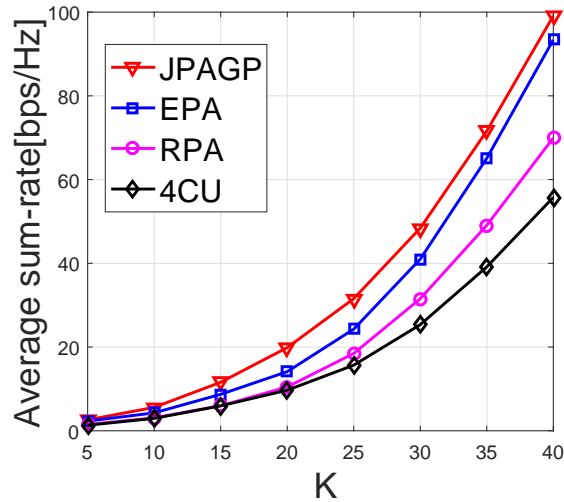
Figure 3.4: Varying the number of subbands K with variable η_b, η_u and η_o.

the proposed and the EPA is reduced as the system now is operating in the high-SNR regime, where equal power itself is close to optimal.

In Fig. 3.4, the sum-rate increases at a linear rate with increasing number of sub-bands until K=20. The sum-rate in Fig 3.4 not only depends on sub-bands but we also vary η_b, η_u and η_o. In Fig. 3.4 we fix $\eta_u = \eta_b = \eta_o \overset{\triangle}{=} \eta = 2$ dB for $K = 5$ subbands, and then we double η with every $K = 5$ subband increment. This is the reason for sum-rate increase at a rate more than linear with increasing number of sub-bands.

3.4.4   GEE comparision with existing methods

We first investigate in Fig. 3.5 the GEE obtained by varying η, which is the maximum power available at the TU, relay and the BS. We also fix the noise power, and assume it to be unity. We also fix $\eta_u = 10$ dB, $\eta_b = 10$ dB, and $\eta_o = 5$ dB with respect to the noise power. Also, $P_s^b = 40$ mW, $P_s^t = 5 - 30$ mW, $P_s^r = 5 - 30$ mW per subband and $P_f^u = 50$ mW and $P_f^b = 2000$ mW. We also fix tolerance $\epsilon = 10^{-3}$, $L = 30$ in Algorithm 1 and $K = 16$ subbands. We observe from Fig. 3.5 that the proposed QTPA algorithm outperforms all the aforementioned state-of-the-art techniques. We also observe that with the proposed algorithm, the GEE increases till $\eta = 5$ dB, and after which it remains constant.

This is because power of $\eta = 5$ dB allows the system to achieve the maximum GEE, and any additional power used by the system will only decrease the GEE for EPA, RPA and GPSRM schemes as the system continues utilising the available power for $\eta > 5$ dB.
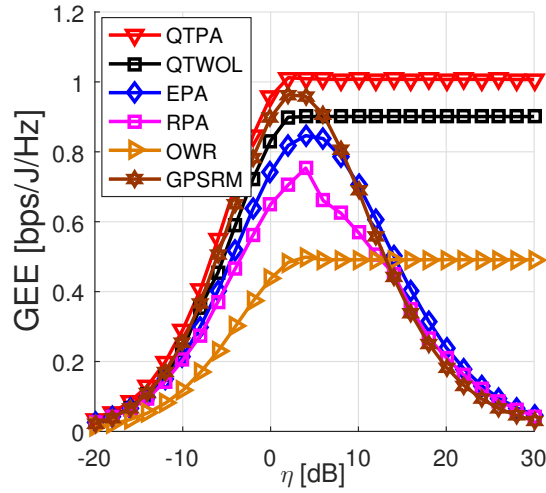
Figure 3.5: GEE vs η for $\eta_b = 10$ dB,$\eta_u = 10$ dB, $\eta_o = 5$ dB and $K = 16$;

3.4.5   GEE versus number of iterations
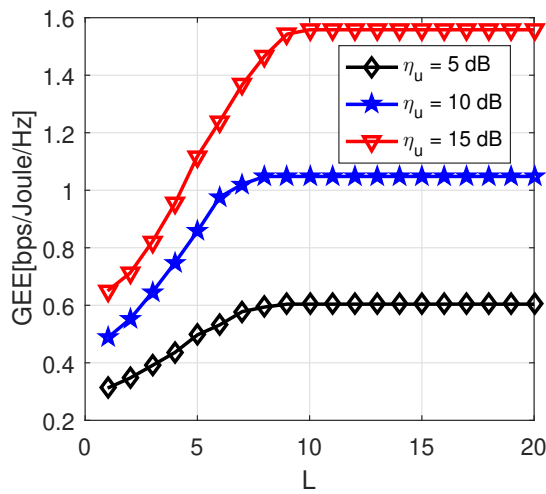
Figure 3.6: GEE versus L for $\eta_b = 10$ dB, $\eta_o = 5$ dB, $\eta = 10$ dB and $K = 16$;

We see from Fig. 3.6, where GEE versus number of iterations is plotted, that the algorithm converges in a few iterations. This also shows that the QT-based algorithm does not increase complexity.

3.4.6 GEE comparison with number of subbands

We next vary the number of subbands K in Fig. 3.7 and Fig. 3.8, and plot the GEE achieved. In Fig. 3.7, we fix $\eta_u = \eta_b = \eta = 10$ dB and $\eta_o = 5$ dB for all K values, whereas in Fig. 3.8 we start by considering $\eta = 2$ dB for $K = 1$ subband and then double it with each $K = 20$ subband increment. We observe that the proposed QTPA algorithm, for different subband values, yields higher GEE than other techniques. In Fig. 3.7, for $K = 70$ subbands, it yields
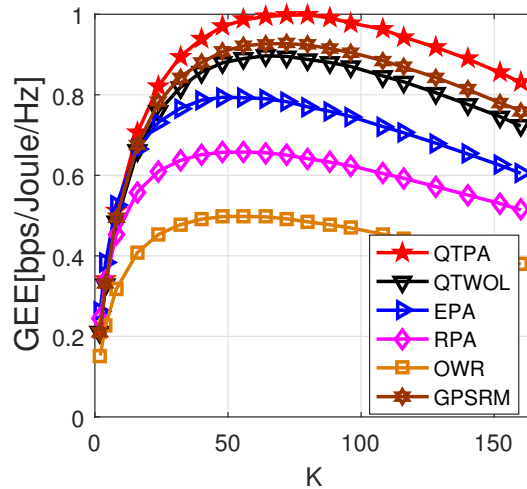
Figure 3.7: GEE versus K for fixed η, η_b, η_u and η_o;

9%, 16%, 22%, and 35% bits/Joule/Hz better GEE than the GPSRM, the QTWOL, the EPA and the RPA, respectively. In Fig. 3.8, for $K = 90$ subbands, the QTPA algorithm yields 9%, 15%, 21%, and 24% bits/Joule/Hz higher GEE than the GPSRM, the QTWOL, the EPA and the RPA, respectively. In Fig. 3.7 and Fig. 3.8, the GEE decreases with increase in subbands K as the circuit power depends on the number of subbands. The GEE decreases after a certain K value as the total power consumed by the system now dominates the increase in SE. In Fig. 3.8, after $K = 40$ subband, the increase in η helped to allocate more and
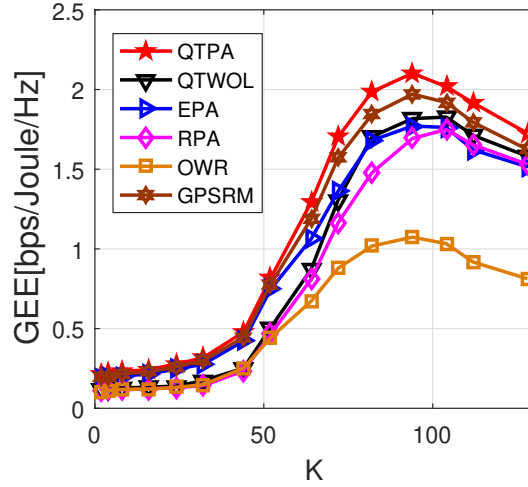
Figure 3.8: GEE versus K

more power during optimization, and hence the rapid increase. However, after a certain point around $K = 90$, the GEE reduces, as the total power consumed by the system, now dominates the increase in SE.

3.4.7   SE versus GEE comparison

We next plot in Fig. 3.9 the system SE-GEE relationship for different η values. We see that for a fixed η, increasing the number of sub-bands K, increases both SE and GEE. Further, for a given K value, increasing η value, reduces both GEE and SE.

3.5   Summary

In this chapter, we first developed a joint power allocation algorithm which solves the non-convex SE optimization using SCA approach. We showed that the proposed algorithm yields better average SE than the baseline equal and random power allocation schemes. Later, we used QT to develop a joint power allocation algorithm to maximize the GEE metric. We showed that the proposed algorithm not only uses lesser than the maximum available power but also achieves as high as 35% average GEE over other state-of-the-art algorithms. We also showed that with the increase in the number of subbands, the ncTWR GEE decreases
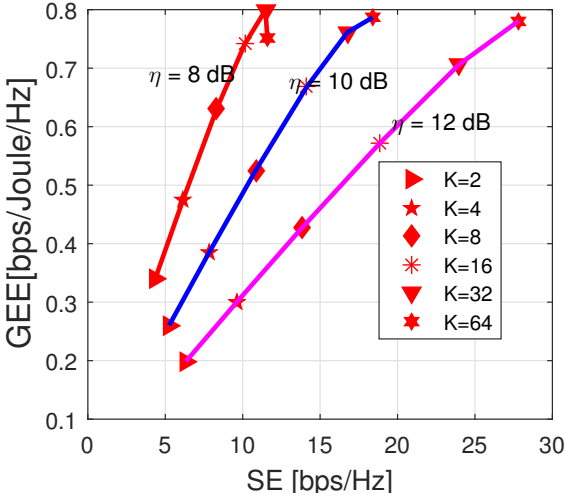
Figure 3.9: GEE vs SE for $\eta_b = 10$ dB,$\eta_u = 10$ dB, $\eta_o = 5$ dB

as the circuit power depends on number of subbands.

Chapter 4

Transceiver Design for MIMO AF ncTWR Relaying

We now extend the ncTWR system model to include MIMO nodes. We will not consider the overhearing protocol to cancel BI here as it becomes extremely difficult for the MIMO users to collect the relevant channel state information. We will also use generalised singular value decomposition (GSVD) to design a transceiver for AF MIMO ncTWR . We will now also include the direct links between BS, RU and TU to further increase the SE. We first discuss the literature survey for MIMO ncTWR.

For the multi-user ncTWR scenario, reference [48] constructed a precoder at the relay and allocated power only at the relay. This design did not epxloit tje the additional precoding gains at the BS and TU. Also, [45] designed a joint transceiver with quality of service constraints and jointly optimized the source and relay precoders unlike the[48]. In [36], a common transceiver is designed with relaxed antenna constraints to work for conventional TWR and ncTWR with reduced complexity. In [61], overhearing-based BI-cancellation approach for OFDM based ncTWR is studied. However, [53, 36, 62, 48, 35, 45, 63, 61] did not consider direct link between the BS and users. The studies mentioned above are summarized in Table. 4.1.

Table 4.1: Summary of MIMO ncTWR focussing on SE and GEE

ncTWR	Summary	Direct link	Precoder using GSVD	Joint power allocation	GEE
[48]	Multi user ncTWR, sum-rate	✗	✗	✗	✗
[35]	Transceiver design of MIMO ncTWR to reduce BER	✗	✗	✗	✗
[36]	Common transceiver design, relaxed antenna constraints	✗	✗	✓	✗
[45]	Transceiver design with quality-of-service (QoS) constraints	✗	✗	✓	✗
[63]	Precoders using zero-forcing and minimum-mean-square-error criteria	✗	✗	✗	✗
[61]	OFDM system, overhearing-based interference cancellation	✗	✗	✓	✗
current work	Direct link ncTWR, Source precoder using GSVD, joint design of Relay precoder and source combiner, Optimized SE power allocation	✓	✓	✓	✓

4.1   System Model

We consider, as shown in Fig. 4.1, the MIMO AF ncTWR system, where the BS communicates with the two users i.e., TU and RU through a HD relay. Each of the BS and two UEs are equipped with M antennas, while the relay is equipped with $N \geq 2M$ antennas. This antenna restriction is required to cancel the BI [35, 64]. We consider a scenario where relays are used to increase the capacity. In such systems, the BS not only exploits the indirect link through relay, but also the direct link. Both TU and BS transmit to relay during MAC phase of ncTWR. The RU and BS also receive direct link signal from BS and TU, respectively. The relay amplifies the sum-signal obtained during initial channel usage and transmits it to the RU and BS during the BC phase of ncTWR.
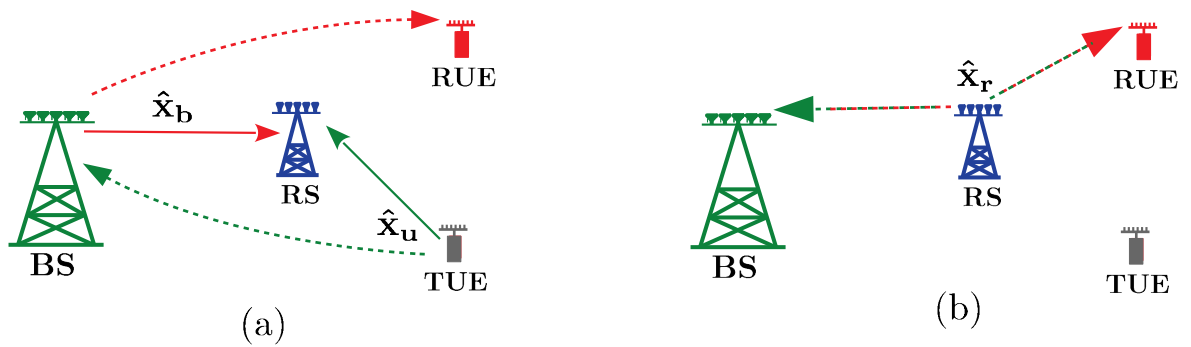
Figure 4.1: Illustration of MIMO ncTWR

The MAC-phase sum-signal received by the relay is $\mathbf{y}_r \in \mathbb{C}^{N \times 1}$, which is given as

$$\mathbf{y}_r = \mathbf{H}_b \widehat{\mathbf{x}}_b + \mathbf{H}_u \widehat{\mathbf{x}}_u + \mathbf{n}_r = \mathbf{H}\widehat{\mathbf{x}} + \mathbf{n}_r. \tag{4.1}$$

Here the matrix $\mathbf{H}_i \in \mathbb{C}^{N\text{x}M}$ for $i = b, u,$[1] are the MAC phase channels for the BS $\to$ relay and the TU $\to$ relay links, and $\mathbf{H} = [\mathbf{H}_b \; \mathbf{H}_u]$ is the MAC-phase composite channel matrix and the vector $\widehat{\mathbf{x}} = [\widehat{\mathbf{x}}_b; \widehat{\mathbf{x}}_u]$. The vector $\mathbf{n}_r \in \mathbb{C}^{N\text{x}1}$ denotes the circular-symmetric complex AWGN at the relay. It is distributed as $\mathcal{CN}(0, \sigma_r^2 \mathbf{I}_N)$. The vector $\widehat{\mathbf{x}}_i \in \mathbb{C}^{M\text{x}1}$ denotes the precoded data by the BS and the TU obtained by multiplying the normalized complex information data $\mathbf{x}_i \in \mathbb{C}^{N\text{x}1}$ with precoder matrix $\mathbf{B}_i \in \mathbb{C}^{M\text{x}M}$, and is given as

$$\widehat{\mathbf{x}}_i = \mathbf{B}_i \mathbf{x}_i. \tag{4.2}$$

We assume that both TU and BS transmit N independent streams such that $\mathbb{E}(\mathbf{x}_i \mathbf{x}_i^H) = \mathbf{\Sigma_i} = \mathbf{I}_M$. The transmit power constraint met by precoded data vector $\widehat{\mathbf{x}}_i$ is

$$\text{Tr}[\mathbb{E}(\widehat{\mathbf{x}}_i \widehat{\mathbf{x}}_i^H] = \text{Tr}(\mathbf{B}_i \mathbf{\Sigma_i} \mathbf{B}_i^H) = \text{Tr}(\Xi) \leq P_i. \tag{4.3}$$

Due to the direct links, the BS in the MAC phase receives the uplink signal transmitted by the TU while the RU receives the downlink signal transmitted by the BS. The uplink and downlink signals are given respectively as

$$\widehat{\mathbf{q}}_b = \mathbf{L}\widehat{\mathbf{x}}_u + \widehat{\mathbf{n}}_{q_b}, \tag{4.4a}$$

$$\widehat{\mathbf{q}}_u = \mathbf{R}\widehat{\mathbf{x}}_b + \widehat{\mathbf{n}}_{q_u}, \tag{4.4b}$$

where $\{\mathbf{L}, \mathbf{R}\} \in \mathbb{C}^{M\text{x}M}$ are the direct link channels of the TU $\to$ BS and the BS$\to$RU links, respectively. The vectors $\{\widehat{\mathbf{n}}_{q_b}, \widehat{\mathbf{n}}_{q_u}\} \in \mathbb{C}^{M\text{x}1}$, distributed as $\mathcal{CN}(0, \sigma^2 \mathbf{I}_M)$, denote the AWGN at the BS and RU, respectively. The BS and RU combine their MAC phase direct link signals using combininig matrices $\mathbf{S}_b$ and $\mathbf{S}_u$ respectively as following.

$$\widetilde{\mathbf{q}}_b = \mathbf{S}_b \widehat{\mathbf{q}}_b, \tag{4.5a}$$

$$\widetilde{\mathbf{q}}_u = \mathbf{S}_u \widehat{\mathbf{q}}_u. \tag{4.5b}$$

---

[1]To avoid repetition, we assume that $i = b, u$ throughout this chapter.

The relay multiplies the signal $\mathbf{y}_r$ it receives with a precoder $\mathbf{W} \in \mathbb{C}^{N \times N}$ during the BC phase of ncTWR. The relay transmi signal is

$$\mathbf{x}_r = \mathbf{W}\mathbf{y}_r, \tag{4.6}$$

which satisfies the following transmit power constraint

$$
\begin{aligned}
P_r &\geq \mathrm{Tr}(\mathbb{E}(\mathbf{x}_r\mathbf{x}_r^H)) \\
&= \mathrm{Tr}(\mathbf{W}\mathbf{H}\boldsymbol{\Sigma}\mathbf{H}^H\mathbf{W}^H + \sigma_r^2\mathbf{W}\mathbf{W}^H).
\end{aligned}
\tag{4.7}
$$

The signals received by the BS and RU in the BC phase

$$
\begin{aligned}
\mathbf{y}_b &= \mathbf{G}_b\mathbf{x}_r + \mathbf{n}_b \\
&= \underbrace{\mathbf{G}_b\mathbf{W}\mathbf{H}_b\widehat{\mathbf{x}}_b}_{\mathbf{BI}} + \mathbf{G}_b\mathbf{W}\mathbf{H}_u\widehat{\mathbf{x}}_u + \mathbf{G}_b\mathbf{W}\mathbf{n}_r + \mathbf{n}_b \\
\mathbf{y}_u &= \mathbf{G}_u\mathbf{x}_r + \mathbf{n}_u \\
&= \mathbf{G}_u\mathbf{W}\mathbf{H}_b\widehat{\mathbf{x}}_b + \underbrace{\mathbf{G}_u\mathbf{W}\mathbf{H}_u\widehat{\mathbf{x}}_u}_{\mathbf{BI}} + \mathbf{G}_u\mathbf{W}\mathbf{n}_r + \mathbf{n}_u.
\end{aligned}
\tag{4.8}
$$

The matrices $\mathbf{G}_b \in \mathbb{C}^{M \times N}$ and $\mathbf{G}_u \in \mathbb{C}^{M \times N}$ are the BC phase channels for the relay $\rightarrow$ BS and the relay $\rightarrow$ RU links, respectively. The vectors $\mathbf{n}_b \in \mathbb{C}^{M \times 1}$ and $\mathbf{n}_u \in \mathbb{C}^{M \times 1}$, distributed as $\sim \mathcal{CN}(0, \sigma^2\mathbf{I}_M)$, represent the AWGN at the BS and the RU, respectively. We assume all the channels are frequency-flat and quasi static. The BS is aware of its own data transmitted during the MAC phase, it can cancel its BI. The RU, in contrast, cannot do that. This BI is canceled by designining precoder $\mathbf{W}$ in the following section. The received signals at the BS and RU, after using the BI-cancelling precoder at the BS, are given respectively as

$$
\begin{aligned}
\widehat{\mathbf{y}}_b &= \mathbf{G}_b\mathbf{W}\mathbf{H}_u\widehat{\mathbf{x}}_u + \mathbf{G}_b\mathbf{W}\mathbf{n}_r + \mathbf{n}_b, \\
\widehat{\mathbf{y}}_u &= \mathbf{G}_u\mathbf{W}\mathbf{H}_b\widehat{\mathbf{x}}_b + \mathbf{G}_u\mathbf{W}\mathbf{n}_r + \mathbf{n}_u.
\end{aligned}
\tag{4.9}
$$

For the BC phase, the BS and the RU employ combiner matrices $\mathbf{K}_b$ and $\mathbf{K}_u$ respectively, to combine their received data as follows

$$
\begin{aligned}
\tilde{\mathbf{y}}_b &= \mathbf{K}_b\widehat{\mathbf{y}}_b = \mathbf{K}_b\mathbf{G}_b\mathbf{W}\mathbf{H}_u\widehat{\mathbf{x}}_u + \mathbf{K}_b\mathbf{G}_b\mathbf{W}\mathbf{n}_r + \mathbf{K}_b\mathbf{n}_b, \\
\tilde{\mathbf{y}}_u &= \mathbf{K}_u\widehat{\mathbf{y}}_u = \mathbf{K}_u\mathbf{G}_u\mathbf{W}\mathbf{H}_b\widehat{\mathbf{x}}_b + \mathbf{K}_u\mathbf{G}_u\mathbf{W}\mathbf{n}_r + \mathbf{K}_u\mathbf{n}_u,
\end{aligned}
\tag{4.10}
$$

where $\mathbf{K}_i \in \mathbb{C}^{M \times M}$.

The BS and RU now add their receive signals i.e., (direct and relay link) before decoding their data.

$$\bar{\mathbf{y}}_b = \tilde{\mathbf{y}}_b + \tilde{\mathbf{q}}_b; \quad \text{and} \quad \bar{\mathbf{y}}_u = \tilde{\mathbf{y}}_u + \tilde{\mathbf{q}}_u. \tag{4.11}$$

The precoder and the combiner are designed such that the overall channel for $\bar{\mathbf{y}}_b$ and $\bar{\mathbf{y}}_u$ reduce to triangular matrix. Both BS and RU employ SIC to decode data. Such an approach, will help us in scalarizing the optimization problems which considerably simplifies them.

4.2 Transceiver design

This section constructs the relay precoder $\mathbf{W}$ to cancel the BI for the RU. To enable this objective, the proposed precoder matrix is partitioned into three matrices as follows

$$\mathbf{W} = \mathbf{MDF}. \tag{4.12}$$

The matrices $\mathbf{M} \in \mathbb{C}^{N \times 2M}$, and $\mathbf{F} \in \mathbb{C}^{2M \times N}$ are contructed to cancel the RU BI alone, and are therefore termed as BI-cancelling precoders. Precoders $\mathbf{M}$ and $\mathbf{F}$ are divided further into $\mathbf{M} = [\mathbf{M}_b \ \mathbf{M}_u]$ and $\mathbf{F} = [\mathbf{F}_b \ ; \mathbf{F}_u]$ respectively, where $\mathbf{M}_i \in \mathbb{C}^{N \times M}$ and $\mathbf{F}_i \in \mathbb{C}^{M \times N}$. Precoder $\mathbf{D} \in \mathbb{C}^{2M \times 2M}$ is defined below.

$$\mathbf{D} = \begin{bmatrix} \mathbf{0} & \mathbf{D}_b \\ \mathbf{D}_u & \mathbf{0} \end{bmatrix}.$$

This precoder $\mathbf{D}$ is contructed to triangularize the end-to-end MIMO channels at the BS and RU. The precoder $\mathbf{D}$ is also used to optimally allocate power to maximize the SE and GEE. The objective of TU and BS precoder, and BS and RU combiners is that the overall channel of the system reduces to a triangular matrix. This, in turn, will enable both BS and RU to decode data by simply applying SIC. We later jointly optimize the power to maximize the SE which summarizes the proposed design as in Algorithm 3.

We now elaborate the proposed design discussed in Algorithm 3 in the following sections.

Algorithm 3: Proposed design.

---

2 *BI-cancelling precoder*: Design $\mathbf{M}$ and $\mathbf{F}$ relay precoder components to mitigate RU's BI.

4 *Design of source precoder using GSVD*: Design of source precoders $\mathbf{B}_u$ and $\mathbf{B}_b$ using GSVD and direct link combiners $\mathbf{S}_u$ $\mathbf{S}_b$.

6 *Joint design of relay precoder and source combiner for relay link*: Design $\mathbf{D}_b$ and $\mathbf{K}_b$ for BS $\rightarrow$ relay $\rightarrow$ RU and $\mathbf{D}_u$ and $\mathbf{K}_u$ for TU $\rightarrow$ relay $\rightarrow$ BS.

4.2.1   Design of BI-Cancelling precoders

The signal received by the BS and the RU in the BC phase in (4.8) are stacked to create a vector $\mathbf{y}$ such that

$$\mathbf{y} = \mathbf{G}\mathbf{x}_r + \mathbf{n}. \tag{4.13}$$

The vector $\mathbf{y} = [\mathbf{y}_b; \mathbf{y}_u]$ and $\mathbf{n} = [\mathbf{n}_b; \mathbf{n}_u]$. The matrix $\mathbf{G} = [\mathbf{G}_b; \mathbf{G}_u]$ is the composite channel of the BC phase. To construct the BI-cancelling precoders, we begin by substituting $\mathbf{y}_r, \mathbf{x}_r$ and $\mathbf{W}$ from (4.1), (4.6) and (4.12) respectively in (4.13).

$$\mathbf{y} = \mathbf{G}\mathbf{W}(\mathbf{H}\widehat{\mathbf{x}} + \mathbf{n}_r) + \mathbf{n}$$

$$= \mathbf{G}\mathbf{W}\mathbf{H}\widehat{\mathbf{x}} + \mathbf{G}\mathbf{W}\mathbf{n}_r + \mathbf{n}$$

$$= \underbrace{\mathbf{G}\mathbf{M}}_{\tilde{\mathbf{G}}}\mathbf{D}\underbrace{\mathbf{F}\mathbf{H}}_{\tilde{\mathbf{H}}}\widehat{\mathbf{x}} + \underbrace{\mathbf{G}\mathbf{W}\mathbf{n}_r + \mathbf{n}}_{\tilde{\mathbf{n}}}$$

$$= \tilde{\mathbf{G}}\mathbf{D}\tilde{\mathbf{H}}\widehat{\mathbf{x}} + \tilde{\mathbf{n}}. \tag{4.14}$$

To cancel the BI only for RU, the BI cancelling precoders $\mathbf{M}$ and $\mathbf{F}$ must be developed to reduce $\tilde{\mathbf{G}}$ and $\tilde{\mathbf{H}}$ into lower and upper block diagonal matrices. With such a design, the vector in (4.14) can be expressed as follows:

$$\mathbf{y} = \begin{bmatrix} \tilde{\mathbf{G}}_b & \mathbf{0} \\ \tilde{\mathbf{G}}_n & \tilde{\mathbf{G}}_u \end{bmatrix} \begin{bmatrix} \mathbf{0} & \tilde{\mathbf{D}}_b \\ \tilde{\mathbf{D}}_u & \mathbf{0} \end{bmatrix} \begin{bmatrix} \tilde{\mathbf{H}}_u & \tilde{\mathbf{H}}_n \\ \mathbf{0} & \tilde{\mathbf{H}}_b \end{bmatrix} \begin{bmatrix} \widehat{\mathbf{x}}_b \\ \widehat{\mathbf{x}}_u \end{bmatrix} + \tilde{\mathbf{n}}$$

$$\mathbf{y} = \begin{bmatrix} (\tilde{\mathbf{G}}_b\mathbf{D}_b\tilde{\mathbf{H}}_b)\widehat{\mathbf{x}}_u \\ \tilde{\mathbf{G}}_u\mathbf{D}_u\tilde{\mathbf{H}}_u\widehat{\mathbf{x}}_b + (\tilde{\mathbf{G}}_n\mathbf{D}_b\tilde{\mathbf{H}}_b + \tilde{\mathbf{G}}_u\mathbf{D}_u\tilde{\mathbf{H}}_n)\widehat{\mathbf{x}}_u \end{bmatrix} + \tilde{\mathbf{n}}.$$

We can observe that the signal the RU received is BI-free whereas the BS experiences the BI. The BI free signal at BS, after it mitigates its BI, and RU are given respectively as

$$\widehat{\mathbf{y}}_b = (\tilde{\mathbf{G}}_b \mathbf{D}_b \tilde{\mathbf{H}}_b)\widehat{\mathbf{x}}_u + \widehat{\mathbf{n}}_b \tag{4.15a}$$

$$\widehat{\mathbf{y}}_u = (\tilde{\mathbf{G}}_u \mathbf{D}_u \tilde{\mathbf{H}}_u)\widehat{\mathbf{x}}_b + \widehat{\mathbf{n}}_u. \tag{4.15b}$$

The BS and RU recover their desired signal using the decoder $\mathbf{K}_b$ and $\mathbf{K}_u$ respectively as follows

$$\tilde{\mathbf{y}}_b = \mathbf{K}_b \widehat{\mathbf{y}}_b = \mathbf{K}_b (\tilde{\mathbf{G}}_b \mathbf{D}_b \tilde{\mathbf{H}}_b)\widehat{\mathbf{x}}_u + \tilde{\mathbf{n}}_b \tag{4.16a}$$

$$\tilde{\mathbf{y}}_u = \mathbf{K}_u \widehat{\mathbf{y}}_u = \mathbf{K}_u (\tilde{\mathbf{G}}_u \mathbf{D}_u \tilde{\mathbf{H}}_u)\widehat{\mathbf{x}}_b + \tilde{\mathbf{n}}_u. \tag{4.16b}$$

The $\tilde{\mathbf{n}}_i$, which has pdf $\mathcal{CN}(0, \mathbf{\Sigma}_{\tilde{\mathbf{n}}_i}) \; \forall \; i \in \{b, u\}$, is the effective noise at the BS and RU.

4.2.2 Precoder design for uplink

We next design BS and TU precoders $\mathbf{B}_b$ and $\mathbf{B}_u$ and the BS and RU decoders $\mathbf{K}_b$ and $\mathbf{K}_u$, respectively. The objective of designing the precoder and decoder is to i) jointly beamform for the relay and direct links; and ii) reduce the end-to-end downlink and uplink channel in (4.11) to a triangular matrix.

To achieve this objective, we rewrite (4.4a) and (4.15a) as follows:

$$\widehat{\mathbf{y}}_b = \tilde{\mathbf{G}}_b \mathbf{D}_b \tilde{\mathbf{H}}_b \mathbf{B}_u \mathbf{x}_u + \widehat{\mathbf{n}}_b \tag{4.17a}$$

$$\widehat{\mathbf{q}}_b = \mathbf{L} \mathbf{B}_u \mathbf{x}_u + \widehat{\mathbf{n}}_{\mathbf{q}_b}. \tag{4.17b}$$

We see from (4.17a) and (4.17b) that the precoder $\mathbf{B}_u$ should be designed to beamform for two links i.e., the direct and the relay link. The GSVD can concurrently decompose two matrices and thus can be used for beamforming for the relay and the direct link. We perform GSVD of MIMO channels $\tilde{\mathbf{H}}_b$ and $\mathbf{L}$ as follows

$$\tilde{\mathbf{H}}_b = \mathbf{U}_{\tilde{H}_b} \mathbf{\Sigma}_{\tilde{\mathbf{H}}_\mathbf{b}} \mathbf{T}_L^H, \quad \mathbf{L} = \mathbf{U}_L \mathbf{\Sigma}_L \mathbf{T}_L^H. \tag{4.18}$$

Here $\{\mathbf{U}_{\tilde{H}_b}, \mathbf{U}_L\} \in \mathbb{C}^{M \times M}$ have M orthonormal rows, $\mathbf{\Sigma}_{\tilde{\mathbf{H}}_b} \in \mathbb{R}_+^{M \times M} = \mathrm{diag}(\sigma_{\tilde{H}_b,1}, \cdots, \sigma_{\tilde{H}_b,M})$, $\mathbf{\Sigma}_L \in \mathbb{R}_+^{M \times M} = \mathrm{diag}(\sigma_{L,1}, ..., \sigma_{L,M})$, $\mathbf{T}_L \in \mathbb{C}^{M \times M}$.

The matrices $\boldsymbol{\Sigma}_{\tilde{\mathbf{H}}_b}$ and $\boldsymbol{\Sigma}_L$ contain generalized singularvalues for MIMO channels $\tilde{\mathbf{H}}_b$ and $\mathbf{L}$, respectively. Substituting the expression of $\mathbf{L}$ in (4.17b), we get

$$\widehat{\mathbf{q}}_b = \mathbf{U}_L \boldsymbol{\Sigma}_L \mathbf{T}_L^H \mathbf{B}_u \mathbf{x}_u + \widehat{\mathbf{n}}_{\mathbf{q}_b}. \tag{4.19}$$

For the TU $\to$ BS link and TU $\to$ relay $\to$ BS link, the precoder $\mathbf{B}_u$ is used at the TU which is designed by using the GSVD of channels $\tilde{\mathbf{H}}_b$ and $\mathbf{L}$. The precoder $\mathbf{B}_u$ is designed by employing LQ decompostion [65] of $\mathbf{T}_L^H$ in (4.18) and given as

$$\mathbf{T}_L^H = \mathbf{L}_L \mathbf{Q}_L$$
$$\mathbf{B}_u = \mathbf{Q}_L^H \boldsymbol{\Lambda}_u. \tag{4.20}$$

Here $\boldsymbol{\Lambda}_u \in \mathbb{R}_+^{M \times M}$ is a power allocation diagonal matrix at the TU such that $\boldsymbol{\Lambda}_u \boldsymbol{\Lambda}_u^H = \mathrm{diag}(\lambda_{u,1} ..... \lambda_{u,M})$. Substituting the expression of $\mathbf{B}_u$ from (4.20) in (4.17b), we get

$$\widehat{\mathbf{q}}_b = \mathbf{U}_L \boldsymbol{\Sigma}_L \mathbf{T}_L^H \mathbf{Q}_L^H \boldsymbol{\Lambda}_u \mathbf{x}_u + \widehat{\mathbf{n}}_{q_b}$$
$$= \mathbf{U}_L \boldsymbol{\Sigma}_L \mathbf{L}_L \boldsymbol{\Lambda}_u \mathbf{x}_u + \widehat{\mathbf{n}}_{q_b}. \tag{4.21}$$

Now, we define the SVD of $\tilde{\mathbf{G}}_b$ as

$$\tilde{\mathbf{G}}_b = \mathbf{U}_{\tilde{\mathbf{G}}_b} \boldsymbol{\Sigma}_{\tilde{\mathbf{G}}_b} \mathbf{V}_{\tilde{\mathbf{G}}_b}^H \tag{4.22}$$

We will now consider the BS $\to$ relay $\to$ RU link. By substituting the expressions of $\tilde{\mathbf{G}}_b$, $\tilde{\mathbf{H}}_b$, $\mathbf{B}_u$ from (4.22), (4.18), (4.20) respectively in (4.17a), we get

$$\widehat{\mathbf{y}}_b = \mathbf{U}_{\tilde{\mathbf{G}}_b} \boldsymbol{\Sigma}_{\tilde{\mathbf{G}}_b} \mathbf{V}_{\tilde{\mathbf{G}}_b}^H \mathbf{D}_b \mathbf{U}_{\tilde{H}_b} \boldsymbol{\Sigma}_{\tilde{\mathbf{H}}_b} \mathbf{L}_L \boldsymbol{\Lambda}_u \mathbf{x}_u + \widehat{\mathbf{n}}_b. \tag{4.23}$$

4.2.3   Precoder design for downlink

Now considering BS $\to$ RU direct link and BS $\to$ relay $\to$ RU relay link, we rewrite (4.4b) and (4.15b) as follows:

$$\widehat{\mathbf{y}}_u = \tilde{\mathbf{G}}_u \mathbf{D}_u \tilde{\mathbf{H}}_u \mathbf{B}_b \mathbf{x}_b + \widehat{\mathbf{n}}_u, \tag{4.24a}$$

$$\widehat{\mathbf{q}}_u = \mathbf{R} \mathbf{B}_b \mathbf{x}_b + \widehat{\mathbf{n}}_{q_u}. \tag{4.24b}$$

The precoder $\mathbf{B}_b$ is designed by using the the GSVD of channels $\tilde{\mathbf{H}}_u$ and $\mathbf{R}$. Now performing the GSVD of $\tilde{\mathbf{H}}_u$ and $\mathbf{R}$

$$\tilde{\mathbf{H}}_u = \mathbf{U}_{\tilde{H}_u} \boldsymbol{\Sigma}_{\tilde{H}_u} \mathbf{T}_R^H, \quad \mathbf{R} = \mathbf{U}_R \boldsymbol{\Sigma}_R \mathbf{T}_R^H. \tag{4.25}$$

Here $\{\mathbf{U}_{\tilde{H}_u}, \mathbf{U}_R\} \in \mathbb{C}^{M \times M}$, $\mathbf{T}_r \in \mathbb{C}^{M \times M}$, $\boldsymbol{\Sigma}_{\tilde{\mathbf{H}}_u} \in \mathbb{R}_+^{M \times M} = \mathrm{diag}(\sigma_{\tilde{\mathbf{H}}_u,1}, ..., \sigma_{\tilde{\mathbf{H}}_u,M})$, $\boldsymbol{\Sigma}_r \in \mathbb{R}_+^{M \times M} = \mathrm{diag}(\sigma_{r,1}, ..., \sigma_{r,M})$.

Substituting the expression of $\mathbf{R}$ (4.24b), we get

$$\widehat{\mathbf{q}}_u = \mathbf{U}_R \boldsymbol{\Sigma}_R \mathbf{T}_R^H \mathbf{B}_b \mathbf{x}_b + \widehat{\mathbf{n}}_{q_u}. \tag{4.26}$$

The precoder $\mathbf{B}_b$ is chosen by LQ decomposition of $\mathbf{T}_R^H$ given by

$$\mathbf{T}_R^H = \mathbf{L}_R \mathbf{Q}_R \tag{4.27}$$

$$\mathbf{B}_b = \mathbf{Q}_R^H \boldsymbol{\Lambda}_b. \tag{4.28}$$

Here $\boldsymbol{\Lambda}_b \in \mathbb{R}_+^{M \times M}$ is a diagonal matrix which is used to allocate power at the BS such that $\boldsymbol{\Lambda}_b \boldsymbol{\Lambda}_{\mathbf{u}}^H = \mathrm{diag}(\lambda_{b,1}, \cdots, \lambda_{b,M})$. Substituting the expression of and $\mathbf{B}_b$ from (4.28) in (4.26) we get

$$\widehat{\mathbf{q}}_u = \mathbf{U}_R \boldsymbol{\Sigma}_R \mathbf{T}_R^H \mathbf{Q}_R^H \boldsymbol{\Lambda}_b \mathbf{x}_b + \widehat{\mathbf{n}}_{q_u}$$

$$= \mathbf{U}_R \boldsymbol{\Sigma}_R \mathbf{L}_R \boldsymbol{\Lambda}_b \mathbf{x}_b + \widehat{\mathbf{n}}_{q_u}. \tag{4.29}$$

Now, the SVD of $\tilde{\mathbf{G}}_u$ is defined as

$$\tilde{\mathbf{G}}_u = \mathbf{U}_{\tilde{\mathbf{G}}_u} \boldsymbol{\Sigma}_{\tilde{\mathbf{G}}_u} \mathbf{V}_{\tilde{\mathbf{G}}_u}^H. \tag{4.30}$$

The BS $\rightarrow$ RU relay link can be rewritten using $\tilde{\mathbf{H}}_u$, $\mathbf{B}_b$, $\tilde{\mathbf{G}}_u$ from (4.25), (4.28), (4.30) respectively in (4.24a) as

$$\widehat{\mathbf{y}}_u = \mathbf{U}_{\tilde{\mathbf{G}}_u} \boldsymbol{\Sigma}_{\tilde{\mathbf{G}}_u} \mathbf{V}_{\tilde{\mathbf{G}}_u}^H \mathbf{D}_u \mathbf{U}_{\tilde{H}_u} \boldsymbol{\Sigma}_{\tilde{\mathbf{H}}_{\mathbf{u}}} \mathbf{L}_R \boldsymbol{\Lambda}_b \mathbf{x}_b + \widehat{\mathbf{n}}_u. \tag{4.31}$$

4.3 Joint design of relay precoder and source combiner

4.3.1 For uplink

We now discuss about the joint design of relay precoder and source combiner for uplink relay link. We will design $\mathbf{K}_b$ in (4.16a). Rewriting (4.16a) using (4.23) as follows:

$$\tilde{\mathbf{y}}_b = \mathbf{K}_b \mathbf{U}_{\tilde{\mathbf{G}}_b} \mathbf{\Sigma}_{\tilde{\mathbf{G}}_b} \mathbf{V}_{\tilde{\mathbf{G}}_b}^H \mathbf{D}_b \mathbf{U}_{\tilde{H}_b} \mathbf{\Sigma}_{\tilde{\mathbf{H}}_b} \mathbf{L}_L \mathbf{\Lambda}_u \mathbf{x}_u + \tilde{\mathbf{n}}_b. \tag{4.32}$$

Observing the above expressions, we choose the precoder $\mathbf{D}_b$ to be $\mathbf{V}_{\tilde{\mathbf{G}}_b} \triangle_b \mathbf{U}_{\tilde{\mathbf{H}}_b}^H$ in (4.32). The diagonal matrix $\triangle_b \in \mathbb{R}^{M \times M}$, with non-negative variables $\sqrt{\delta_{b,m}}$, $\sqrt{\delta_{u,m}}$ $\forall$ $m = 1$ to M, allocates power allocation to the streams. We also choose the combiner $\mathbf{K}_b = \mathbf{U}_{\tilde{\mathbf{G}}_b}^H$ in (4.32). So, by substituting the designed precoder and combiner for the uplink, we get

$$\begin{aligned}
\tilde{\mathbf{y}}_b &= \mathbf{U}_{\tilde{\mathbf{G}}_b}^H \mathbf{U}_{\tilde{\mathbf{G}}_b} \mathbf{\Sigma}_{\tilde{\mathbf{G}}_b} \mathbf{V}_{\tilde{\mathbf{G}}_b}^H \mathbf{V}_{\tilde{\mathbf{G}}_b} \triangle_b \mathbf{U}_{\tilde{\mathbf{H}}_b}^H \mathbf{U}_{\tilde{H}_b} \mathbf{\Sigma}_{\tilde{\mathbf{H}}_b} \mathbf{L}_L \mathbf{\Lambda}_u \mathbf{x}_u + \tilde{\mathbf{n}}_b \\
&= \underbrace{\mathbf{\Sigma}_{\tilde{\mathbf{G}}_b} \triangle_b \mathbf{\Sigma}_{\tilde{\mathbf{H}}_b} \mathbf{L}_L \boldsymbol{\lambda}_u}_{\mathbf{T}_b} \mathbf{x}_u + \tilde{\mathbf{n}}_b.
\end{aligned} \tag{4.33}$$

Here, the term $\mathbf{T}_b$ in (4.33) result in reflected lower triangular structure. We now design the source combiners for the direct uplink. Substituting (4.21) in (4.5a) we get

$$\tilde{\mathbf{q}}_b = \mathbf{S}_b \mathbf{U}_L \mathbf{\Sigma}_L \mathbf{L}_L \boldsymbol{\lambda}_u \mathbf{x}_u + \mathbf{S}_b \widehat{\mathbf{n}}_b. \tag{4.34}$$

The direct link combiner $\mathbf{S}_b$ in the direct uplink is chosen as $\mathbf{U}_L^H$. After substituting it in the above equation, the decoded signal at the BS is given as

$$\tilde{\mathbf{q}}_b = \underbrace{\mathbf{\Sigma}_L \mathbf{L}_L \mathbf{\Lambda}_u}_{\mathbf{T}_{q_b}} \mathbf{x}_u + \underbrace{\mathbf{U}_L^H \widehat{\mathbf{n}}_b}_{\mathbf{n}_{\tilde{q}_b}}. \tag{4.35}$$

Here the term $\mathbf{T}_{q_u}$ also form lower triangular structure due to our precoder design which helps in SIC. The combined uplink signals i.e., direct and relay signals at the BS are

$$\tilde{\mathbf{c}}_b = \tilde{\mathbf{y}}_b + \tilde{\mathbf{q}}_b. \tag{4.36}$$

The combined signals at the BS i.e., $\mathbf{c}_b$ in (4.36) will have a lower triangular structure as

shown below:

$$
\begin{bmatrix}
\tilde{c}_{b,1} \\
\tilde{c}_{b,2} \\
\cdot \\
\cdot \\
\tilde{c}_{b,M-1} \\
\tilde{c}_{b,M}
\end{bmatrix}
=
\begin{bmatrix}
\times & 0 & \ldots & 0 & 0 & 0 \\
\times & \times & \ldots & 0 & 0 & 0 \\
\cdot & \cdot & \cdot & \cdot & \cdot & \cdot \\
\cdot & \cdot & \cdot & \cdot & \cdot & \cdot \\
\times & \times & \ldots & \times & \times & 0 \\
\times & \times & \ldots & \times & \times & \times
\end{bmatrix}
\begin{bmatrix}
\mathbf{x}_{b,1} \\
\mathbf{x}_{b,2} \\
\cdot \\
\cdot \\
\mathbf{x}_{b,M-1} \\
\mathbf{x}_{b,M}
\end{bmatrix}
+ \widehat{\mathbf{n}}_{c_b}
$$

Here, $\widehat{\mathbf{n}}_{c_b}$ is the effective uplink noise. This structure prevents inter-stream interference on the first transmit stream, which is also the first to be decoded. The $(M - k)$th transmit stream is then decoded by subtracting the inter-stream interference generated by the $(M - k - 1)$th to first streams that have previously been decoded.

After the inter stream interference cancellation, the expression of the mth stream received by the BS through the TU$\rightarrow$ BS direct link and relay link is given by

$$
\begin{aligned}
\tilde{c}_b(m) &= \sqrt{\delta_{b,m}}\sqrt{\lambda_{u,m}}[\boldsymbol{\Sigma}_{\tilde{\mathbf{G}}_b}]_{m,m}[\boldsymbol{\Sigma}_{\tilde{\mathbf{H}}_b}]_{m,m}[\mathbf{L}_L]_{m,m}x_u(m) + \sqrt{\lambda_{u,m}}[\boldsymbol{\Sigma}_l]_{m,m}[\mathbf{L}_L]_{m,m}x_u(m) + \widehat{\mathbf{n}}_{c_b}(m) \\
&= \sqrt{\delta_{b,m}}\sqrt{\lambda_{u,m}}\sigma_{\tilde{\mathbf{G}}_b,m}\sigma_{\tilde{\mathbf{H}}_b,m}[\mathbf{L}_L]_{m,m}x_u(m) + \tilde{\mathbf{n}}_b(m) + \sqrt{\lambda_{u,m}}\sigma_{l,m}[\mathbf{L}_L]_{m,m}x_u(m) + \widehat{\mathbf{n}}_{c_b}(m).
\end{aligned}
\tag{4.37}
$$

The combined effective covariance matrix of noise at BS i.e., $\widehat{\mathbf{n}}_{c_b}$ is

$$
\boldsymbol{\Xi}_{\tilde{\mathbf{n}}_b} = \sigma_r^2 \Big\{ \mathbf{T}_b \mathbf{T}_b^H + \mathbf{I}_M \Big\} + \sigma^2 \mathbf{I}_M,
\tag{4.38}
$$

where $\mathbf{T}_b = \mathbf{U}_{\tilde{\mathbf{G}}_u}^H \tilde{\mathbf{G}}_n \mathbf{D}_b$.

The SNR observed by the mth stream received by the BS can be computed by using (4.37) and (4.38) is shown in (4.39)

$$
\text{SNR}_{b,m} = \frac{\Big\{\lambda_{u,m}\sigma_{l,m}^2\big|[\mathbf{L}_L]_{m,m}\big|^2 + \delta_{b,m}\sigma_{\tilde{G}_b,m}^2\sigma_{\tilde{H}_b,m}^2\lambda_{u,m}\big|[\mathbf{L}_L]_{m,m}\big|^2 + 2\sqrt{\delta_{b,m}}\lambda_{u,m}\sigma_{l,m}\sigma_{\tilde{\mathbf{G}}_b,m}\sigma_{\tilde{\mathbf{H}}_b,m}\big|[\mathbf{L}_L]_{m,m}\big|^2\Big\}}{\delta_{b,m}\sigma_{\tilde{G}_b,m}^2\sigma_r^2 + \sigma_r^2 + \sigma^2}.
\tag{4.39}
$$

4.3.2 For downlink

Similarly, we now discuss the joint design of relay precoder and source combiner for the downlink relay link. We will design $\mathbf{K}_u$ in (4.16b). Rewriting (4.16b) using (4.31) as:

$$
\tilde{\mathbf{y}}_u = \mathbf{K}_u \mathbf{U}_{\tilde{\mathbf{G}}_u} \boldsymbol{\Sigma}_{\tilde{\mathbf{G}}_u} \mathbf{V}_{\tilde{\mathbf{G}}_u}^H \mathbf{D}_u \mathbf{U}_{\tilde{H}_u} \boldsymbol{\Sigma}_{\tilde{\mathbf{H}}_u} \mathbf{L}_R \boldsymbol{\Lambda}_b \mathbf{x}_b + \tilde{\mathbf{n}}_u.
\tag{4.40}
$$

Observing the above expression, we choose the precoder $\mathbf{D}_u$ to be $\mathbf{V}_{\tilde{\mathbf{G}}_u} \triangle_u \mathbf{U}_{\tilde{\mathbf{H}}_u}^H$ in (4.40). The diagonal matrix $\triangle_u \in \mathbb{R}^{M \times M}$, with non-negative variables $\sqrt{\delta}_{u,m} \, \forall \, \mathrm{m} = 1 \, \mathrm{to} \, \mathrm{M}$, allocated the power to the downlink streams. We also choose the combiner $\mathbf{K}_u = \mathbf{U}_{\tilde{\mathbf{G}}_u}^H$ in (4.40). So, by substituting the designed downlink precoder and combiner for the downlink relay link, we get

$$\begin{aligned}
\tilde{\mathbf{y}}_u &= \mathbf{U}_{\tilde{\mathbf{G}}_u}^H \mathbf{U}_{\tilde{\mathbf{G}}_u} \boldsymbol{\Sigma}_{\tilde{\mathbf{G}}_u} \mathbf{V}_{\tilde{\mathbf{G}}_u}^H \mathbf{V}_{\tilde{\mathbf{G}}_u} \triangle_u \mathbf{U}_{\tilde{\mathbf{H}}_u}^H \mathbf{U}_{\tilde{\mathbf{H}}_u} \boldsymbol{\Sigma}_{\tilde{\mathbf{H}}_u} \mathbf{L}_R \boldsymbol{\Lambda}_b \mathbf{x}_b + \tilde{\mathbf{n}}_u \\
&= \underbrace{\boldsymbol{\Sigma}_{\tilde{\mathbf{G}}_u} \triangle_u \boldsymbol{\Sigma}_{\tilde{\mathbf{H}}_u} \mathbf{L}_R \boldsymbol{\Lambda}_b}_{\mathbf{T}_u} \mathbf{x}_b + \tilde{\mathbf{n}}_u.
\end{aligned} \tag{4.41}$$

Here, the term $\mathbf{T}_u$ in (4.41) results in reflected lower triangular structure. We now design the source combiners for the downlink direct link. Substituting (4.29) in (4.5b) we get

$$\tilde{\mathbf{q}}_u = \mathbf{S}_u \mathbf{U}_R \boldsymbol{\Sigma}_R \mathbf{L}_R \boldsymbol{\Lambda}_b \mathbf{x}_b + \mathbf{S}_u \widehat{\mathbf{n}}_u. \tag{4.42}$$

The direct link downlink combiner $\mathbf{S}_u$ is chosen as $\mathbf{U}_R^H$. After substituting it in the above equations, the decoded signal at the RU is given by

$$\tilde{\mathbf{q}}_u = \underbrace{\boldsymbol{\Sigma}_R \mathbf{L}_R \boldsymbol{\Lambda}_b}_{\mathbf{T}_{q_u}} \mathbf{x}_b + \underbrace{\mathbf{U}_R^H \widehat{\mathbf{n}}_u}_{\mathbf{n}_{\tilde{q}_u}}. \tag{4.43}$$

Here the term $\mathbf{T}_{q_u}$ also form lower triangular structure due to our downlink precoder design which helps in SIC. The combined signals i.e., direct and relay signals at the RU is

$$\tilde{\mathbf{c}}_u = \tilde{\mathbf{y}}_u + \tilde{\mathbf{q}}_u. \tag{4.44}$$

The combined signals at RU i.e., $\mathbf{c}_u$ in (4.44) will also have a lower triangular structure as shown below:

$$\begin{bmatrix} \tilde{c}_{u,1} \\ \tilde{c}_{u,2} \\ . \\ . \\ \tilde{c}_{u,M-1} \\ \tilde{c}_{u,M} \end{bmatrix} = \begin{bmatrix} \times & 0 & ... & 0 & 0 & 0 \\ \times & \times & ... & 0 & 0 & 0 \\ . & . & . & . & . & . \\ . & . & . & . & . & . \\ \times & \times & ... & \times & \times & 0 \\ \times & \times & ... & \times & \times & \times \end{bmatrix} \begin{bmatrix} \mathbf{x}_{u,1} \\ \mathbf{x}_{u,2} \\ . \\ . \\ \mathbf{x}_{u,M-1} \\ \mathbf{x}_{u,M} \end{bmatrix} + \widehat{\mathbf{n}}_{c_u}.$$

Here, $\widehat{\mathbf{n}}_{c_u}$ is effective combined noise.

Similar to the uplink structure, this structure prevents inter-stream interference on the first transmit stream, which is also the first to be decoded. The $(M - k)$th transmit stream is then decoded by subtracting the inter-stream interference generated by the $(M - k - 1)$th to first streams that have previously been decoded.

After the inter stream interference cancellation, the expression of the mth stream received by the RU through the RU $\rightarrow$ BS downlink direct and relay links is given by

$$
\begin{aligned}
\tilde{c}_u(m) &= \sqrt{\delta}_{u,m}\sqrt{\lambda}_{b,m}[\boldsymbol{\Sigma}_{\tilde{\mathbf{G}}_u}]_{m,m}[\boldsymbol{\Sigma}_{\tilde{\mathbf{H}}_u}]_{m,m}[\mathbf{L}_R]_{m,m}x_b(m) + \sqrt{\lambda}_{b,m}[\boldsymbol{\Sigma}_R]_{m,m}[\mathbf{L}_R]_{m,m}x_b(m) + \widehat{\mathbf{n}}_{c_u}(m) \\
&= \sqrt{\delta}_{u,m}\sqrt{\lambda}_{b,m}\sigma_{\tilde{\mathbf{G}}_u,m}\sigma_{\tilde{\mathbf{H}}_u,m}[\mathbf{L}_R]_{m,m}x_b(m) + \sqrt{\lambda}_{b,m}\sigma_{r,m}[\mathbf{L}_R]_{m,m}x_b(m) + \widehat{\mathbf{n}}_{c_u}(m).
\end{aligned}
$$
(4.45)

The combined effective covariance matrix of noise at RU i.e., $\tilde{\mathbf{n}}_{c_u}$ is

$$
\boldsymbol{\Xi}_{\tilde{\mathbf{n}}_{c_u}} = \sigma_r^2\Big\{\mathbf{T}_n\mathbf{T}_n^H + \mathbf{T}_u\mathbf{T}_u^H + \mathbf{I}_M\Big\} + \sigma^2\mathbf{I}_M,
$$
(4.46)

where $\mathbf{T}_u = \mathbf{U}_{\tilde{\mathbf{G}}_u}^H\tilde{\mathbf{G}}_u\mathbf{D}_u$ and $\mathbf{T}_n = \mathbf{U}_{\tilde{\mathbf{G}}_u}^H\tilde{\mathbf{G}}_n\mathbf{D}_b$.

The SNR observed by the mth stream received by the RU, can be computed by using (4.45) and (4.46) is shown in (4.47).

$$
\mathrm{SNR}_{u,m} = \frac{\Big\{\lambda_{b,m}\sigma_{r,m}^2\big|[\mathbf{L}_R]_{m,m}\big|^2 + \delta_{u,m}\sigma_{\tilde{\mathbf{G}}_u,m}^2\sigma_{\tilde{\mathbf{H}}_u,m}^2\lambda_{b,m}\big|[\mathbf{L}_R]_{m,m}\big|^2 + 2\sqrt{\delta}_{u,m}\lambda_{b,m}\sigma_{r,m}\sigma_{\tilde{G}_u,m}\sigma_{\tilde{H}_u,m}\big|[\mathbf{L}_R]_{m,m}\big|^2\Big\}}{\sigma_r^2\sum_{k=1}^M\Big\{\delta_{b,k}\big([\mathbf{U}_{\tilde{G}_u}^H\tilde{\mathbf{G}}_n\mathbf{V}_{\tilde{G}_b}]_{m,k}[\mathbf{U}_{\tilde{G}_u}^H\tilde{\mathbf{G}}_n\mathbf{V}_{\tilde{G}_b}]_{m,k}^*\big)\Big\} + \delta_{u,m}\sigma_{\tilde{G}_u,m}^2\sigma_r^2 + \sigma_r^2 + \sigma^2}.
$$
(4.47)

4.4 Summary

In this chapter, we first looked at the MIMO ncTWR system model, which includes weak direct links between the BS and UEs in addition of the indirect relay links. After that, we designed a precoder and decoder to beamform the relay and direct links simultaneously. This design also decomposes the end-to-end downlink and uplink channel to a triangular matrix. This enables the receive decoding only with successive interference cancellation technique.

Chapter 5

Optimization of SE and GEE for MIMO AF ncTWR Relaying

In this chapter, we joint allocate power across different nodes for the proposed GSVD transceiver in the previous chapter. Even though the direct links are weak, the proposed novel GSVD-based joint precoder design and optimization exploits them efficiently, and provides these gains. We first maximize the non-convex SE metric by casting it as a GP. We then later maximize the GEE by combining the Dinkelbach algorithm [66] with the GP framework. We also show the improved performance of two algorithms over the state-of-the-art methods.

5.1 SE maximization using geometric programming

The SE expression for the GSVD-based transceiver is given as

$$\mathbf{R}_{sum}(\boldsymbol{\delta}, \boldsymbol{\lambda}_u, \boldsymbol{\Lambda}_b) = \frac{1}{2} \sum_{i \in \{u,b\}} \sum_{m=1}^{M} \log(1 + \mathrm{SNR}_{i,m}(\boldsymbol{\delta}, \boldsymbol{\lambda}_i)). \tag{5.1}$$

The power allocation variables are stacked as $\boldsymbol{\delta} = [\delta_{u,1}, \cdots, \delta_{u,M}, \delta_{b,1}, \cdots, \delta_{b,M}]$ at the RS. The power allocation variables are stacked at the source to create the vector $\boldsymbol{\lambda}_i = [\lambda_{i,1}..., \lambda_{i,M}]$, $i \in \{u, b\}$ where $\boldsymbol{\lambda}_i \in \mathbb{R}^{M \times 1}$. To show that SE maximization can be treated as a GP, we begin the optimization by presenting two lemmas.

Lemma 4 *The transmit power of the node $\widehat{\mathbf{x}}_i$ depicted in (4.3), is a posynomial in optimization variable λ_i.*

$$\mathrm{Tr}(\mathbf{B}_u\mathbf{B}_u^H) = \mathrm{Tr}(\mathbf{Q}_l^H\boldsymbol{\Lambda}_u\boldsymbol{\Lambda}_u^H\mathbf{Q}_l) = \sum_{j=1}^{M} \lambda_{u,j}$$

$$\mathrm{Tr}(\mathbf{B}_b\mathbf{B}_b^H) = \mathrm{Tr}(\mathbf{Q}_p^H\boldsymbol{\Lambda}_b\boldsymbol{\Lambda}_b^H\mathbf{Q}_p) = \sum_{j=1}^{M} \lambda_{b,j} \tag{5.2}$$

The above equalities use the trace operator circular property . Due to positive coefficients of optimization variable $\lambda_{i,j}$ $\forall j$, the transmit power is a posynomial in λ_i. For ease of notation, the transmit power of the nodes TU and BS is written as $p_u(\boldsymbol{\lambda}_u)$ and $p_b(\boldsymbol{\lambda}_b)$, respectively.

Lemma 5 *The RS transmit power described in* (4.7) *is a posynomial in* $\boldsymbol{\lambda}_u, \boldsymbol{\lambda}_b$ *and* $\boldsymbol{\delta}$.

Proof. Please see Appendix C.1.

The SE maximization problem can be stated as

$$\underset{\boldsymbol{\delta},\boldsymbol{\lambda}_u,\boldsymbol{\lambda}_b}{\mathrm{Maximize}}\ R_{\mathrm{sum}}(\boldsymbol{\delta},\boldsymbol{\lambda}_u,\boldsymbol{\lambda}_b) \tag{5.3a}$$

$$\mathrm{s.t.} \qquad p_r(\boldsymbol{\delta},\boldsymbol{\lambda}_u,\boldsymbol{\Lambda}_b) \leq P_r \tag{5.3b}$$

$$p_u(\boldsymbol{\lambda}_u) \leq P_u, \quad p_b(\boldsymbol{\lambda}_b) \leq P_b. \tag{5.3c}$$

In its current state, the optimization problem is non-convex. We now cast the problem in epigraph form [55].

$$\underset{\boldsymbol{\delta},\boldsymbol{\lambda_u},\boldsymbol{\lambda_b},\gamma_u,\gamma_b}{\mathrm{Maximize}}\ \sum_{m=1}^{M}\frac{1}{2}\log(1+\gamma_u(m))+\frac{1}{2}\log(1+\gamma_b(m))$$

$$\mathrm{s.t.} \qquad \gamma_u(m) \leq \mathrm{SNR}_{u,m} \tag{5.4a}$$

$$\gamma_b(m) \leq \mathrm{SNR}_{b,m} \tag{5.4b}$$

$$p_r(\boldsymbol{\delta},\boldsymbol{\lambda}_u,\boldsymbol{\Lambda}_b) \leq P_r$$

$$p_u(\boldsymbol{\lambda}_u) \leq P_u, \quad p_b(\boldsymbol{\lambda}_b) \leq P_b.$$

We next state the following lemma regarding the constraints.

Lemma 6 *The inequality constraints* (5.4a) *and* (5.4b) *are upper bounded posynomials in optimization variables* $\boldsymbol{\delta}, \boldsymbol{\lambda}_u, \boldsymbol{\lambda}_b$.

Proof. Please see Appendix C.2.

The above optimization problem can be equivalently written as

$$\underset{\boldsymbol{\delta},\boldsymbol{\lambda}_u,\boldsymbol{\lambda}_b,\boldsymbol{\gamma}_u,\boldsymbol{\gamma}_b}{\text{Maximize}} \frac{1}{2}\log\Big(\prod_{m=1}^{M}(1+\gamma_u(m))(1+\gamma_b(m))\Big)$$

$$\text{s.t.} \quad \gamma_u(m) \leq \text{SNR}_{u,m}$$

$$\gamma_b(m) \leq \text{SNR}_{b,m}$$

$$p_r(\boldsymbol{\delta},\boldsymbol{\lambda}_u,\boldsymbol{\Lambda}_b) \leq P_r$$

$$p_u(\boldsymbol{\lambda}_u) \leq P_u, \quad p_b(\boldsymbol{\lambda}_b) \leq P_b.$$

Since $\log(\cdot)$ is non-decreasing function, the $(1/2)\log$ term is dropped from objective function.

$$\underset{\boldsymbol{\delta},\boldsymbol{\lambda}_u,\boldsymbol{\lambda}_b,\boldsymbol{\gamma}_u,\boldsymbol{\gamma}_b}{\text{Minimize}} \prod_{m=1}^{M}\Big[(1+\gamma_u(m))(1+\gamma_b(m))\Big]^{-1}$$

$$\text{s.t.} \quad \gamma_u(m) \leq \text{SNR}_{u,m}$$

$$\gamma_b(m) \leq \text{SNR}_{b,m}$$

$$p_r(\boldsymbol{\delta},\boldsymbol{\lambda}_u,\boldsymbol{\Lambda}_b) \leq P_r$$

$$p_u(\boldsymbol{\lambda}_u) \leq P_u, \quad p_b(\boldsymbol{\lambda}_b) \leq P_b.$$

Equation (5.3a) is product of inverse of two posynomials and consequently not a posynomial. We now approximate these posynomials as monomials using the following Lemma from [67].

Lemma 7 *For $\gamma_i(\xi) \geq 0$, $f(\gamma_i(\xi)) = (1+\gamma_i(\xi))$ can be lower bounded by a monomial function*

$$g(\gamma_i(\xi)) = c_i(\xi)\gamma_i(\xi)^{a_i(\xi)} \tag{5.4e}$$

The expressions of $c_i(\xi)$ and $a_i(\xi)$ that results in best monomial approximation in the neighbourhood of $\widehat{\gamma}_i(m) \geq 0$ are

$$a_i(\xi) = \widehat{\gamma}_i(\xi)(1+\widehat{\gamma}_i(\xi))^{-1}$$

$$c_i(\xi) = \widehat{\gamma}_i(\xi)^{-a_i(\xi)}(1+\widehat{\gamma}_i(\xi)) \tag{5.4f}$$

We use Lemma (7) to define $g(m \mid m_t)$, which majorizes the objective function.

$$g(m \mid m_t) = \prod_{m=1}^{M}\Big[\Big(\gamma_u(m)^{\left(\frac{\widehat{\gamma}_u(m)}{1+\widehat{\gamma}_u(m)}\right)}\Big)\Big(\gamma_b(m)^{\left(\frac{\widehat{\gamma}_b(m)}{1+\widehat{\gamma}_b(m)}\right)}\Big)\Big]^{-1}. \tag{5.4g}$$

We now re-cast the optimization problem using the surrogate function in (5.4e) as

$$\underset{\boldsymbol{\delta},\boldsymbol{\lambda}_u,\boldsymbol{\lambda}_b,\boldsymbol{\gamma}_u,\boldsymbol{\gamma}_b}{\text{Minimize}} \; g(m \mid m_t)$$

$$\text{s.t.} \qquad (5.4\text{a}), (5.4\text{b}), (5.3\text{b}), (5.3\text{c}).$$

We see that the objective function is the product of monomials, and hence a monomial. This is because monomials are closed under multiplication [49]. We have already shown in Lemma 4, Lemma 5 and Lemma 6 that the constraints are upper-bounded posynomials. As a result, the optimization problem is a GP with varibles $\boldsymbol{\gamma}_u, \boldsymbol{\gamma}_b$ in posynomial objective and with $\boldsymbol{\delta}, \boldsymbol{\lambda}_u, \boldsymbol{\lambda}_b, \boldsymbol{\gamma}_u, \boldsymbol{\gamma}_b$ variables as upper bounded posynomial.

The above approximation is iteratively improved in the algorithm summarized below. The initial values of $\widehat{\boldsymbol{\gamma}}_u, \widehat{\boldsymbol{\gamma}}_b$ in the algorithm are derived using the equal power allocation and

---

Algorithm 4: Algorithm for joint power allocation

Input: Given a tolerance $\epsilon > 0$ and the maximum number of iterations L.

Output: $\boldsymbol{\delta}, \boldsymbol{\lambda}_u, \boldsymbol{\lambda}_b, \boldsymbol{\gamma}_b, \boldsymbol{\gamma}_u$ as the solutions.

2 *Initialization*: Calculate initial values $\widehat{\boldsymbol{\gamma}}_b^1, \widehat{\boldsymbol{\gamma}}_u^1$ by allocating equal power.

4 for $m \leftarrow 1$ **to** L **do**

6 $\quad$ Given a feasible $\boldsymbol{\delta}, \boldsymbol{\lambda}_u, \boldsymbol{\lambda}_b, \forall i = u, b$ compute $\left(\frac{\widehat{\gamma}_u(m)}{1+\widehat{\gamma}_u(m)}\right), \left(\frac{\widehat{\gamma}_b(m)}{1+\widehat{\gamma}_b(m)}\right) \forall k = 1, \cdots, K.$

8 $\quad$ Solve the GP to calculate $\boldsymbol{\delta}, \boldsymbol{\lambda}_u, \boldsymbol{\lambda}_b, \boldsymbol{\gamma}_b, \boldsymbol{\gamma}_u$

$$\underset{\boldsymbol{\delta},\boldsymbol{\lambda}_u,\boldsymbol{\lambda}_b,\boldsymbol{\gamma}_u,\boldsymbol{\gamma}_b}{\text{Minimize}} \qquad \prod_{m=1}^{M}\left[\gamma_u(m)^{\left(\frac{\widehat{\gamma}_u(m)}{1+\widehat{\gamma}_u(m)}\right)}\gamma_b(m)^{\left(\frac{\widehat{\gamma}_b(m)}{1+\widehat{\gamma}_b(m)}\right)}\right]^{-1}$$

$$\text{s.t.} \qquad\qquad (5.4\text{a}), (5.4\text{b}), (5.3\text{b}), (5.3\text{c}). \qquad\qquad (5.4\text{i})$$

10 $\quad$ Do until convergence

$\qquad$ **if** $\max |\boldsymbol{\gamma}_b - \widehat{\boldsymbol{\gamma}}_b^m| \leq \epsilon$ *and* $\max |\boldsymbol{\gamma}_u - \widehat{\boldsymbol{\gamma}}_u^m| \leq \epsilon$ **then**

11 $\quad$ break

12 $\quad$ **else** $\widehat{\boldsymbol{\gamma}}_u^{m+1} = \boldsymbol{\gamma}_u, \widehat{\boldsymbol{\gamma}}_b^{m+1} = \boldsymbol{\gamma}_b.$

14 return $\mathbf{p}_r, \mathbf{p}_b, \mathbf{p}_u.$

---

the values of $\left(\frac{\widehat{\gamma}_u}{1+\widehat{\gamma}_u}\right), \left(\frac{\widehat{\gamma}_b}{1+\widehat{\gamma}_b}\right)$ are calculated accordingly.

5.1.1 Simulation Results

Now that the GSVD-GP design has been developed, we quantitatively analyse how well the ncTWR performs. The constituents of $\mathbf{H}_i$ and $\mathbf{G}_i$ are assumed to be i.i.d. complex Gaussian random variables with zero mean and variance h_i^2 and g_i^2, respectively for $i \in \{u, b\}$. We specify the average SNR of TU $\to$ RS and RS$\to$ RU as $\eta_b = h_b^2 = g_b^2$ and of BS $\to$ RS and RS $\to$ BS links as $\eta_u = h_u^2 = g_u^2$ and of TU $\to$ BS and BS $\to$ RU direct links as η_d by fixing noise power at all nodes to unity. We choose $\alpha_{i,1} = \alpha_{i,2} = 3$ and fix $\epsilon = 10^{-4}$. We also assume power at different nodes as $P_r = 10$ dB and $P_u = 5$ dB and $P_b = 10$ dB. We observe from Fig. 5.1 with joint optimal power allocation of proposed method, spectral efficiency (SE) significantly improves with conventional ncTWR, baseline equal power allocation (EPA) [60], Random power allocation (RPA) [60] and one way relaying (OWR). Our proposed joint power allocation of iterative GP algorithm dominated over other power allocation schemes as well for all SNR values.

5.1.2 SE comparison

We compare in Fig. 5.1 the SE of the proposed algorithm (labelled as PNCTWR) with conventional ncTWR (labelled as CNCTWR), which neglects the direct link. We consider $M = 3$ antennas at the BS and TU/RU and and $N = 6$ antennas at the relay. We assume $\eta = \eta_u = \eta_b$. We observe from Fig. 5.1 that the proposed PNCTWR system which also considers the weak links, for all η values, vastly outperforms conventional ncTWR , which does not consider direct link. It shows the importance of considering even "weak" direct links for ncTWR. The proposed design also has much higher SE than EPA, RPA and conventional OWR. Recall that RPA algorithm randomly allocates power to all the node such that their power constraints are met. The degraded performance of OWR is because it requires four channel uses when compared with two in the current design.

We next consider in Fig. 5.2 the same parameters as above analysis except that the SNR η_b is fixed at 10 dB. We now only vary the SNR η_u. Such a study helps in analyzing the unbalanced links. We again observe that the proposed algorithm outperforms the conventional ncTWR, EPA, RPA and OWR for all η_u values.
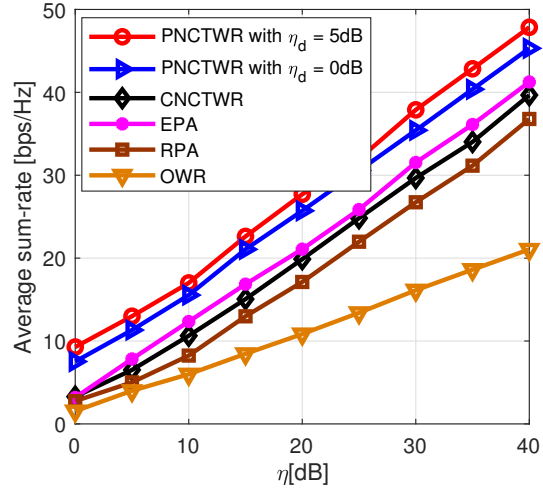
Figure 5.1: SE comparision of two protocols for $\eta = \eta_u = \eta_b$ with different antenna configurations M=3 and N=6 antennas
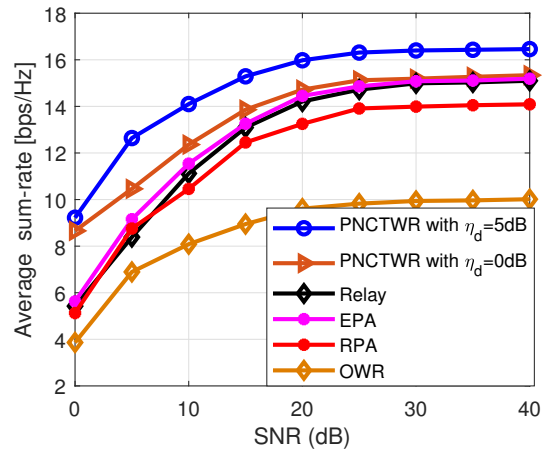
Figure 5.2: SE comparision of two protocols for fixed η_b with antenna configuration M=3 and N=6 antennas.

5.1.3   Numerical convergence analysis

The proposed algorithm's convergence is then examined by plotting the average SE attained throughout each iteration. We consider the same parameters as in Fig. 5.1. We observe that for various η values, the SE of the proposed algorithm saturates within 5 iterations.
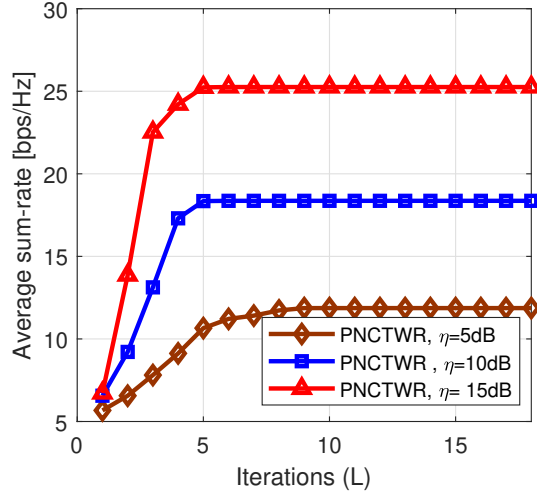
Figure 5.3: SE vs L with M=4 and N=8 antennas, and $\eta_d = 5$ dB

5.2   GEE using Dinkelbach and geometric programming approach

The GEE is defined as the ratio of the system SE and its total power consumption [44].

$$\text{GEE} = \frac{\frac{1}{2}\sum_{i\in\{u,b\}}\sum_{m=1}^{M}\log(1+\text{SNR}_{i,m}(\boldsymbol{\delta},\boldsymbol{\lambda}_i))}{\sum_{m=1}^{M}\delta_{u,m}+\delta_{b,m}+\lambda_{u,m}+\lambda_{b,m}+P_{CP}}. \tag{5.4j}$$

Here P_{CP} is the fixed circuit power consumed by the system, which consists of the power required by the transceiver chains, signal processing and the backhaul network [68]. We next formulate the GEE maximization problem as follows:

$$\underset{\boldsymbol{\delta},\boldsymbol{\lambda_u},\boldsymbol{\lambda_b},}{\text{Maximize}}\frac{\frac{1}{2}\sum_{i\in\{u,b\}}\sum_{m=1}^{M}\log(1+\text{SNR}_{i,m}(\boldsymbol{\delta},\boldsymbol{\lambda}_i))}{\sum_{m=1}^{M}\delta_{u,m}+\delta_{b,m}+\lambda_{u,m}+\lambda_{b,m}+P_{CP}}$$

$$\text{s.t.} \qquad (5.3b),(5.3c).$$

5.2.1 Realistic power consumption model:

We consider the realistic power consumption model, which similar to [68], is given as follows:

$$P_{CP} = P_{FIX} + P_{TC} + P_{BH} + P_{LP}. \tag{5.4l}$$

The constant power P_{FIX} is required for the control signaling, site-cooling, backhaul infrastructure and the baseband processors. The power P_{TC}, P_{BH} and P_{LP} are consumed by the transceiver chain, load-dependent backhaul, and linear processing, respectively.

We recall from our earlier discussion while maximizing SE, that the SE optimization is non-convex as it is a ratio of two posynomials, which is not a posynomial. The GEE problem is a fractional function of non-convex numerator and a linear denominator. We now solve the GEE optimization problem by combining the GP and Dinkelbach algorithms [66]. We begin by using the GP approach, similar to SE maximization problem, to cast the numerator as concave function

$$\underset{\delta, \lambda_u, \lambda_b, \gamma_u, \gamma_b}{\text{Maximize}} \frac{g(m \mid m_t)^{-1}}{\sum_{m=1}^{M} \delta_{u,m} + \delta_{b,m} + \lambda_{u,m} + \lambda_{b,m} + P_{CP}}$$

$$\text{s.t.} \qquad (5.4a), (5.4b), (5.3b), (5.3c).$$

We assert the following proposition in order to apply the Dinkelbach algorithm [66].

Proposition 3 *Consider a function of ratio problem*

$$\underset{x}{Max} \frac{f(x)}{g(x)} \quad subject\ to\ x \in \chi, \tag{5.4n}$$

where χ is a convex set, and $f(x)$ is a non-negative, differential and a concave function of x and $g(x)$ is a positive, differential and convex function of x. The function $z(x) = \frac{f(x)}{g(x)}$ is known to be pseudo-concave (PC) with respect to x and the optimization problem with $z(x)$ as objective function similar to (5.4n) are called as concave-convex fractional program (CCFP). We note that $x^\star$ (stationary point) of $z(x)$ is its global maximizer and it is identical to determining positive zero of $D(\lambda)$, which is defined as

$$D(\lambda) = \underset{x}{Max} f(x) - \lambda g(x) \quad subject\ to\ x \in \chi, \tag{5.4o}$$

Here, $D(\lambda)$ is a continuous, strictly monotonically decreasing, convex function, and the Dinkelbach technique is used to determine its zero.

The equivalent problem of (5.4p) using Dinkelbach algorithm is given as follows

$$\underset{\boldsymbol{\delta},\boldsymbol{\lambda_u},\boldsymbol{\lambda_b},\boldsymbol{\gamma_u},\boldsymbol{\gamma_b}}{\text{Minimize}}\, g(m \mid m_t) + \lambda \sum_{m=1}^{M} \delta_{u,m} + \delta_{b,m} + \lambda_{u,m} + \lambda_{b,m} + P_{CP}$$

s.t.   (5.4a), (5.4b), (5.3b), (5.3c).

The iterative GP-Dinkelbach procedure for GEE maximization is summarized in Algorithm 4.

Algorithm 5: GP Dinkelbach algorithm for GEE maximization

Input: Given a tolerance $\epsilon > 0$ and the maximum number of iterations L.

Output: $\boldsymbol{\delta}, \boldsymbol{\lambda}_u, \boldsymbol{\lambda}_b, \boldsymbol{\gamma}_b, \boldsymbol{\gamma}_u$ as the solutions.

2 *Initialization*: Calculate initial values $\widehat{\boldsymbol{\gamma}}_b^1, \widehat{\boldsymbol{\gamma}}_u^1$ by allocating equal power .

4 for $m \leftarrow 1$ **to** L **do**

6   Given a feasible $\boldsymbol{\delta}, \boldsymbol{\lambda}_u, \boldsymbol{\lambda}_b, \forall i = u, b$ compute $\left(\frac{\widehat{\gamma}_u(m)}{1+\widehat{\gamma}_u(m)}\right), \left(\frac{\widehat{\gamma}_b(m)}{1+\widehat{\gamma}_b(m)}\right) \forall k = 1, \cdots, K.$

8   Solve the GP to calculate $\boldsymbol{\delta}, \boldsymbol{\lambda}_u, \boldsymbol{\lambda}_b, \boldsymbol{\gamma}_b, \boldsymbol{\gamma}_u$

$$\underset{\boldsymbol{\delta},\boldsymbol{\lambda_u},\boldsymbol{\lambda_b},\boldsymbol{\gamma_u},\boldsymbol{\gamma_b}}{\text{Minimize}}\, g(m \mid m_t) + \lambda \sum_{m=1}^{M} \delta_{u,m} + \delta_{b,m} + \lambda_{u,m} + \lambda_{b,m} + P_c$$

s.t.   (5.4a), (5.4b), (5.3b), (5.3c).

10   Do until convergence

        if $\max |\boldsymbol{\gamma}_b - \widehat{\boldsymbol{\gamma}}_b^m| \leq \epsilon$ *and* $\max |\boldsymbol{\gamma}_u - \widehat{\boldsymbol{\gamma}}_u^m| \leq \epsilon$ **then**

11   break

12   **else** $\widehat{\boldsymbol{\gamma}}_u^{m+1} = \boldsymbol{\gamma}_u$, $\widehat{\boldsymbol{\gamma}}_b^{m+1} = \boldsymbol{\gamma}_b$.

14 return $\mathbf{p}_r, \mathbf{p}_b, \mathbf{p}_u$.

5.3   Simulation results

5.3.1   GEE maximization comparison

We compare in Fig. 5.4 the GEE of the proposed GP-Dinkelbach Algorithm (PGPD) with that of the equal power allocation (EPA), and the random power allocation (RPA). We also consider a conventional ncTWR system which neglects the direct link. The power allocation algorithms for this system is labeled as conventional equal power allocation (lCEPA), conventional random power allocation (CRPA). We consider $M = 5$ and $N = 10$; all other parameters are same as the SE analysis in Fig. 5.1. We assume a circuit power consumption of $P_c = 5$ dB. We observe that GEE of the proposed Algorithm 5 increases till $\eta = 8$ dB, and remains constant after that. The GEE of all other algorithms reduces. This is because till $\eta = 8$ dB, the increase in SE is proportionate with the power expended to achieve it. For $\eta \geq 8$ dB, this does not happen. The proposed algorithm then stops allocating power, and the GEE consequently saturates. Other algorithms, on contrast, continues to expend power, which reduces their GEE. We also note that the system GEE increases considerably by considering the direct link.
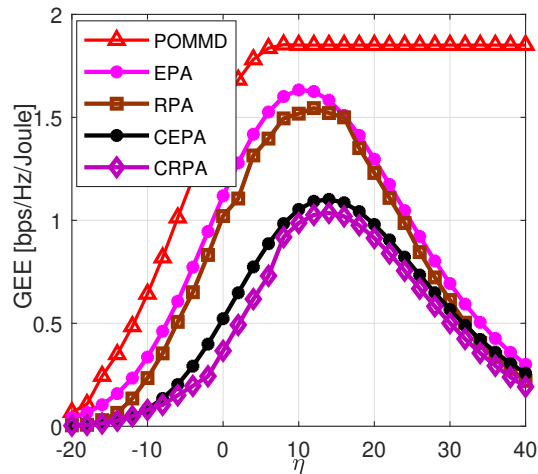
Figure 5.4: GEE vs η with M = 5 and N = 10 antennas, and $\eta_d = 5$ dB

5.3.2 Numerical convergence analysis

Figure 5.5 evaluates the performance of GP-Dinkelbach's Algorithm 5 in maximizing the GEE with respect to number of iterations L. We observe that algorithm converges within 8 iterations.
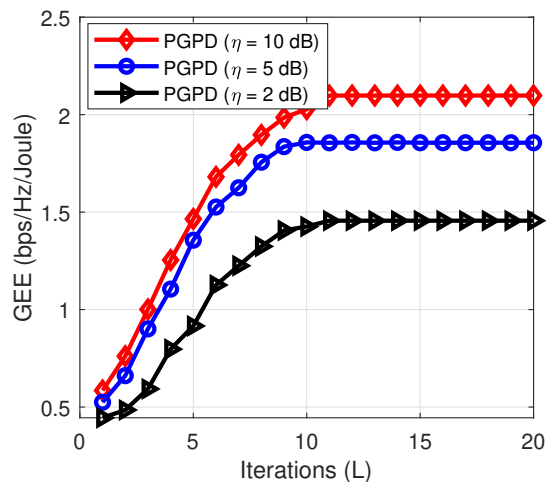
Figure 5.5: GEE vs vs L with M=5 and N=10 antennas, and $\eta_d = 5$ dB

5.4 Summary

We proposed a novel GSVD-based transceiver design for ncTWR by considering the direct link, an aspect none of the existing ncTWR works have exploited. We also developed two optimization algorithms to optimize the SE and GEE of this system. The first uses only GP, while the second one combines GP with Dinkelbach algorithm. We numerically investigated the SE and GEE of above transceiver design and the optimization algorithms, and showed their improved performance.

Chapter 6

Summary and Future Directions

6.1   Thesis Summary

Conventional two-way relaying (TWR) assumes data flows back and forth between a user and the BS. Typically, cellular networks do not operate under the premise that traffic flows in both directions. For instance, a receive-only user RU requests data in the downlink alone, while a transmit-only user TU sends data in the uplink only. TWR becomes to spectrally inefficient one-way relaying in such situations when there is a one-way traffic flow. To re-establish the two-way traffic flow, we considered non-concurrent TWR (ncTWR). In this protocol, the uplink phase of TU is followed by the downlink phase of RU to transmit its downlink data to the RU. But unlike TWR, the RU can no longer eliminate the back-propagating interference (BI).

We first considered OFDM-based ncTWR with all single-antenna modes, and introduced a novel overhearing-based BI cancellation method to cancel BI at the RU. We optimize the non-convex SE for the proposed model by developing a joint power allocation algorithm, which optimizes it using successive convex approximation approach (SCA). We showed that the proposed algorithm yields better SE rate than the baseline equal and random power allocation schemes.

Next, with the goal of reducing energy consumption, we designed an algorithm to maximize the global energy efficiency (GEE) for OFDM ncTWR. To maximise GEE, we simultaneously optimized the relay and user powers. The objective function in GEE maximization

is non-convex. We used a novel quadratic transformation to develop a joint power allocation algorithm for GEE optimization. We showed that the proposed algorithm uses less than the maximum available power, and outperforms other state-of-the-art algorithms.

We then extended the ncTWR system to MIMO nodes with direct links. We developed a novel GSVD-based transceiver design for MIMO ncTWR by exploiting the weak direct link. We developed GP and Dinkelbach-based algorithms for this transceiver design to maximize the SE and GEE metrics. We again showed that the proposed algorithms yields higher SE and GEE than the other power allocation schemes.

6.2   Scope for future work

1. For OFDM ncTWR and MIMO ncTWR, other relaying techniques including compress and forward, compute and forward, and decode and forward have not yet been studied. Future research might look into incorporating the aforementioned relaying techniques into the existing framework.

2. Future research could also consider MIMO nodes for OFDM ncTWR. This is a challenging area, with multiple possible novel OFDM-based MIMO ncTWR transceiver designs.

3. Designing SE optimum transceivers for multi-antenna OFDM-based ncTWR systems is an additional future objective.

4. Design of OFDM ncTWR schedulers must be explored. Designing a hybrid BS and relay scheduler that maximizes throughput while maintaining fairness is an intersting topic.

Appendix A

Appendix for Chapter 2

A.1 Derivations for Eq. 2.10, 2.11, 2.12

The expressions for $\tilde{y}_b[k]$ and $\tilde{y}_u[k]$ are as follows:

$$\tilde{y}_b[k] = \sqrt{p_r[k]} g_b[k] h_u[k] x_u[k] + \bar{n}_b[k].$$

$$\tilde{y}_u[k] = \sqrt{p_r[k]} g_u[k] h_b[k] x_b[k] + \bar{n}_u^2[k] - \frac{\sqrt{p_r[k]} g_u[k] h_u[k]}{h_0[k]} n_u^1[k].$$

From the above expressions, using Shannon's theorem, we write $R_b[k]$ and $R_u[k]$ as follows:

$$R_b[k] = \frac{1}{2} \log_2 \left(1 + \mathrm{SNR}_b[k] \right)$$

$$R_u[k] = \frac{1}{2} \log_2 \left(1 + \mathrm{SNR}_u[k] \right).$$

The factor $\frac{1}{2}$ is because the HD relay cannot transmit and receive simultaneously on the same spectral resource. The expression $\mathrm{SNR}_b[k]$ is defined as ratio of signal power to noise power from $R_b[k]$ and similarly the $\mathrm{SNR}_u[k]$ is defined as ratio of signal power to noise power from $R_u[k]$.

$$\mathrm{SNR}_b[k] = \frac{|h_u[k] g_b[k]|^2 p_r[k] p_u[k]}{1 + |g_b[k]|^2 p_r[k]}$$

$$\mathrm{SNR}_u[k] = \frac{|g_u[k] h_b[k]|^2 p_r[k] p_b[k]}{1 + |g_u[k]|^2 p_r[k] + |\frac{g_u[k] h_u[k]}{h_o[k]}|^2 p_r[k]}.$$

Appendix B

Appendix for Chapter 3

B.1   Geometric Programming

We briefly discuss about the terminology of geometric programming from [**?**].

A function $f : \mathbb{R}^n_{++} :\to \mathbb{R}$ is described to be monomial if

$$f(x) = px_1^{c_1} x_2^{c_2} \cdots x_n^{c_n}. \tag{5.4a}$$

where $p > 0$ and $c_j \in \mathbb{R}$. A sum of monomials. i.e.,

$$f(x) = \sum_{k=1}^{K} p_k x_1^{c_{1k}} x_2^{c_{2k}} \cdots x_n^{c_{nk}}. \tag{5.4b}$$

where $p_k > 0$ is called a posynomial and $\mathbb{R}^n_{++}$ is a collection of positive real vectors with n dimensions. A posynomial serves as the objective in a standard from GP, and upper bounded posynomials serve as the inequality constraints whereas the monomials serve as the equality constraints. Following a logarithmic shift in the variables, the posynomial objective can be turned into a convex function and upper-bounded posynomial constraints can be turned into a convex set. There is no division closure for the posynomials, although they are closed under addition and multiplication.

B.2   Proof of Lemma 2

Using the first-order Taylor series approximation [59], any function in two variables x and y i.e., f(x,y) is estimated around a point (a, b) as

$$f(x, y) = f(a, b) + \left[\frac{\partial f(x, y)}{\partial x}\right]_{a,b} (x - a) + \left[\frac{\partial f(x, y)}{\partial x}\right]_{a,b} (x - b).$$

We apply the above approximation for the terms $p_r[k]p_b[k]$ and $p_r[k]p_u[k]$ around the points $\tilde{p}_r[k]$, $\tilde{p}_u[k]$ and $\tilde{p}_b[k]$, and

$$p_r[k]p_b[k] \approx \tilde{p}_r[k]\tilde{p}_b[k] + \tilde{p}_b[k](p_r[k] - \tilde{p}_r[k]) + \tilde{p}_r[k](p_b[k] - \tilde{p}_b[k]),$$

$$p_r[k]p_u[k] \approx \tilde{p}_r[k]\tilde{p}_u[k] + \tilde{p}_u[k](p_r[k] - \tilde{p}_r[k]) + \tilde{p}_r[k](p_u[k] - \tilde{p}_u[k]).$$

We used the fact that the first-order Taylor series approximation of a convex function provides a lower bound on the function [59]. The bound, as discussed in [59], is a tight one, and is a commonly used heuristic to approximate the problem as convex which leads close-to-optimal results.

Appendix C

Appendix for Chapter 5

C.1   Proof of Lemma 5

The transmit power of the RS is given in (4.7). To prove the lemma, we proceed in the following way. The channel-triangularizing preocoder matrix $\mathbf{D}$ is rewritten as

$$\mathbf{D} = \underbrace{\begin{bmatrix} \mathbf{V}_{\tilde{\mathbf{G}}_b} & 0 \\ 0 & \mathbf{V}_{\tilde{\mathbf{G}}_u} \end{bmatrix}}_{\mathbf{V}} \underbrace{\begin{bmatrix} 0 & \triangle_b \\ \triangle_u & 0 \end{bmatrix}}_{\triangle} \underbrace{\begin{bmatrix} \mathbf{U}_{\tilde{\mathbf{H}}_u}^H & 0 \\ 0 & \mathbf{U}_{\tilde{\mathbf{H}}_b}^H \end{bmatrix}}_{\mathbf{U}}.$$

The matrices $\mathbf{V}_{\tilde{\mathbf{G}}_i}$ and $\mathbf{U}_{\tilde{\mathbf{H}}_i}^H$ are the unitary matrices and $\triangle$ is an anti-diagonal matrix. The precoder $\mathbf{W} = \mathbf{MDF}$ is now written as $\mathbf{W} = \mathbf{MV}\triangle\mathbf{UF} = \overline{\mathbf{M}}\triangle\overline{\mathbf{F}}$ where $\overline{\mathbf{M}} = \mathbf{MV}$ and $\overline{\mathbf{F}} = \mathbf{UF}$. The columns of $\overline{\mathbf{M}}$ and the rows of $\overline{\mathbf{F}}$ will be orthonormal. Now, the constraint in (4.7) can be expressed more simply as an upper-bounded posynomial.

Here in the following proof, $\mathbf{H}_j^b$ and $\mathbf{H}_j^u$ define the j th column of $\mathbf{H}_b$ and $\mathbf{H}_u$, respectively. Also, $\overline{\mathbf{H}}_j^b = \overline{\mathbf{F}}\mathbf{H}_j^b = [\overline{\mathbf{H}}_{j,1}^b ..., ..., \overline{\mathbf{H}}_{j,M}^b]^T$, $\overline{\mathbf{H}}_j^u = \overline{\mathbf{F}}\mathbf{H}_j^u = [\overline{\mathbf{H}}_{j,1}^u ..., ..., \overline{\mathbf{H}}_{j,M}^u]^T$, $\widehat{m} = 2M - m + 1$ and $m = M - m + 1$. We make use of the orthonormal columns that the $\overline{M}$ possesses by design in (a). The following facts are used to derive equality in clause (b):

1. $\mathrm{Tr}(\mathbf{AB}) = \mathrm{Tr}(\mathbf{BA})$ for a given compatible matrices $\mathbf{A}$ and $\mathbf{B}$.

2. Orthonormal columns exist in $\overline{M}$ and orthonormal rows exist in $\overline{F}$. Since of $\delta_{u,m}$ and $\delta_{b,m}$ coefficients are non-negative, the above constraint can be stated as upper bounded posynomial.

$$P_r \geq \mathrm{Tr}(\mathbb{E}(\mathbf{x}_r \mathbf{x}_r^H))$$

$$= \mathrm{Tr}(\mathbf{W}\mathbf{H}\mathbf{\Xi}\mathbf{H}^H \mathbf{W}^H + \sigma_r^2 \mathbf{W}\mathbf{W}^H)$$

$$= \sum_{j=1}^{M} \left\{ \lambda_{u,j} \parallel \mathbf{W}\mathbf{H}_j^u \parallel^2 + \lambda_{b,j} \parallel \mathbf{W}\mathbf{H}_j^b \parallel^2 \right\} + \sigma_r^2 \mathrm{Tr}(\mathbf{W}\mathbf{W}^H)$$

$$= \sum_{j=1}^{M} \left\{ \lambda_{u,j} \parallel \overline{\mathbf{M}}\triangle\overline{\mathbf{F}}\mathbf{H}_j^u \parallel^2 + \lambda_{b,j} \parallel \overline{\mathbf{M}}\triangle\overline{\mathbf{F}}\mathbf{H}_j^b \parallel^2 \right\} + \sigma_r^2 \mathrm{Tr}(\mathbf{W}\mathbf{W}^H)$$

$$= \sum_{j=1}^{M} \left\{ \lambda_{u,j} \parallel \overline{\mathbf{M}}\triangle\overline{\mathbf{H}}_j^u \parallel^2 + \lambda_{b,j} \parallel \overline{\mathbf{M}}\triangle\overline{\mathbf{H}}_j^b \parallel^2 \right\} + \sigma_r^2 \mathrm{Tr}(\mathbf{W}\mathbf{W}^H)$$

$$\overset{(a)}{=} \sum_{j=1}^{M} \left\{ \lambda_{u,j} \parallel \triangle\overline{\mathbf{H}}_j^u \parallel^2 + \lambda_{b,j} \parallel \triangle\overline{\mathbf{H}}_j^b \parallel^2 \right\} + \sigma_r^2 \mathrm{Tr}(\triangle\triangle^H)$$

$$\overset{(b)}{\geq} \sum_{m=1}^{M} \sum_{j=1}^{M} \left\{ \lambda_{b,j} |\overline{\mathbf{H}}_{j,\widehat{m}}^b|^2 + \lambda_{u,j} |\overline{\mathbf{H}}_{j,\widehat{m}}^u|^2 + \sigma_r^2 \right\} \delta_{b,m} + \left\{ \lambda_{u,j} |\overline{\mathbf{H}}_{j,\widehat{m}}^u|^2 + \lambda_{b,j} |\overline{\mathbf{H}}_{j,\widehat{m}}^b|^2 + \sigma_r^2 \right\} \delta_{u,m}.$$

$$(5.4a)$$

C.2   Proof of Lemma 4

For notational convinence, we consider $\boldsymbol{\Upsilon} = \mathbf{U}_{\tilde{g}_u}^H \tilde{\mathbf{G}}_n \mathbf{V}_{\tilde{g}_b}$. Consider the inequality constraint in (5.4a) i.e., $\gamma_u(m) \leq \mathrm{SNR}_{u,m}$. By substituting the expression of $\mathrm{SNR}_{u,m}$ from (4.47) in the above constraint we rewrite the inequality constraint as shown in (5.4b).

$$\gamma_u(m) \leq \frac{\lambda_{b,m}\sigma_{r,m}^2\left|[\mathbf{L}_R]_{m,m}\right|^2 + \delta_{u,m}\sigma_{\tilde{g}_u,m}^2\sigma_{\tilde{h}_u,m}^2\lambda_{b,m}\left|[\mathbf{L}_R]_{m,m}\right|^2 + 2\sqrt{\delta_{u,m}}\lambda_{b,m}\sigma_{r,m}\sigma_{\tilde{g}_u,m}\sigma_{\tilde{h}_u,m}\left|[\mathbf{L}_r]_{m,m}\right|^2}{\sigma_p^2\sum_{k=1}^M\left\{\delta_{b,k}\left(\boldsymbol{\Upsilon}_{m,k}\boldsymbol{\Upsilon}_{m,k}^*\right)\right\} + \delta_{u,m}\sigma_{\tilde{g}_u,m}^2\sigma_p^2 + \sigma^2 + \sigma^2}$$

$$(5.4\mathrm{b})$$

$$\gamma_u(m)\left\{\sigma_p^2\sum_{k=1}^M\delta_{b,k}\boldsymbol{\Upsilon}_{m,k}\boldsymbol{\Upsilon}_{m,k}^* + \delta_{u,m}\sigma_{\tilde{g}_u,m}^2\sigma_p^2 + 2\sigma^2\right\} \leq \lambda_{b,m}\sigma_{r,m}^2\left|[\mathbf{L}_R]_{m,m}\right|^2\left\{1 + \frac{\delta_{u,m}\sigma_{\tilde{g}_u,m}^2\sigma_{\tilde{\mathbf{h}}_u,m}^2}{\sigma_{r,m}^2}\right.$$
$$\left. + \frac{2\sqrt{\delta_{u,m}}\sigma_{\tilde{g}_u,m}\sigma_{\tilde{h}_u,m}}{\sigma_{r,m}}\right\}. \quad (5.4\mathrm{c})$$

Here, the equations on LHS and RHS of the equation (5.4c) are posynomials. The ratio of two posynomials is obtained when we take their ratio. Given that a posynomial is not closed under division, the resultant of the ratio is not a posynomial. In GP, we need to have the inequality constraint to be upper bounded posynomial. We rewrite (5.4c) as (5.4d).

$$\gamma_u(m)\left\{\sigma_p^2\sum_{k=1}^M\left\{\delta_{b,k}\left(\boldsymbol{\Upsilon}_{m,k}\boldsymbol{\Upsilon}_{m,k}^*\right)\right\} + \delta_{u,m}\sigma_{\tilde{g}_u,m}^2\sigma_p^2 + 2\sigma^2\right\} \leq \lambda_{b,m}\sigma_{r,m}^2\left|[\mathbf{L}_R]_{m,m}\right|^2\left\{1 + \beta_u(m)\right\}^2.$$

$$(5.4\mathrm{d})$$

Here, $\beta_u(m) = \frac{\sqrt{\delta_{u,m}}\sigma_{\tilde{g}_u,m}\sigma_{\tilde{h}_u,m}}{\sigma_{r,m}}$. Rewriting (5.4d) as (5.4e), we can observe it as ratio of two posynomials.

$$\frac{\lambda_{b,m}^{-1}\sigma_{r,m}^{-2}\left|[\mathbf{L}_R]_{m,m}\right|^{-2}\gamma_u(m)\left\{\sigma_p^2\sum_{k=1}^M\left\{\delta_{b,k}\left(\boldsymbol{\Upsilon}_{m,k}\boldsymbol{\Upsilon}_{m,k}^*\right)\right\} + \delta_{u,m}\sigma_{\tilde{g}_u,m}^2\sigma_p^2 + 2\sigma^2\right\}}{\left\{1 + \beta_u(m)\right\}^2} \leq 1. \quad (5.4\mathrm{e})$$

So to prove this lemma, we use a similar approach as in [56]. A posynomial in the ratio's denominator is reduced to a monomial using this method. This results in the overall term to be posynomial. As a result, the problem is solved iteratively to enhance the approximation at each stage. Using the monomial approximation i.e., Lemma (6), we can reduce the denominator in LHS expression in (5.4e) into monomial. The resulting expression after the monomial

approximation expression is given as in (5.4f). By using the monomial approximation, our aim of showing the (5.4b) to be upper bounded posynomial is achieved and shown in (5.4f). Similarly, (5.4b) can be showed to be upper bounded posynomial.

$$
\frac{\lambda_{b,m}^{-1}\sigma_{r,m}^{-2}\left|[\mathbf{L}_R]_{m,m}\right|^{-2}\gamma_u(m)\left\{\sigma_p^2\sum_{k=1}^M\left\{\delta_{b,k}\left(\mathbf{\Upsilon}_{m,k}\mathbf{\Upsilon}_{m,k}^*\right)\right\}+\delta_{u,m}\sigma_{\tilde{g}_u,m}^2\sigma_p^2+2\sigma^2\right\}}{\left\{\beta_u(m)^{r_u(m)}\right\}^2}\leq 1.
$$

$$(5.4f)$$

References

[1] T. Mekkawy, R. Yao, N. Qi, and Y. Lu, "Secure relay selection for two way amplify-and-forward untrusted relaying networks," *IEEE Trans. Veh. Technol.*, vol. 67, no. 12, pp. 11 979–11 987, 2018.

[2] A. K. Dutta, K. Hari, and L. Hanzo, "Linear transceiver design for an amplify-and-forward relay based on the mber criterion," *IEEE Trans. Commun.*, vol. 62, no. 11, pp. 3765–3777, 2014.

[3] J. Sydir and R. Taori, "An evolved cellular system architecture incorporating relay stations," *IEEE Commun. Mag.*, vol. 47, no. 6, pp. 115–121, 2009.

[4] Q. Li, S. Feng, X. Ge, G. Mao, and L. Hanzo, "On the performance of full-duplex multi-relay channels with df relays," *IEEE Trans. Veh. Technol.*, vol. 66, no. 10, pp. 9550–9554, 2017.

[5] Y. Hu, C. Xu, Y. Zhang, and L. Ping, "Joint power and rate allocation for df two-path relay systems," *IEEE Commun. Lett.*, vol. 5, no. 6, pp. 620–623, 2016.

[6] I. Ahmad, K. D. Nguyen, N. Letzepis, and A. Pollok, "On the hopping loss in mimo decode-and-forward cooperative relaying," *IEEE Trans. Commun.*, vol. 66, no. 1, pp. 54–63, 2018.

[7] Z. Chen, T. Q. S. Quek, and Y.-C. Liang, "Spectral efficiency and relay energy efficiency of full-duplex relay channel," *IEEE Trans. Wireless Commun.*, vol. 16, no. 5, pp. 3162–3175, 2017.

[8] A. Almradi, P. Xiao, and K. A. Hamdi, "Hop-by-hop zf beamforming for mimo full-duplex relaying with co-channel interference," *IEEE Trans. Commun.*, vol. 66, no. 12, pp. 6135–6149, 2018.

[9] H. Shen, Z. He, W. Xu, S. Gong, and C. Zhao, "Is full-duplex relaying more energy efficient than half-duplex relaying?" *IEEE Commun. Lett.*, vol. 8, no. 3, pp. 841–844, 2019.

[10] S. Sohaib and M. Uppal, "Full-duplex compress-and-forward relaying under residual self-interference," *IEEE Trans. Veh. Technol.*, vol. 67, no. 3, pp. 2776–2780, 2018.

[11] Y. Jin, X.-G. Xia, Y. Chen, and R. Li, "Full-duplex delay diversity relay transmission using bit-interleaved coded ofdm," *IEEE Trans. Commun.*, vol. 65, no. 8, pp. 3250–3258, 2017.

[12] G. Chen, P. Xiao, J. R. Kelly, B. Li, and R. Tafazolli, "Full-duplex wireless-powered relay in two way cooperative networks," *IEEE Access*, vol. 5, pp. 1548–1558, 2017.

[13] J. Hou, S. Narayanan, N. Yi, Y. Ma, and M. Shikh-Bahaei, "Symbol-level selective full-duplex relaying with power and location optimization," *IEEE Trans. Commun.*, vol. 66, no. 11, pp. 5097–5111, 2018.

[14] A. Nordio and C. F. Chiasserini, "Mimo full-duplex networks with limited knowledge of the relay state," *IEEE Trans. Commun.*, vol. 20, no. 4, pp. 2516–2529, 2021.

[15] A. Sabharwal, P. Schniter, D. Guo, D. W. Bliss, S. Rangarajan, and R. Wichman, "In-band full-duplex wireless: Challenges and opportunities," *IEEE J. Sel. Areas Commun.*, vol. 32, no. 9, pp. 1637–1652, 2014.

[16] Z. Zhang, K. Long, A. V. Vasilakos, and L. Hanzo, "Full-duplex wireless communications: Challenges, solutions, and future research directions," *Proceedings of the IEEE*, vol. 104, no. 7, pp. 1369–1409, 2016.

[17] C. Raman, G. J. Foschini, R. A. Valenzuela, R. D. Yates, and N. B. Mandayam, "Half-duplex relaying in downlink cellular systems," *IEEE Trans. Wireless Commun.*, vol. 10, no. 5, pp. 1396–1404, 2011.

[18] B. Radunovic and A. Proutiere, "On downlink capacity of cellular data networks with wlan/wpan relays," *IEEE/ACM Trans. Netw.*, vol. 21, no. 1, pp. 286–296, 2013.

[19] L. Sanguinetti, A. A. D'Amico, and Y. Rong, "A tutorial on the optimization of amplify-and-forward mimo relay systems," *IEEE J. Sel. Areas Commun.*, vol. 30, no. 8, pp. 1331–1346, 2012.

[20] I. Hammerstrom and A. Wittneben, "Power allocation schemes for amplify-and-forward mimo-ofdm relay links," *IEEE Trans. Wireless Commun.*, vol. 6, no. 8, pp. 2798–2802, August 2007.

[21] O. Munoz-Medina, J. Vidal, and A. Agustin, "Linear transceiver design in nonregenerative relays with channel state information," *IEEE Trans. Signal Process.*, vol. 55, no. 6, pp. 2593–2604, June 2007.

[22] D. Hwang, S.-G. Hong, and T.-J. Lee, "Multiuser two way relaying schemes in the future cellular network," *IEEE Transactions on Wireless Communications*, vol. 12, no. 10, pp. 5200–5207, 2013.

[23] H. Li and X. Zhao, "Joint resource allocation for ofdm-based cognitive two-way multiple af relays networks with imperfect spectrum sensing," *IEEE Trans. Veh. Technol.*, vol. 67, no. 7, pp. 6286–6300, 2018.

[24] S. Katti, H. Rahul, W. Hu, D. Katabi, M. Medard, and J. Crowcroft, "Xors in the air: Practical wireless network coding," *IEEE/ACM Trans. Netw.*, vol. 16, no. 3, pp. 497–510, June 2008.

[25] B. Rankov and A. Wittneben, "Spectral efficient protocols for half-duplex fading relay channels," *IEEE J. Sel. Areas Commun.*, vol. 25, no. 2, pp. 379–389, February 2007.

[26] C. Sun, C. Yang, Y. Li, and B. Vucetic, "Transceiver design for multi-user multi-antenna two-way relay cellular systems," *IEEE Trans. Commun.*, vol. 60, no. 10, pp. 2893–2903, 2012.

[27] M. Alaaeldin, E. A. Alsusa, and K. G. Seddik, "Irs-assisted physical layer network coding over two-way relay fading channels," *IEEE Trans. Veh. Technol.*, pp. 1–1, 2022.

[28] V. T. Muralidharan and B. S. Rajan, "Wireless network coding for mimo two-way re-laying," *IEEE Trans. Wireless Commun.*, vol. 12, no. 7, pp. 3566–3577, 2013.

[29] G. Cai, Y. Fang, G. Han, J. Xu, and G. Chen, "Design and analysis of relay-selection strategies for two-way relay network-coded dcsk systems," *IEEE Trans. Veh. Technol.*, vol. 67, no. 2, pp. 1258–1271, 2018.

[30] H. Pan, T.-T. Chan, V. C. M. Leung, and J. Li, "Age of information in physical-layer network coding enabled two-way relay networks," *IEEE Trans. Mobile Comput.*, pp. 1–1, 2022.

[31] C. Peng, F. Li, and H. Liu, "Optimal power splitting in two-way decode-and-forward relay networks," *IEEE Commun. Lett.*, vol. 21, no. 9, pp. 2009–2012, 2017.

[32] S. C. Liew, S. Zhang, and L. Lu, "Physical-layer network coding: Tutorial, survey, and beyond," *Physical Communication*, vol. 6, pp. 4 – 42, 2013, network Coding and its Applications to Wireless Communications.

[33] J. You, E. Liu, R. Wang, and W. Su, "Joint source and relay precoding design for MIMO two-way relay systems with transceiver impairments," *IEEE Commun. Lett.*, vol. 21, no. 3, pp. 572–575, 2017.

[34] B. Rankov and A. Wittneben, "Spectral efficient protocols for half-duplex fading relay channels," *IEEE J. Sel. Areas Commun.*, vol. 25, no. 2, pp. 379–389, 2007.

[35] R. Budhiraja and B. Ramamurthi, "Joint transceiver design for non-concurrent MIMO two-way AF relaying," *IEEE Wireless Commun. Lett.*, vol. 4, no. 5, pp. 497–500, 2015.

[36] R. Budhiraja and A. K. Chaturvedi, "A common transceiver design for nonregenerative asymmetric and symmetric two-way relaying with relaxed antenna constraints," *IEEE Trans. Veh. Technol.*, vol. 66, no. 8, pp. 7026–7037, Aug 2017.

[37] Z. Liu, X. Tao, and W. ur Rehman, "Resource allocation for two-way amplify and forward ofdm relay networks," *China Communications*, vol. 14, no. 8, pp. 76–82, 2017.

[38] S. Berger, M. Kuhn, A. Wittneben, T. Unger, and A. Klein, "Recent advances in amplify-and-forward two-hop relaying," *IEEE Communications Magazine*, vol. 47, no. 7, pp. 50–56, 2009.

[39] C. Li, J. Wang, F. C. Zheng, J. M. Cioffi, and L. Yang, "Overhearing-based co-operation for two-cell network with asymmetric uplink-downlink traffics," *IEEE Trans. Signal Inf. Process. Netw.*, vol. 2, no. 3, pp. 350–361, 2016.

[40] C. Li, H. J. Yang, F. Sun, J. M. Cioffi, and L. Yang, "Multiuser overhearing for cooperative two-way multiantenna relays," *IEEE Trans. Veh. Technol.*, vol. 65, no. 5, pp. 3796–3802, 2016.

[41] F. Sun, T. M. Kim, A. J. Paulraj, E. de Carvalho, and P. Popovski, "Cell-edge multi-user relaying with overhearing," *IEEE Commun. Lett.*, vol. 17, no. 6, pp. 1160–1163, June 2013.

[42] R. Budhiraja and B. Ramamurthi, "Joint precoder and receiver design for af non-simultaneous two-way mimo relaying," *IEEE Trans. Wireless Commun.*, vol. 14, no. 6, pp. 2942–2955, 2015.

[43] P. Sudharshan Babu, R. Budhiraja, and A. K. Chaturvedi, "Joint power allocation for OFDM-based non-concurrent two-way AF relaying," *IEEE Commun. Lett.*, vol. 22, no. 10, pp. 2100–2103, Oct 2018.

[44] K. Shen and W. Yu, "Fractional programming for communication systems—part i: Power control and beamforming," *IEEE Trans. Signal Process.*, vol. 66, no. 10, pp. 2616–2630, May 2018.

[45] R. Budhiraja and B. Ramamurthi, "Joint transceiver design for QoS-constrained MIMO two-way non-regenerative relaying using geometric programming," *IEEE Trans. Wireless Commun.*, vol. 15, no. 5, pp. 3453–3465, May 2016.

[46] M. Grant and S. Boyd, "CVX: Matlab software for disciplined convex programming, version 2.1," Mar. 2014.

[47] M. Chiang, C. W. Tan, D. P. Palomar, D. O'neill, and D. Julian, "Power control by geometric programming," *IEEE Trans. Wireless Commun.*, vol. 6, no. 7, pp. 2640–2651, July 2007.

[48] R. Budhiraja and B. Ramamurthi, "Multiuser two-way nonregenerative mimo relaying with nonconcurrent traffic," *IEEE Trans. Veh. Technol.*, vol. 64, no. 7, pp. 3268–3273, July 2015.

[49] S. P. Boyd, S. J. Kim, L. Vandenberghe, and A. Hassibi, "A tutorial on geometric programming," vol. 8, no. 1, p. 67, 2007.

[50] A. Zappone and E. Jorswieck, "Energy efficiency in wireless networks via fractional programming theory," *Foundations and Trends of Communications and Information Theory*, vol. 11, no. 3-4, pp. 185–399, 2014.

[51] Q. Wu, W. Chen, M. Tao, J. Li, H. Tang, and J. Wu, "Resource allocation for joint transmitter and receiver energy efficiency maximization in downlink OFDMA systems," *IEEE Trans. Commun.*, vol. 63, no. 2, pp. 416–430, Feb 2015.

[52] Y. Han, T. Hsu, C. Wen, K. Wong, and S. Jin, "Efficient downlink channel reconstruction for FDD multi-antenna systems," *IEEE Trans. Wireless Commun.*, vol. 18, no. 6, pp. 3161–3176, June 2019.

[53] B. Dutta, R. Budhiraja, and R. D. Koilpillai, "High-diversity joint precoder design for non-concurrent two-way af MIMO relaying," *IEEE Trans. Commun.*, vol. 66, no. 7, pp. 2855–2872, July 2018.

[54] P. S. Babu, R. Budhiraja, and A. K. Chaturvedi, "Optimization for energy-efficient ofdm amplify and forward non-concurrent two-way relaying," vol. 24, no. 2, pp. 405–409, 2020.

[55] S. Boyd and L. Vandenberghe, *Convex Optimization.* New York, NY, USA: Cambridge University Press, 2004.

[56] M. Chiang, "Geometric programming for communication systems," *Found. Trends Commun. Inf. Theory*, vol. 2, no. 1-2, Jul. 2005.

[57] M. Chiang, C. W. Tan, D. Palomar, D. O'Neill, and D. Julian, "Power control by geometric programming," *IEEE Trans. Wireless Commun.*, vol. 6, no. 7, pp. 2640–2651, Jul. 2007.

[58] Y. J. A. Zhang, L. Qian, and J. Huang, "Monotonic optimization in communication and networking systems," *Found. Trends Netw.*, vol. 7, no. 1, pp. 1–75, Oct. 2013.

[59] Y. Sun, P. Babu, and D. P. Palomar, "Majorization-minimization algorithms in signal processing, communications, and machine learning," *IEEE Trans. Signal Process.*, vol. 65, no. 3, pp. 794–816, Feb 2017.

[60] G. Xu, W. Ma, Y. Ren, Q. Huang, and Y. Wang, "Joint resource allocation for multi-user and two-way multi-relay OFDMA networks," in *Proc. IEEE 79th Veh. Technol. Conf. (VTC)*, 2014, pp. 1–5.

[61] P. Sudharshan Babu, R. Budhiraja, and A. K. Chaturvedi, "Joint power allocation for OFDM-based non-concurrent two-way AF relaying," *IEEE Commun. Lett.*, vol. 22, no. 10, pp. 2100–2103, Oct 2018.

[62] H. Zhang and L. Cai, "Hepnc: A cross-layer design for mimo networks with asymmetric two-way relay channel," in *2015 IEEE Global Communications Conference (GLOBECOM)*, Dec 2015, pp. 1–6.

[63] R. Budhiraja and B. Ramamurthi, "Precoder design for asymmetric two-way af shared relay," in *2013 National Conference on Communications (NCC)*, Feb 2013, pp. 1–5.

[64] R. Budhiraja and B. Ramamurthi, "Transceiver design for nonconcurrent two-way mimo af relaying with qos guarantees," *IEEE Trans. Veh. Technol.*, vol. 65, no. 12, pp. 9651–9661, Dec 2016.

[65] G. H. Golub and C. F. Van Loan, *Matrix Computations*, 3rd ed. The Johns Hopkins University Press, 1996.

[66] W. Dinkelbach, "On nonlinear fractional programming," *Management Science*, vol. 13, no. 7, pp. 492–498, 1967.

[67] Y. Dai and X. Dong, "Power allocation for multi-pair massive mimo two-way af relaying with linear processing," *IEEE Trans. Wireless Commun.*, vol. 15, no. 9, pp. 5932–5946, Sep 2016.

[68] E. Björnson, L. Sanguinetti, J. Hoydis, and M. Debbah, "Optimal design of energy-efficient multi-user mimo systems: Is massive mimo the answer?" *IEEE Trans. Wireless Commun.*, vol. 14, no. 6, pp. 3059–3075, 2015.

Publications

Published in Referred Journals:

[1] P. S. Babu, R. Budhiraja and A. K. Chaturvedi, "Optimization For Energy-Efficient OFDM Amplify and Forward Non-Concurrent Two-Way Relaying," in IEEE Communications Letters, vol. 24, no. 2, pp. 405-409, Feb. 2020.

[2] P. Sudharshan Babu, R. Budhiraja and A. K. Chaturvedi, "Joint Power Allocation for OFDM-Based Non-Concurrent Two-Way AF Relaying," in IEEE Communications Letters, vol. 22, no. 10, pp. 2100-2103, Oct. 2018.

Under Preparation

[3] P. Sudharshan Babu, R. Budhiraja and A. K. Chaturvedi, "Transceiver Design and Joint Power Allocation for Non-Concurrent Two-Way AF MIMO Relaying in Cellular Networks," to be submitted to IEEE Transactions on Vehicular Technology.